Photobioreactor Technologies for High-Throughput Microalgae Cultivation

Ebenezer Olusegun Ojo

A thesis submitted to the University College London for the degree of
Doctor of Philosophy

Department of Biochemical Engineering
University College London
Torrington Place, London
WC1E 6BT

DECLARATION

I, Ebenezer Olusegun Ojo, confirms that the work presented in this thesis is my own. Where information has been derived from other sources, I confirm that this has been indicated in the thesis.

Signature: _____ Date:___17/02/2015_____

ABSTRACT

The evaluation and optimisation of microalgae cultivation process for biomass, lipid and high value chemicals production requires experimental investigation of several interacting variables. This thesis addresses the development of a range of small-scale photobioreactor technologies and shows how they can be applied for rapid, early stage evaluation and scale-up of microalgae cultivation processes. In particular, the work focuses on the engineering evaluation of a novel shaken miniature photobioreactor (mPBr) and a single-use photobioreactor (SUPBr) that can be adapted for both phototrophic and heterotrophic cultivation.

A prototype twin-well mPBr was initially designed and fabricated with light provided from cool white light emitting diodes (LED). This was scaled-out to a 24-well mPBr system (4 mL working volume) on a novel shaken platform. High power warm white LEDs provided a maximum light intensity of 2000 $\mu molm^{-2}s^{-1}$. In both systems, surface aeration (via a semipermeable membrane) and mixing were provided by orbital shaking. Real-time control of temperature, relative humidity and CO_2 levels was achieved via incubator level control. Amongst the tested geometries of the mPBr, round base and pyramid base gave the best performance. The mass transfer coefficient (k_La) values in the 24-well were measured between $20 - 88$ h^{-1} and visual observation of fluid hydrodynamics showed an increase in total surface area with increased shaking frequency. Negligible evaporation was observed at 90% relative humidity for light intensity of < 400 $\mu molm^{-2}s^{-1}$ and at 32 °C, while light intensity variation across the platform is in the range $\pm$ 20 $\mu molm^{-2}s^{-1}$.

Evaluation of phototrophic culture kinetics of *Chlorella sorokiniana* in both mPBr designs showed good reproducibility between wells. The best culture performance occurred at 380 $\mu molm^{-2}s^{-1}$, 300 rpm and 5% CO_2, where final biomass concentration and total lipid concentration achieved were 9 ± 0.2 gL^{-1} and 55% w/w respectively. The SUPBr comprised a transparent polymeric CultiBag^{TM} operated on the illuminated rotary shaken platform described above. Mixing time values were determined over the range 40 - 220 rpm and were generally less than 40 s. Hydrodynamic studies showed three distinct flow regimes at various shaking frequencies: in-phase, transitional and out-of-phase. Under optimal flow regime, the highest cell concentrations achieved was 6.7 gL^{-1} $\pm$ 0.3. Doubling the total working

volume resulted in 35 - 40% reduction in biomass concentration due to an increase in the light path length. Phototrophic scale-up criteria from mPBr to SUPBr was successfully achieved based on light–path length and k_La values. Comparison of final biomass concentrations showed similar performance of 6 ± 0.2 gL^{-1} and comparable total lipid production of $25 - 30\%$ by weight at a light intensity of 180 ± 20 $\mu molm^{-2}s^{-1}$.

Furthermore, application of the shaken 24-well system for heterotrophic cultivation of microalgae and scale-up to a 7.5 L stirred tank bioreactor was also shown. Cells were cultured in 24 parallel wells, shake flasks and a 7.5 L bioreactor with working volumes of 4 mL, 100 mL and 4000 mL respectively using glucose (10 gL^{-1}) as the main carbon source. Constant k_La was chosen as scale-up criteria and the values range between $30 - 60$ h^{-1}. Final biomass concentrations showed good agreement in the range of 4.5 ± 0.5 gL^{-1} and total lipid production of $43 - 50\%$ by weight for the three systems. Overall, the results show the utility of the mPBr and SUPBr technologies for the rapid evaluation and scale-up of both phototrophic and heterotrophic microalgae cultivation conditions.

ACKNOWLEDGMENTS

DEDICATION

I would like to dedicate this thesis to Mrs. Jana Small of Biochemical Engineering Department, UCL, for her support and help in 2009, when I almost missed my admission. Much appreciated.

CONTENTS

Section

LIST OF FIGURES

13

14

17

18

LIST OF TABLES

NOMENCLATURE

A	Area (m^2)
A_H	Heat transfer area (m^2)
A_{pbr}	Bioreactor illuminated surface area (m^2)
B	Bag width (m)
C	Concentration (kgm^{-3})
$C_{chl-a,b}$	Chlorophyll concentration (a and b) (mgL^{-1})
C_H	Dimensionless mixing number (–)
C_L	Dissolved oxygen concentration in the liquid (kgm^{-3})
$C_{L,O2}{}^*$	Saturation concentration of the oxygen in the liquid (kgm^{-3})
$C_{L,O2}{}^*$–$C_{L,O2}$	Difference of dissolved oxygen in the fluid (kgm^{-3})
C_p	Dimensionless power input coefficient (–)
C_{ppc}	Carotenoids concentration (mgL^{-1})
C_T	Tracer concentration (kgm^{-3})
$C_{T,\,0}$	Tracer concentration at the start of the experiment (kgm^{-3})
$C_{T,\,\omega}$	Tracer concentration at the end of the determination (kgm^{-3})
C_x	Cell concentration ($cellsmL^{-1}$)
C_p	Heat capacity ($kgs^{-2}m^{-1}K^{-1}$)
C	Correlation factor (–)
d_a	Agitator diameter (m)
d_o	Orbital shaking diameter (mm)
d_v or d	Vessel diameter (m)
d_{VF}	Reference floc diameter (ms^{-1})
D	Dilution rate (s^{-1})
h	High level of the bag (m)
H	Homogeneity (–)
H_o	Initial height of liquid (m)
H	Maximum height of the liquid (m)
H_N	Normalised height
k_La	Volumetric mass transfer coefficient (s^{-1})
L	Quartz cuvette path length (mm)
m	Mass (kg)
M	Torque (kgm^2s^{-2})
M_d	Dead weight torque (kgm^2s^{-2})
Ne	Newton number (–)
$N=f_s$	Rotation/shaking frequency (s^{-1})
$\overline{N}$	Average rotary frequency (s^{-1})
OTR	Oxygen transfer rate ($kg_{O2}m^{-3}s^{-1}$)
OUR	Oxygen uptake rate ($kg_{O2}m^{-3}s^{-1}$)
PE	Photosynthetic efficiency (%)
Ph	Phase number
P	Power input (kgm^2s^{-3})
p/v	Specific power input ($kgm^{-1}s^{-3}$)
$q0_2$	Specific oxygen uptake rate ($kg_{o2}s^{-1}cells^{-1}$)
r	Rocking rate (s^{-1})
Re	Reynolds number (–)
Re_{mod}	Reynolds number modified for single-use bioreactor
$\underline{t}$	Time (s)
$\overline{t}$	Mean residence time (s)

T_E	Fluid temperature (K)
t_m	Mixing time (s)
T_o	Environment / bioreactor wall temperature (K)
u_G	Superficial gas velocity (ms^{-1})
u_{max}	Maximal fluid velocity [ms^{-1}]
$u_{max, mod}$	Modified maximal fluid velocity (ms^{-1})
u_{Tip}	Tip speed (ms^{-1})
U	Heat transfer coefficient ($kgK^{-1}s^{-3}$)
V_1	Sample volume (m^3)
V_2	Extraction solvent volume (m^3)
v	Characteristic velocity (ms^{-1})
V or V_L	Working volume (m^3)
$\tilde{V}$	Flow rate (liquid) (m^3s^{-1})
$\tilde{V}_G$	Flow rate of gas (m^3s^{-1})
V_f	Fill volume / total volume
X_1	Initial dry cell weight (gL^{-1})
X_2	Final dry cell weight (gL^{-1})
y	Amplitude (m)
$Y_{x,E}$	Biomass yield on photon energy ($gmol^{-1}$)

Greek symbols

η_L	Fluid viscosity ($kgm^{-1}s^{-1}$)
θ_m	Mixing time (s)
$\rho_L \& \rho$	Fluid density (kgm^{-3})
ω_y	Angular velocity (s^{-1})

ABBREVIATIONS

BBM	Bold basal medium
CCAP	Culture collection of algae and protozoan
CO_2	Carbon dioxide (%)
CP	Closed photobioreactors
DOT	Dissolved oxygen tension (%)
EG	*Euglena gracilis*
FAME	Fatty acid methyl ester
FID	Flame ionization detector
HPH	High pressure homogeniser
HSH	High speed homogeniser
HSM	High salt medium
IEA	International energy agency
IPAR	Illuminated photosynthetic active radiation (400nm -700nm)
JAH	Jerusalem artichoke hydrolysate
LED	Light emitting diodes
mPBr	Miniature photobioreactor
MTP	Microtitre plate
MUFA	Monounsaturated fatty acids
NADPH	Nicotinamide adenine dinucleotide phosphate
OD	Optical density (nm)
PAME	Palmitic acid methyl ester
PAR	Photosynthetic active radiation
PDC	Pyruvate dehydrogenase complex
PE	Photosynthetic efficiency (%)
PI	Photosynthetic rate and light intensity relationship
PUFA	Polyunsaturated fatty acids
RH	Relative humidity
RO	Reverse osmosis
RQ	Respiratory quotient
SFA	Saturated fatty acids
STR	Stirred tank reactor
SUB	Single-use bioreactors
SUPBr	Single-use photobioreactor
S/V	Surface area to volume ratio (m^{-1})
TAP	Tris-acetate phosphate
TBP	Tris-base phosphate
TMSH	Trimethyl sulfonium hydroxide
UFA	Unsaturated fatty acids
URS	User requirement specifications

1.INTRODUCTION

1.1 Biofuels from Microalgae

1.1.1 Biofuels an Alternative Energy Source

The increasing dependence of global economic developments on natural energy sources have placed significant demand on the continuous supply of fossil fuels (crude-oil and gas) in order to meet rising demand. Despite the impact of fossil fuel utilisation on global warming, the International Energy Agency (IEA) has forecast a probable 40% increase in use by 2030. Biofuels are alternative sources of clean energy that have received increasing attention in recent years. Referred to as liquid and gaseous fuel produced from biomass, biofuels are classified into four different generations (first to fourth) based on advances in the underpinning technology. The current status of biofuel technology development is shown in Figure 1.1 (IEA, 2011).

Microalgae are currently considered as a prime feedstock for biofuel production amongst others such as lignin, organic waste and plant crops. Avoiding the use of arable land for microalgae cultivation lessens the impact on the food chain supply (Singh et al., 2011) and converts excess carbon dioxide (CO_2) present in the atmosphere into valued products (Guedes et al., 2011; Jeong et al., 2003). Microalgae are ubiquitous organisms which grow in fresh and saline water bodies, cold mountain streams, hot inland swamps and ponds (Mata et al., 2010). Algae range in sizes from a few micrometers to over 30 m in length and have been classified into macroalgae and microalgae of which the latter are the focus of this work.

Microalgae are tiny (micrometers in dimension) unicellular organisms that grow in suspension or on solid substrates. Microalgae cells are eukaryotic containing internal organelles such as chloroplasts, nucleus, etc (Figure 1.2 (A)) and are comparable to most terrestrial plants. Their ability to grow rapidly with doubling times in the range of 3.5-24 hr enables their utilisation as an alternative source of biofuels (Chisti, 2007; Illman et al., 2000; Xu et al., 2006; Liu et al., 2010; Metting, 1996).
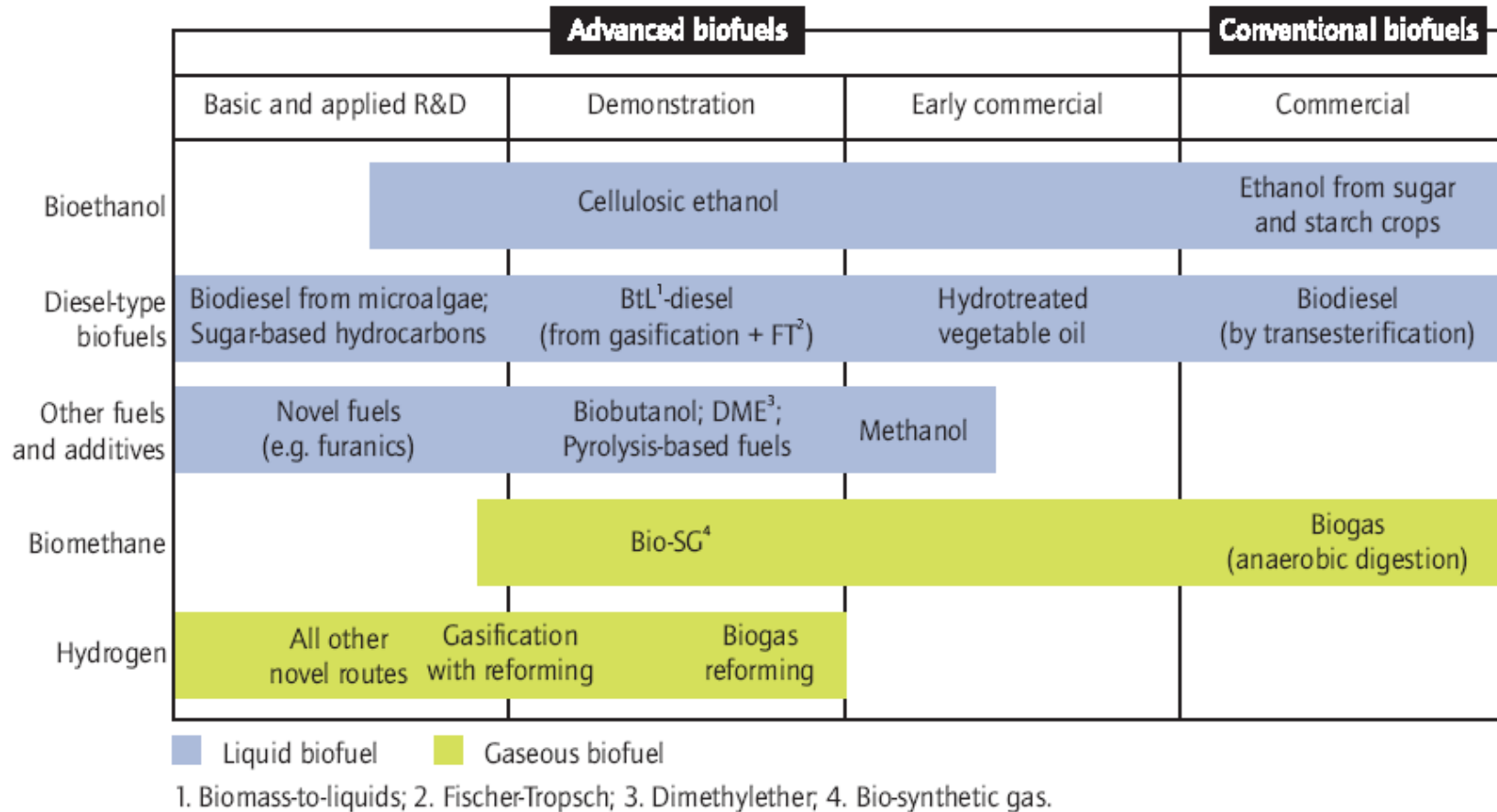
Figure 1.1: The commercialisation status of key biofuel technologies categorised according to the production technologies used. Reproduced from IEA (2011).

Photosynthetic microalgae convert CO_2 in the presence of light to algal biomass, which is used as feedstock for other bioproducts (Chen et al., 2010; Chisti, 2007a). Many microalgae species have the ability to synthesise and accumulate large amounts of neutral oil/lipids (the main precursor to biodiesel production) as shown in Figure 1.2 (B) (Chen and Chen, 2006; Chisti, 2008). This lipid can account for 20–50% of dry cell weight (Hu et al., 2008) while some strains can reach as high as 80% (Spolaore et al, 2006). Oil-rich microalgae are therefore considered an ideal feedstock for biodiesel production via trans-esterification of triglycerides (lipids/oil). Glycerol is released as the main by-product, and this could be further converted to many other by-products (Chisti, 2007). A generalise biosynthetic pathway for biodiesel production is shown in Figure 1.3.

The biochemical composition of different strains of microalgae has been extensively studied due to the various applications of algal biomass and metabolites (Guedes et al., 2011). This knowledge enhances strain selection for different applications such as biofuels, biopharmaceuticals and bioremediation. The choice of algal strain depends largely on the intended bioproducts, the bioprocess engineering environment it will be used and the cell genetic make up. In certain instances, strains are selected based on the knowledge of their genetic compositions and understanding of their metabolic pathways and growth rates. In other instances, selection is based on their ability to synthesize either extra or intra-cellular metabolites of high value. In general, most algae exhibit a similar biochemical composition as shown in Table 1-1. Microalgae cell walls are typically tri-layered structures which include; polysaccharides such as cellulose, uronic acid, protein, mannose, xylan, or tri-laminar layers of algaenan, glycoproteins and minerals such as calcium or silicates (Allard et al., 2002; Allard and Templier, 2001; Blumreisinger et al., 1983; Carpita, 1985; Sugiyama et al., 1991).

Photosynthesis undergoes either light or dark steps (or Calvin cycle). The initial step is the conversion of light energy absorbed at a specific wavelength into chemical energy (adenosine triphosphate (ATP) and nicotinamide adenine dinucleotide phosphate (NADPH)) during the light reactions. The ATP and NADPH is thereafter utilised during CO_2 fixation (dark reactions) to produce glyceraldehyde-3-phosphate (G3P). This is further converted into biomass building blocks and production of other useful metabolites.

(A)

(B)
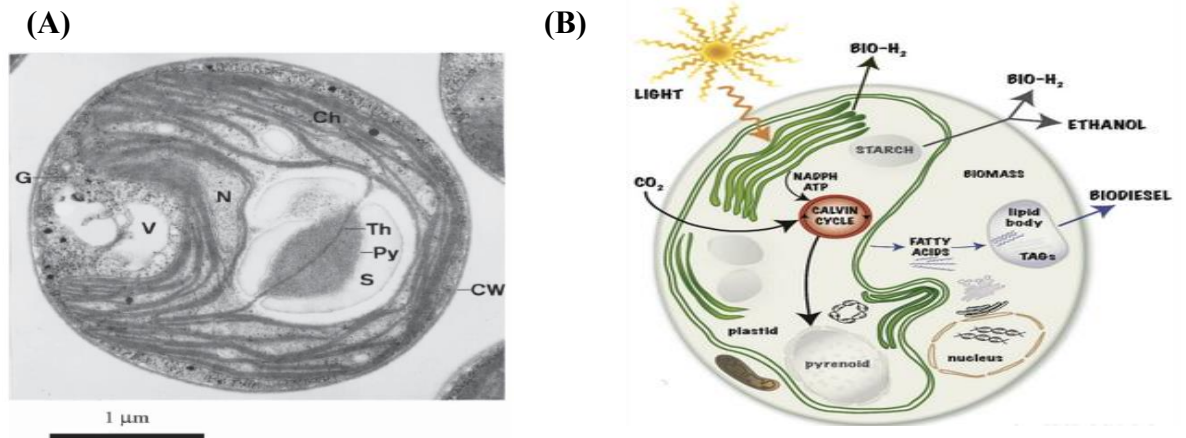
Figure 1.2: Microalgae physiology. (A) Transmission electron micrograph of *C.sorokiniana* HO-1 showing cellular structures and organelles. Ch, chloroplast; CW, cell wall; G, granule; N, nucleus; Py, pyrenoid; S, starch; Th, thylakoid; V, vacuole. (B) Typical pictorial representation of green microalgae cells showing growth requirements and potential final products. Figures reproduced from Masahiko et al. (2000).
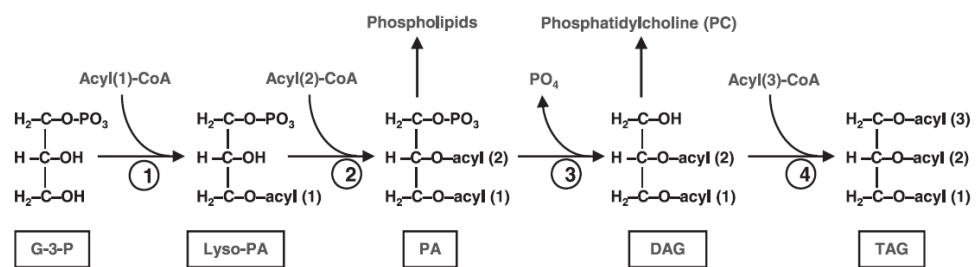
Figure 1.3: Simplified schematic diagram of triacylglycerol biosynthesis pathway in algae. (1) Cytosolic glycerol-3-phosphate acyl transferase, (2) lyso-phosphatidic acid acyl transferase, (3) phosphatidic acid phosphatase, and (4) diacylglycerol acyl transferase. Figure reproduced from Hu et al. (2008).

Table 1-1: Biochemical composition of various microalgal species as wt. % of dry biomass. Reproduced from (Becker, 1994; Halim et al, 2013)

Strain	Protein (%)	Carbohydrates (%)	Lipids (%)	Nucleic acid (%)
Scenedesmus obliquus	50-56	10-17	12-14	3-6
Scenesdesmus quadricauda	47	-	1.9	-
Scenesdesmus dimorphus	8 -18	21-52	16-40	-
Chlamydomonas rheinhardii	48	17	21	-
Chlorella vulgaris	51-58	12-17	14-22	4-5
Chlorella pyrenoidosa	57	26	2	-
Spirogyra species	6 -20	33-64	11-21	-
Unaliella bioculata	49	4	8	-
Dunaliella salina	57	32	6	-
Euglena gracilis	39-61	14-18	14-20	-
Prymnesium parvum	28-45	25-33	22-38	1-2
Tetraselmis maculata	52	15	3	-
Porphyridium cruentum	28-39	40-57	9-14	-
Spirulina platensis	46-63	8-14	4-9	2-5
Spirulina maxima	60-71	13-16	6-7	3-4.5
Synechoccus sp	63	15	11	5
Anabaena cylindrica	43-56	25-30	4-7	-

During respiration, oxygen taken up enables oxidation of NADH in the mitochondria. This process generates energy in the form of ATP along with cellular CO_2. The extra energy produced enhances biomass formation and also provides maintenance support to other cellular processes. Photorespiration involves oxygen fixation via the oxygenase activity of rubisco to form glycolate. This is further converted to glyceraldehyde-3-phospahte which is reused for other biosysnthetic processes. In general, CO_2 and ammonia lost will require energy in the form of ATP and NADH for re-fixing.

Oleaginous microalgae, generally known as lipid accumulating microorganisms (Ratledge, 2002), are known for syntheses of polyunsaturated fatty acids (PUFAs) and many other bioactive compounds such as pigments, antioxidants, antibiotics, toxins and biofuels. Several of these are currently being investigated as a viable and sustainable source of new products for the nutraceutics and biopharmaceutics industries (Bellou and Aggelis, 2012). Besides, algal biomass and lipid have been considered for biofuel production either by direct combustion, pretreated wet biomass or trans-esterification of the extracted lipid to biodiesel. The success of the latter approach tends to improve on the economic viability of its use as an alternative fuel.

1.1.1.1 Lipid Biosynthesis Process

The lipid components of microalgae differ from strain to strain and are divided into neutral (eg. triacylglycerides and cholesterol) and polar lipids (eg. phospholipids and galactolipids) (Huang et al., 2010). In order to synthesise neutral lipid, a precursor called glyceraldehyde phosphate (GAP) is synthesised from the conversion of CO_2 during photosynthesis by the activities of different photosystems and other cell organelles required for light capturing (Bellou and Aggelis, 2012). The produced G3P is first converted to pyruvate and then to acetyl-CoA through an enzyme catalysed step by "pyruvate dehydrogenase complex (PDC)". The acetyl-CoA produced is then used as precursor for fatty acid synthesis in the plastid (Ngangkham et al., 2012; Packer et al., 2011; Prathima Devi et al., 2013; Qiao and Wang, 2009; Rodolfi et al., 2009; Sakthivel et al., 2011; Xin et al., 2010).

Alternatively, G3P can be directed towards production of polysaccharides which serves structural purposes and as storage materials. With G3P serving as a key

precursor for lipid and polysaccharides metabolism, a systematic switch in the metabolic pathway via nutrient limitation is adopted to enhance production of one over the other (Packer et al., 2011a; Rodolfi et al., 2009; Sharma et al., 2012). During catabolic process in the cytosol, energy from sugar is liberated via glycolysis and is immediately followed by the citric acid cycle in the mitochondrion. However, under limiting conditions of nitrate and phosphate, the metabolic pathway for citric acid cycle could be altered due to the inhibition of the isocitrate dehydrogenase (ICDH) enzyme that catalyses the conversion of isocitrate to ketoglutarate (Bellou and Aggelis, 2012).

In this case, citrate is accumulated in the mitochondrion and then excreted into the cytosol where, in the presence of ATP dependent citrate-lyase (ATP:CL), it is converted into acetyl-CoA and oxaloacetate. Again, acetyl-CoA generated from citrate could be used for fatty acid synthesis. Besides acetyl-CoA, a supply of NADPH (generated from NADH via a small cycle in which malic enzyme – ME participates) is also required for the fatty acids synthesis. The biochemical pathway described above, permitting the conversion of polysaccharides to lipids, is common in oleaginous heterotrophs (Ratledge, 2002).

1.1.2 Culture Conditions for Microalgae

The growth kinetics of microalgae are known to depend significantly on the cultivation conditions. There are four types of cultivation modes namely: phototrophic, heterotrophic, mixotrophic and photoheterotrophic cultivation (Katarzyna and Facundo-Joaquin, 2004). Phototrophic cultivation occurs when microalgae depend on a light source and inorganic carbon (e.g., carbon dioxide) for metabolic activities (Chen and Chen, 2006). Growth under this condition is closely related to the photosynthetic activities described in Section 1.1.1, with light and CO_2 being the frequent growth limiting substrates (Katarzyna and Facundo-Joaquin, 2004). Table 1-2 summarises data reported for the growth of *Chlorella* strains under phototrophic conditions.

The major advantage of adopting phototrophic cultivation to produce microalgal oil is the utilisation of CO_2 as the carbon source for cell growth and lipid production. However, utilisation of CO_2 for large-scale production requires citing of microalgae ponds close to factories or power plants where an adequate supply of CO_2 can be

Table 1-2: Summary of biomass and lipid productivity in different *Chlorella* strains. Reproduced from Chen et al. (2010).

Microalgae strains	CO_2 (%)	Volumetric biomass productivity ($\mu gL^{-1}d^{-1}$)	Lipid content (% of DCW)	Lipid productivity ($mgL^{-1}d^{-1}$)	References
C. emersonii CCAP211/11N	atm. air	40.0	25.0-34.0	10.3-12.2	Scragg et al. (2002)
C. emersonii CCAP211/11N	CO_2	30.0 – 50.0	29.0-63.0	8.1-49.9	Illman et al. (2000)
C. minutissima	CO_2	20.0 – 30.0	31.0-57.0	9.0-10.2	Illman et al. (2000)
C. protothecoides CCAP 211/8D	CO_2	2.0 – 20.0	11.0-23.0	0.2-5.4	Illman et al. (2000)
C. sorokiniana UTEX 1230	CO_2	3.0 – 5.0	20.0-22.0	0.6-1.1	Illman et al. (2000)
C. sorokiniana IAM-212	CO_2	230.0	19.3	44.7	Rodolfi et al. (2009)
C. sp. F&M-M48	CO_2	230.0	18.7	42.1	Rodolfi et al. (2009)
C. sp	CO_2	370.0 – 530.0	32.0-34.0	121.3–178.8	Chiu et al. (2009)
C. vulgaris KCTC AG10032	CO_2	100.0	6.6	6.9	Yoo et al. (2010)
C. vulgaris #259	CO_2	10.0	33.0-38.0	4.0	Liang et al. (2009)
C. vulgaris INETI 58	atm. air	180.0	5.1	7.4	Gouveia and Oliveira, (2009)
C. vulgaris Beijerinck CCAP 211/11B	CO_2	31.0 – 40.0	18.0-40.0	5.4–14.9	Illman et al. (2000)
C. vulgaris CCAP 211/11B	CO_2	170.0	19.2	32.6	Rodolfi et al. (2009)
C. vulgaris Beijerinck CCAP 211/11B	atm. air	20.0 – 40.0	28.0-58.0	11.2–13.9	Scragg et al. (2002)
C. vulgaris F&M-M49	CO_2	200.0	18.4	36.9	Rodolfi et al. (2009)

atm = atmospheric, DCW = dry cell weight, CO_2 = carbon dioxide

obtained. In addition, contamination problem is less severe with phototrophic culture condition, thus enhancing operation of outdoor large-scale cultivation systems, such as open ponds and raceway ponds (Mata et al., 2010).

Reductions in the cost of microalgal biomass and oil production under heterotrophic conditions were reported by Miao and Wu, (2006). This is, however, subject to different economic parameters. The situation when microalgae use organic carbon as both energy and carbon source is called heterotrophic cultivation (Katarzyna and Facundo-Joaquin, 2004). Heterotrophic cultivation avoids the effects of limited light saturation during high cell density culture in large-scale photobioreactors (Huang et al., 2010) thus making large-scale production more feasible. The use of cheaper organic carbon source, such as corn powder hydrolysate (CPH) and Jerusalem artichoke hydrolysate (JAH), in place of glucose, acetate and glycerol have been studied. Table 1-3 reviews different heterotrophic cultivation of microalgae in which the highest lipid productivity is nearly 20 times higher than that obtained under phototrophic cultivation (Chen et al., 2010).

Mixotrophic cultivation occurs when microalgae photosynthesis uses a combination of both carbon source and illumination for growth. During cellular respiration, the CO_2 released by microalgae is trapped and reused under phototrophic mode (Mata et al., 2010). Compared with phototrophic and heterotrophic cultivation, mixotrophic cultivation is rarely used in microalgae oil production.

Finally, photoheterotrophic cultivation occurs when the microalgae require light when using organic carbon as the carbon source. The main difference between mixotrophic and photoheterotrophic cultivation is that the latter requires light as the energy source, while mixotrophic cultivation can use organic compounds to serve this purpose. Hence, photoheterotrophic cultivation needs both sugars and light at the same time (Katarzyna & Facundo-Joaquin, 2004). Although the production of some light-regulated useful metabolites can be enhanced by using photoheterotrophic cultivation, using this approach to produce biodiesel is very rare, as is the case with mixotrophic cultivation.

Table 1-3: Heterotrophic cultivation of microalgae on different carbon sources and their respective biomass and lipid productivity. Reproduced from Chen et al. (2010).

Microalgae species	Carbon source	Biomass productivity $(gL^{-1}d^{-1})$	Lipid content (% of DCW)	Lipid productivity $(mgL^{-1}d^{-1})$	References
C. protothecoides	JAH	4.0–4.4	43.0–46.0	1881.3–1840.0	Cheng et al. (2009)
C. protothecoides	Glucose	2.2–7.4	50.3–57.8	1209.6–3701.1	Xiong et al. (2008)
C. protothecoides	Glucose	1.7–2.0	43.0–48.7	732.7–932.0	Li et al. (2007)
C. protothecoides	CHP/Glucose	2.0	46.1	932.0	Xu et al. (2006)
C. vulgaris	Glucose and Acetate	0.08–0.15	23.0–36.0	27.0–35.0	Liang et al. (2009)

atm = atmospheric, DCW = dry cell weight, CO_2 = carbon dioxide

1.1.3   Medium Composition and Formulation

The extent of cell growth and metabolic activities during microalgae cultivation depends largely on the medium composition. The carbon and nitrogen contents are critical for biomass and lipid production irrespective of the cultivation mode (Xu et al., 2006). Also included in the media formulations are; phosphates, silicon, iron, and trace elements specifically required by some strains. Synthetic media are frequently designed for the purpose of studying a strain of interest. Several reported studies highlighted the importance of each of these compounds and their concentration on growth (Agrawal and Manisha, 2007; Chen et al., 2010; Ghoshal and Goyal, 2001; Illman et al., 2000; Khalil et al., 2009; Lehana, 1990; Liang et al., 2009; O'Grady and Morgan, 2010; Pyle et al., 2008; Robertson and Jane, 2010; Tam and Wong, 1996). Understanding the metabolic fluxes in individual microalgae strains could enable formulation of novel and specific media supporting both high biomass yield and lipid production.

Utilisation of CO_2 by photosynthetically growing microalgae is of global interest for the capture of gaseous CO_2 from industrial and fermentation effluents (Chen et al., 2008; Chen and Chang, 2006). Effective CO_2 capture is achieved via chemical absorption with aqueous sodium hydroxide (Dindore et al., 2005) to produce sodium bicarbonate. This is further utilised by microalgae to produce high carbohydrate or high lipid containing biomass (Raoof et al., 2006; Hsueh et al., 2007). Residual bicarbonate ions and dissolved CO_2 (as carbonic acid) in the media often leads to increase in broth acidity. This decreases pH values to below those that can be tolerated by the cells resulting in growth limitation.

It is therefore important that culture media are specifically formulated to provide the right environment for optimal biomass production and ideally maintains a constant pH within an acceptable range throughout the culture period. In order to achieve this, the choice of media components and concentrations becomes crucial alongside the basic understanding of chemical interactions between the different ions and free radicals Becker (1994). A practical approach to this problem is further discussed in Chapter 3 of this thesis.

1.2   Photobioreactor Technology

1.2.1   Photobioreactors for Microalgae Cultivation

Given the likely requirement for large-scale growth of microalgae for biofuel and other high value chemical production, phototrophic cultivation is considered to be more economically feasible than heterotrophic or mixotrophic cultivation. There is also the advantage of phototrophic cultivation enabling assimilation of carbon dioxide from the atmosphere as mentioned in Section 1.1.1. Depending on the production scale envisaged, two main bioreactor types have been developed namely; open pond and closed photobioreactors (Borowitzka, 1999).

The former is most often used for large-scale production while closed photobioreactors are often used for smaller scale, high productivity cultures. The illumination of closed bioreactors is either internal or external (Chen et al., 2011; Ugwu et al., 2005). The overall productivity in each system is influenced by the properties of selected microalgae strains, facility set-up, culture conditions and the operational costs (Borowitzka, 1992).

1.2.2   Light Intensity Estimation in Photobioreactors

Estimation of light intensity within the culture medium is usually performed using Beer Lambert's law. Most conventional PBr are designed based on the light attenuation along the depth of the liquid volume (Aiba, 1982). Dark zones in the PBr are minimized through optimisation of the average light path length (Liao et al., 2014; Zhang, 2013). A common phenomenon observed in the presence of photosynthetic microorganism is the effect of light scattering. It is therefore important to understand the relationship between photosynthetic rate and light intensity (PI).

1.2.2.1   Light Intensity and Photosynthetic Rate (PI)

As culture density increases, photon flux dispersion in the PBr system reduces. However, at full scale these two parameters are less controllable and thereby impact on net algal biomass productivity significantly (Béchet et al., 2010; Béchet et al., 2011; Grobbelaar, 2009; Mata et al., 2010). Béchet et al., (2013) reported the effect of specific rate of oxygen production and the specific growth rate on PI relationship. Under poor mixing conditions, concentrations gradient could lead to localised

nutrients and oxygen limitations. However, this can be mitigated by optimal design and operations of photobioreactor system (Mata et al., 2010).

For optimal performance of a photobioreactor, the effect of light intensity on the rate of photosynthesis has been classified into three different light regimes as shown in Figure 1.4.

- **Low light intensities**: A condition where the rate of photosynthesis is often proportional to light intensity because of limited photon capture.

- **Saturation threshold of light intensity**: Growth of light saturated microalgae under these conditions is independent of light intensity and photosynthetic rate is usually maximal. However, the rate of reaction following photon capture limits the photosynthetic rate.

- **Inhibitory threshold of light intensity**: Deactivation of key proteins in the photosynthetic unit starts at light intensity above an inhibitory threshold

1.2.2.2   Modeling Photosynthesis in Well-Mixed Dense Cultures

In order to optimise productivity, microalgae cultivation is performed at high cell density which introduces light gradients into the system (Cuaresma et al., 2009; Mairet et al., 2011). The gradient leads to cells experiencing different light intensities depending on their location and the rate of mixing. In well-mixed systems, microalgae experience short light cycles travelling from high light zones to near dark zones. This reduces light inhibition and creates a flashing light effect (Béchet et al., 2013; Mirón et al., 1999).

Models for photosynthetic microalgae cultivation can be categorised based on their ability to account for light gradients and short light cycles experienced in well-mixed dense outdoor cultures. Some of the models highlighted include: Poisson, light inhibition, tangent and modified hyperbolic models. The three model types described by Bechet et al. (2013) are summarised below:

- Type 1: These models predict the rate of photosynthesis of the entire culture as a function of the incident or the average light intensity reaching the culture. Type I model development is largely dependent on the operating

37

conditions specified during development and validation, and should therefore be used within this range of conditions.

● Type II: These models quantify the impact of the light gradient on the local rate of photosynthesis. Light distribution in the broth is quantified, followed by selection of a biological model that expresses the local rate of photosynthesis as a function of light intensity and finds the aggregate of the local rate of photosynthesis to obtain the global rate of photosynthesis. Yun and Park (2003) and Cornet and Dussap (2009) were able to show the versatility and accurate prediction of Type II models under a wide range of operating conditions. However, for very large-scale production, overestimation of the impact of light inhibition may be encountered (Bosma et al., 2007).

● Type III: These models account for both light gradients and short light cycles, as the microalgae cells move across in the system over time. A dynamic biological model is used to determine the photosynthetic rate based on the prior interaction with light in the system and the photosynthetic rates of individual cells is thereafter summed up to determine the total rate of photosynthesis in the cultivation system. Computational fluid dynamics have been applied in determining the flow field which represents light interactions (Perner-Nochta and Posten, 2007; Pruvost et al., 2006).

Light Intensity (I)
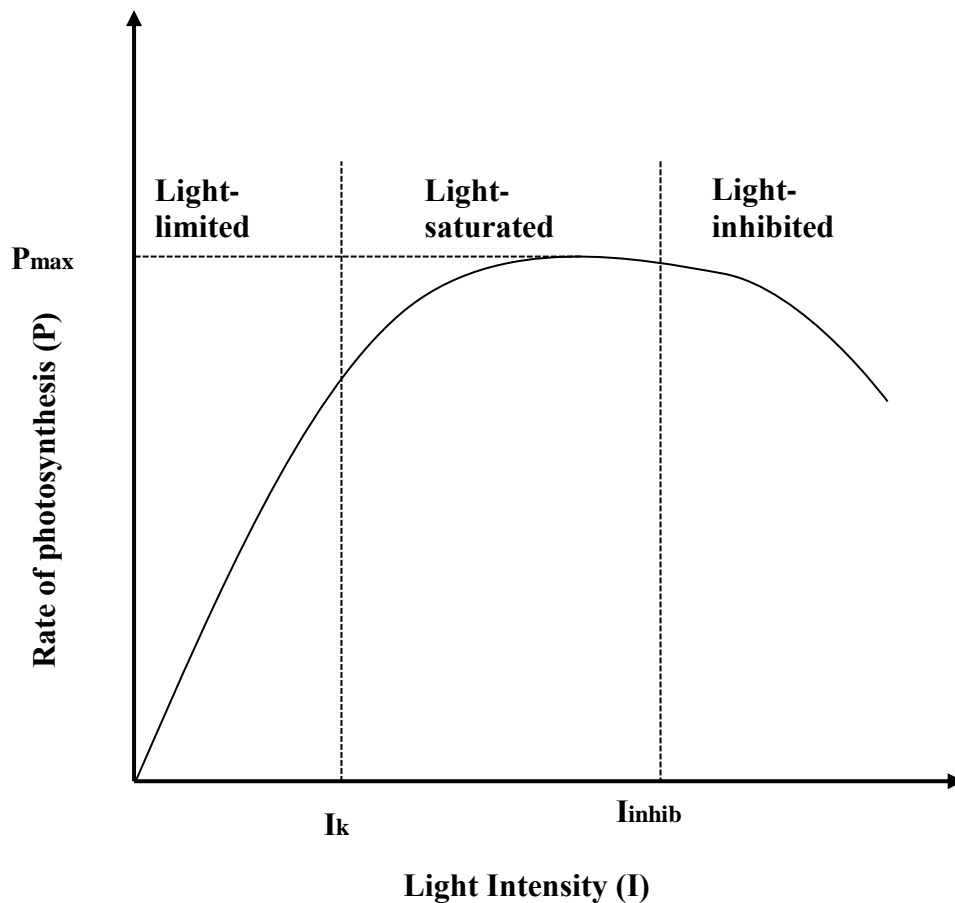
Figure 1.4: Typical PI relationship showing the light limited-limited ($I<I_k$), light saturated ($I_k<I<I_{inhib}$), and light-inhibited ($I>I_{inhib}$) regimes of microalgae light response. Reproduced from Béchet et al. (2013).

1.2.3 Comparison of Large-Scale Phototrophic Cultivation Systems

Different large-scale cultivation systems have been developed and these are categorised into open and closed production systems (Section 1.2.1). The advantages and disadvantages of the different types are highlighted in Table 1.4.

Open pond systems for microalgae production have been used since the 1950s (Borowitzka, 1999) and are categorised into natural waters (such as lakes, lagoons, and ponds) and artificial ponds or containers. The most common design is the raceway pond (Jimenez et al., 2003). Mixing and circulation are achieved using a paddle wheel in order to stabilize microalgae growth, productivity and enhance homogeneity, especially in a continuous system requiring additional broth and nutrients.

Closed photobioreactor systems help to overcome some of the major problems associated with the open pond production systems such as pollution and contamination risks. In contrast, closed photobioreactors allow culture of single-species of microalgae for prolonged durations with a lower risk of contamination (Chisti, 2007). Closed systems include tubular, flat plate, and column photobioreactors. These systems are more appropriate for sensitive strains because the closed configuration enables better control of bioprocess parameters and ensures sterility. Owing to the higher cell mass productivities attained, harvesting costs can also be significantly reduced (Carvalho et al., 2006). Table 1.5 shows selected examples of different bioreactors.

1.2.4 Need for Small-Scale Cultivation Systems for Microalgae

In recent times, novel small-scale cultivation systems are rapidly replacing conventional laboratory scale experimentation because it offers a parallel platform to obtain key bioprocess data early and cost effectively (Lye et al., 2003). This capability is combined with easy automation (Doig et al., 2002) and implementation of advanced operating strategies such as liquid addition for pH control (Elmahdi, 2003) and fed-batch operation. Doig et al. (2005) identified four key steps required

Table 1.4: Advantages and limitations of different photobioreactor systems.

Production Systems	Advantages	Limitations
Raceway pond	Relatively cheap Easy to clean Utilises non-agricultural land Low energy input Easy maintenance	Poor biomass productivity Large area of land required Limited to a few strains of microalgae Poor mixing, light and CO_2 utilisation Cultures are easily contaminated
Tubular photobioreactor	Large illumination surface area Suitable for outdoor cultures Relatively cheap Good biomass productivities	Some degree of wall growth Fouling Requires large land space Gradients of pH, dissolved oxygen and CO_2 along the tubes
Flat plate photobioreactor	High biomass productivities Easy to sterilise Low oxygen build-up Good light path Large illumination surface area Suitable for outdoor cultures.	Difficult scale-up Difficult temperature control Some degree of wall growth
Column photobioreactor	Compact High mass transfer Low energy consumption Good mixing with low shear stress Easy to sterilise Reduced photo-inhibition and photo-oxidation	Small illumination area Expensive compared to open ponds Shear stress Sophisticated construction

for the design and optimisation of most industrial scale fermentation which are also similar for microalgae cultivation processes. These four steps are: (i) strain identification (ii) strain enhancement (iii) process design and optimisation and (iv) process scale-up and validation.

Depending on the products of interest, strain identification could end with more than one strain with significant differences in their responses to the biochemical environment. Process requirements and optimisation of the leading strains are further evaluated for increase productivity. These steps involve comparing several growth parameters such as light intensity, pH, temperature, mass transfer, percentage carbon dioxide, organic carbon sources and media composition. However, the best strain is further used to define the process boundaries and scale-up based on experimentally validated scale-up criteria.

Several studies on the engineering characterisation and applications of microscale technology for microbial and mammalian cell bioprocess development have been reported (Barrett et al., 2010; Hussain et al., 2013; Klöckner and Büchs, 2012; Mukhopadhyay et al., 2011; Silk et al., 2010; Zhou et al., 2009). However, for microalgae, illuminated shake flask systems remain the most widely used bioreactor format for early stage phototrophic cultivation.

Design of a photobioreactor for microalgae cultivation requires careful consideration of microalgae growth requirements. These include maintenance of axenic conditions and control of physical and engineering parameters, particularly: light intensity, temperature, pH and dissolved CO_2. Listed in Table 1.5 are some of the parameters considered in various design of various miniature PBRs. The most commonly used small-scale systems are briefly described in the sections below.

At present illuminated shake flasks are most commonly used for microalgae cultivation. These are typically operated with working volumes between 25 - 1000 mL in 250 – 2000 mL Erlenmeyer flasks (Büchs et al., 2001; Fernandes and Cabral, 2006). A well-lit shaker incubator provides light and mixing with a measure of temperature control. However, adoption of light emitting diode technologies and

42

Table 1.5: Comparison of different photobioreactor designs and their specific applications. The table highlights key design and operating features. Nomenclature: T = temperature, DOT = dissolved oxygen, OD = optical density, N/A = not applicable, N/R = not reported.

Photobioreactor Design	Total Volume/ Working Volume (mL)	No. of Parallel Units	Mixing Pattern / Stirrer Type / Agitation Speed / S/V Ratio	Aeration rate / Method	Mode of Operation	Lightening System	Online Monitoring	Max. Light Intensity ($\mu mol m^{-2} s^{-1}$)	Strain Type	Reference
(a) Cylindrical										
Cylindrical, externally illuminated PBR	2 L /1.8 L	1	Stirred tank/ Rushton stirrer with Stirrer/vessel ratio of 0.63 – 250 rpm	63mL/min / Air pump	Batch and Continuous	Warm white SMD-LEDs	T, pH, DOT, LI	5000/500Hz	*Chlamydomonas reinhardtii* wt	Jacobi et al., (2012).
Cuvette shaped commercial bioreactor converted to photobioreactor	0.35 L	2	Airlift 0	Mass controller/0.3 L.min^{-1}	Batch	LEDs/Blue-Red-white LED Arrays	T, pH, DOT, LI	3500	Cyanobacteria	Nedbal et al., (2008).
Novel stirred plate reactor. externally illuminated via optical fibre	3 L		Stirrer		Batch and continuous	150-Watt cold light reflector lamp	T, pH, DOT, LI	100 Light shutter generation	Axenic *Porphyridum purpuruem*	Csogor et al., (2001).
Cylindrical and Flat Torus PBR	5 L	1	Stirred vessel	NM	Batch, chemostat and continuous	55 (20 W, 12 V) halogen lamps	T, pH, DOT, OD	1000	*C.reinhardtii wild AH typr strain 137*	Takache et el., (2009).

Table continued on the next page

Table 1.5 Continued

Photobioreactor Design	Total Volume/ Working Volume (mL)	No. of Parallel Units	Mixing Pattern / Stirrer Type / Agitation Speed / S/V Ratio	Aeration rate / Method	Mode of Operation	Lightening System	Online Monitoring	Max. Light Intensity (μmolm^{-2}s^{-1})	Strain Type	Reference
(b) Bubble Columns										
Vertical rectangular slab shaped PBR (Illumination chamber)	80 cm^3 / 52 cm^3	1	Internal sparging	100 mLmin^{-1}	Batch	LED using gallium aluminium	T, pH, DOT	23 mWcm^{-2}	*C. vulgaris* UTEX 398	Lee & Palsson., (1994).
Glass bubbled tube	600 mL / 500 mL		Air bubble		Batch	Day light fluorescent tubes	T, pH, DOT	200	Multiple strains	Rodolfi et al., (2008).
(c) Shake Flasks / Flat Panels										
FAP Photobioreactor	20 - L	6	Air bubble	0.5 LL^{-1}min^{-1}	Batch	Day light fluorescent tubes	T, pH	115	*Eustigmatophyte nannochloropsis*	Rodolfi et al., (2008).
GWP Photobioreactor	110 L	4	Airlift	0.3 LL^{-1}min^{-1}	Fed-Batch		N/R			Rodolfi et al., (2008).

better control technologies for shaking incubators are enabling more efficient phototrophic cultivation. Some of the advantages of phototrophic shake flask systems include; ease of operation, reduced cost and adequate information on performance characteristics (Büchs et al., 2000; Doig et al., 2005; Tan et al., 2011).

Recent advances have improved the amount of process information obtainable from shake flask systems. Integration of probes and sensor spots such as pH, optical density, oxygen uptake rate (OUR), Carbon dioxide transfer rate (CTR) and respiratory quotient (RQ) have enabled real-time data acquisition (Betts and Baganz, 2006). However, for phototrophic cultivation, more investigation is required into the development of probes that are not light sensitive.

1.3 Single-Use Bioreactors

Single-use bioreactors (SUB) were first developed in the 1990's for animal cell culture and comprise of a flexible plastic bag (Eibl et al., 2009; Eibl et al., 2010; Singh, 1999) made from approved Food and Drug Administration (FDA) polymeric materials. They are however made of specific components such as the bag film, stirrers, spargers, filters, tubes, connectors, and clamps. Once assembled, they are pre-sterilised by gamma irradiation before delivery to end users (Weber et al., 2013). The pre-sterilised SUB come in different geometries from L to m^3 scale (Lopes, 2013; Shukla and Gottschalk, 2013). Furthermore, SU stirred tank reactors are being currently developed with operations similar to conventional stirred tank bioreactor. Power input into the SU-system is achieved by either mechanically or pneumatically or a combination of the two (Löffelholz et al., 2013).

Mixing is achieved by rocking of the bioreactor bag on a platform which induces a wave motion in the fluid (Eibl et al., 2009; Lopes, 2013). The SUB is made from modern bags consists of three well-defined layers with specific functions such as; support, thermal resistance, strength and chemical resistance (Löffelholz et al., 2013; Meusel et al., 2013). Nonetheless, advantages over conventional stainless steel bioreactors have been identified in terms of applications (Löffelholz et al., 2013; Szarafinski, 2013).

The use of SUB has been known to release leachates and extractables into the broth. These are caused by continuous mixing and cells interactions with the inner layer of the bag. Studies into the amount of leachables and extractables becomes necessary if the application is designed for high-grade therapeutics and biopharmaceutics (Löffelholz et al., 2014; Steiger and Eibl, 2013). The impact of high light intensity on the leachates and how these affect photosynthetic microalgae cultivation has not yet been reported. Other limitations that have been improved include insertion of probes for online monitoring of culture performance (Hillig et al., 2014a) and possible biosafety concerns (Merseburger et al., 2014; Weber et al., 2013).

Recently developed SUB comprises of sensor patches that are installed and pre-sterilised with the cultivation bag. These bags compares with modern single-use sensor technology which ensures the same level of control that traditional sensors possess (Hillig et al., 2014a). However, reusable probes can be inserted into SUB through sensor ports for a culture control.

At present, commercially available working volumes range between 2 - 2000 L (Shukla and Gottschalk, 2013). The system accessories include, a stainless steel bag holder which supports the flexible, single-use cultivation chamber during cell culture, a direct digital-control unit (DCU), and a single-use cultivation chamber (CultiBag STR) (Weber et al., 2013) as shown in Figure 1.5. The design of the cultivation chamber was similar to a conventional STR with similar impeller types, convex bottom and a harvest port at the base. Likewise, the aspect ratio (H/D) and the ratio of the impeller's diameter to the bag's diameter are 1.8:1 and 0.38 respectively. Base on all these similarities, the risks of process transfers between existing steel and SU Biostat STR system is considered to be minimal (Lopes, 2013; Weber et al., 2013).

1.3.1 Bioreactor Engineering Characterisation

Conventional bioreactors SUB need to be characterised in terms of impeller tip speed, specific power input per volume, mixing time, and $k_L a$ (Löffelholz et al., 2013; Weber et al., 2013). These parameters are often used as basis for predictive scale-up. Methods for engineering characterisation of single-use systems are those already established for conventional bioreactors namely: (1) parametric, (2)
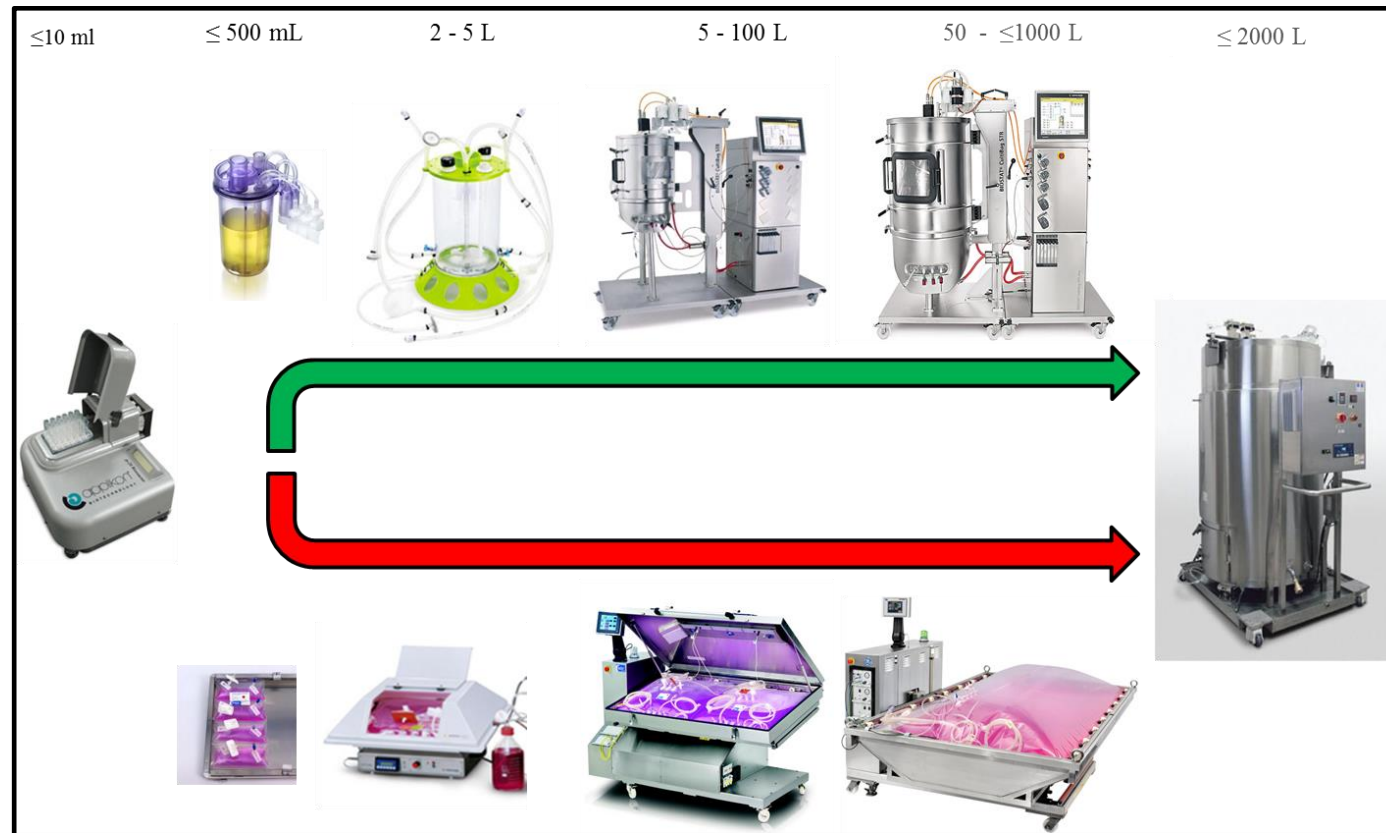
Figure 1.5: Representation of the different SUB geometries used at different operational scales. The green line represents stirred bioreactor systems while the red line represents rocked mixing platform. (All figures adapted from the following company's webpage; Applikon biotechnology, TAP Biosystems, Millipore, Sartorious, Thermoscientific, GE Life Sciences).

experimental and (3) computer-based numeric analysis. Application of each method further enhances understanding of system performance (Löffelholz et al., 2013).

Volumetric mass transfer coefficient ($k_L a$): Oxygen is sparingly soluble in a culture broth at the conditions normally used for cell cultivation. As a result, oxygen supply to growing cells is usually a rate-limiting operation as scale increases (Kirk and Szita, 2013). It is important for the oxygen or carbon dioxide requirements of the cells to be met by the gas-liquid transfer rate of the bioreactor system (Weber et al., 2013). The oxygen transfer rate (OTR) is typically expressed as the overall volumetric mass transfer coefficient $k_L a$ which is determined by different methods (Kirk and Szita, 2013; Löffelholz et al., 2013; Suresh et al., 2009). However, conditions involving temporary depletion of dissolved oxygen during aerobic fermentations or inadequate CO_2 during photosynthetic culture could result in irreversible cell damage and significant lower productivity (Suresh et al., 2009).

Nevertheless, maintaining constant $k_L a$ during process scale-up is one basis for scale translation. This can be achieved in different sized vessels using different correlations (Linek et al., 2004; Zhu et al., 2001). $k_L a$ values can either be estimated from correlations (Table 1.6) or measured experimentally by various methods as described below:

- **Static gassing out:** Based on the measurement of the DO in the absence of biomass, Nitrogen is first introduced to eliminate oxygen in the fluid before sparging with air.
- **Sulfite method:** Based on the chemical reaction of sulphite (SO_3^{2-}) to (SO_4^{2-}) in the presence of DO. The reaction is catalysed by copper, ferric, cobalt or manganese ions.
- **Dynamic gassing out:** Based on the measurement of DO during active cell growth.

Fluid hydrodynamics: Fluid hydrodynamics in stirred bioreactors have been described based on experimentally established flow regimes which are: laminar, transitional and turbulent flow. The dimensionless Reynold's number (Re) estimation for single-use and reusable bioreactors have been identified to be related to flow regime. This can be predicted using model described in Table 1.6 (Löffelholz et al., 2013).

Table 1.6: Summary of litreature correlations and methods available for bioreactor engineering characterisation for stirred, rocked or orbitally shaken bioreactors (Büchs et al., 2001; Kauling et al., 2013; Löffelholz et al., 2013; Marques et al., 2010; Oncül et al., 2009; Raval et al., 2007).

Engineering characterisation of single-use bioreactor/photobioreactors			
Methods	**Mathematical models**		
Parametrical	**Stirred**	**Wave-mixed**	**Orbital shaken/Transient rotatory**
Flow regime	$Re = \dfrac{\rho_L N d_a^2}{\eta_L}$ $Ne = \dfrac{P}{\rho_L N^3 d_a^5}$	$Re_{mod} = \dfrac{V k C \rho_L}{\eta_L (2h + B)}$	$Ph = \dfrac{d_o}{d}\left\{1 + 3\log_{10}\left[\dfrac{\rho(2\pi n)d^2}{4\eta}\left(1 - \sqrt{1 - \dfrac{4}{\pi}\left(\dfrac{V_L^{1/3}}{d}\right)^2}\right)^2\right]\right\}$ $Ph > 1.26$
Fluid velocity	$\mu_{max} = \mu_{Tip} = \pi N d_a$		$U_{max} = U_{max,BaySHAKE} = \pi N d_v$ $u_{max} = U_{max,Vibromix} = \gamma \omega_\gamma \cos(\omega_\gamma dt)$
Superficial gas velocity	$U_G = \dfrac{V_G}{A}$		
Power consumption	$\dfrac{P}{V} = \dfrac{(M - M_d)2\pi N}{V}$	NA	$\dfrac{P}{V} = Ne'\rho\dfrac{N^3 d^4}{V^{\frac{2}{3}}} = C_3\rho\dfrac{N^3 d^4}{V^{\frac{2}{3}}}\mathrm{Re}^{-0.2}$
Torque	$-mC_p\dfrac{dT_E}{dt} = UA_H(T_E - T_o) - P$ $P_o = N_p\rho N^3 T^5$	NA	$-mC_p\dfrac{dT_E}{dt} = UA_H(T_E - T_o) - P$

Continued on the next page

Table 1.6 Continued

Engineering Characterisation of single-use bioreactor/photobioreactors			
Methods	**Mathematical models**		
Parametrical	**Stirred**	**Wave-mixed**	**Orbital shaken/Transient rotatory**
Mixing time distribution	$H(t) = \dfrac{C\tau,o - C(t)}{C\tau,o - C\tau,\omega}$	$H(t) = \dfrac{C\tau,o - C(t)}{C\tau,o - C\tau,\omega}$	$H(t) = \dfrac{C\tau,o - C(t)}{C\tau,o - C\tau,\omega}$
	Residence time method $\bar{t} = \dfrac{\bar{V}}{\bar{V}}$		
Volumetric mass transfer coefficient	$k_L a = C_1 \left(\dfrac{P}{V}\right)^{C_2} \left(V_g\right)^{C_3}$		
Sulphite-method	$SO_4^{2-} + 0.5O_2 \xrightarrow{Cu^{2+},Fe^-,Mn^+,Cu^+} SO_4^{2-}$		
Respiratory method	$\dfrac{dC}{dt} = OTR = k_L a(C^* - C)$	$\dfrac{dC_L}{dt} = OUR = -qO_2 Cx$	$q_{O2}C_x\Delta t + \Delta C_{L,O2} k_L a(C^*_{L,O2} - C_{L,O2})\Delta t$

All symbols are defined in the nomenclature.

Mixing time determination: Successful operation of bioreactor systems depend on the creation of homogenous cell suspensions throughout the cultivation period. It is important to prevent poor mixing which results in formation of pH, biomass and nutrient gradients thereby reducing cell growth and protein expression. Mixing time could be determined using different methods such as iodometry-decolorisation or neutralisation based on redox reaction (Betts et al., 2014). Other methods include conductivity method, optical or visual technique using high speed camera, residence time distribution and sensors which measures at least one physical component (John Bett).

Superficial gas velocity: For the prediction of liquid dispersal in single-use bioreactors, the calculated superficial gas velocity (U_G) is necessary for an aerated process. The correlation for U_G is shown in Table 1.6. For turbulent flow regime, U_G has a direct influence on the bubble diameter (Löffelholz et al., 2013)

Specific power input: Often used as a scale-up criterion, specific power input is a well described parameter for understanding bioreactor operations. One of the standard methods for determining specific power input in the STR is the torque which is an indirect determination of the power input for mechanically driven systems. According to Weber et al., (2013), the power input for most STR is within the range of 1-220 Wm^{-3} and is dependent on operation scale, impeller configuration and rate of agitation. Other methods used for determining the power input include: temperature and numerical dimensionless correlations (Table 1.6). Estimation of the power input enables the prediction of the Newton number (Ne) also called dimensionless power number, the specific power input (P/V), the power input coefficient (C_P) and the Kolmogorov length scale (Büchs et al., 2000a; Büchs et al., 2000b; Doran, 1995; Löffelholz et al., 2013).

Fluid velocity: Calculation of fluid velocity is an important bioprocess parameter that is dependent of the bioreactor type and design. It refers to the maximal fluid velocity (u_{max}) generated by the agitation system (especially STR) and is influenced by the diameter of the agitator, cultivation vessel and the support container or tray dimensions (Löffelholz et al., 2013).

1.4   Scale-up of Microalgae Cultivation Processes

1.4.1   Concept of Predictive Scale-up

Scale-up methods normally rely on regime analysis (Löffelholz et al., 2013) and the maintenance of key engineering parameters, such as $k_L a$, constant at increasing scales of operation (Islam et al., 2008). The early traditional methods based on geometry similarities are less effective as the process scale increases from micro to industrial. Large-scale operations are characterised by significant changes in vessels configuration, number of accessories required, increased process parameters and huge economic implications. Other approaches suggested for scale-up include fundamental methods, semi-fundamental methods, dimensional analysis and rule of thumb according to Oosterhuis and Kossen (1981). Realistically, determination of scale-up criteria for a given process may require a combination of more than one criterion in order to satisfy the required optimum scale-up criteria.

1.4.2   Strategies for Predictive Scale-up

No generic approach or strategy has been developed for bioprocess scale-up. However, microalgae cultivations are affected by various parameters of which the relevant ones for phototrophic cultivation include carbon dioxide, water, minerals, and light while heterotrophic requires a carbon source with sufficient aeration. Others are categorised under process, biochemical and physical parameters shown in Figure 1.6. The overall effect of individual factor on the overall productivity and optimum performance of growth system depends largely on the mode of cultivation and combination of different factors as shown on Figure 1.6.

Stanbury et al. (1995) identified the following as critical parameters that have direct impact on the scale of operations: Nutrient availability, temperature, dissolved carbon dioxide concentration, foam production, hydrodynamic shear, pH, and dissolved oxygen concentration. While these remain valid for heterotrophic cultivation of microalgae, phototrophic culture of microalgae requires parameters such as light intensity and photobioreactor geometry design.
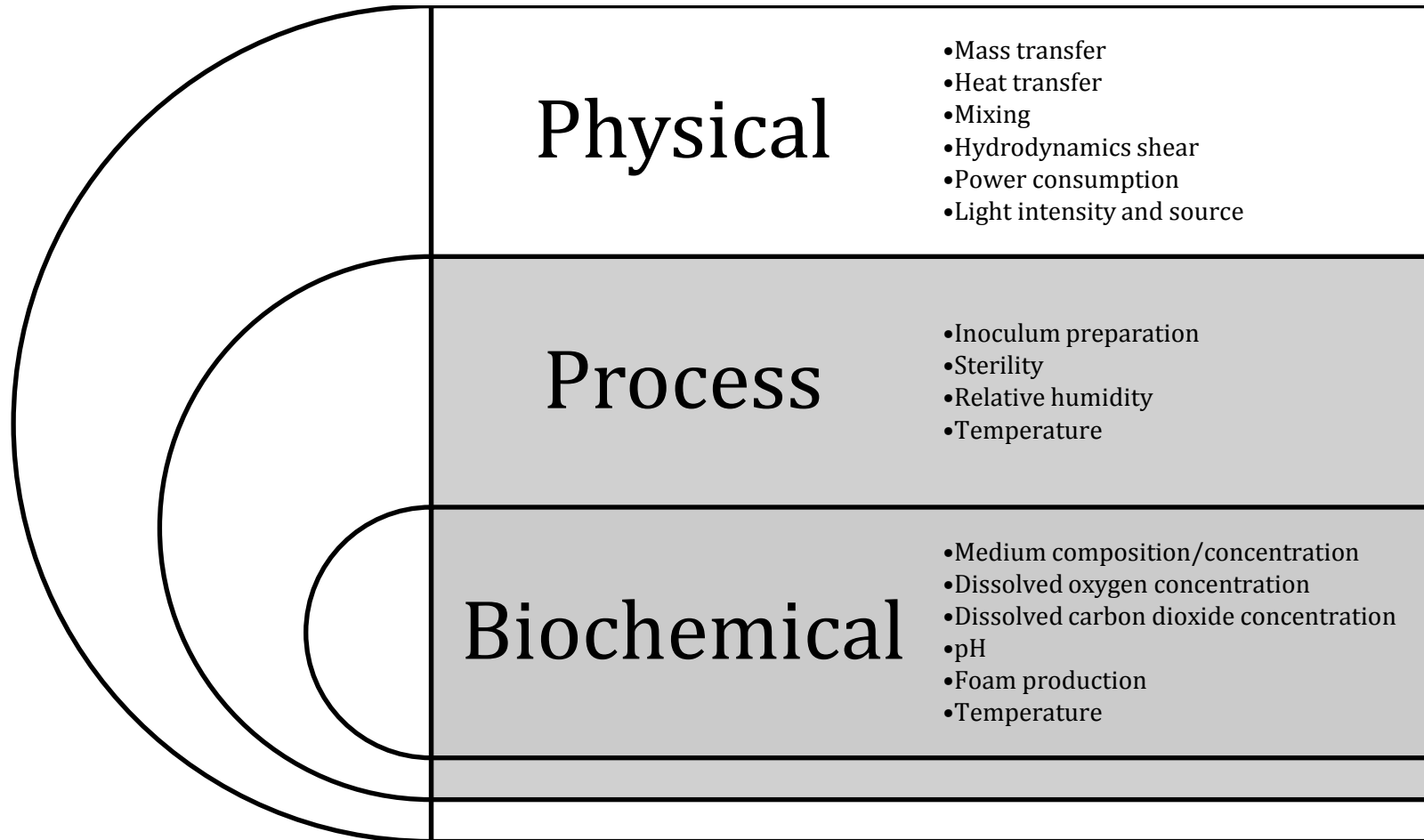
Figure 1.6: Key parameters affecting microalgae bioprocess development.

1.4.3 Microalgae Bioprocess Scale Translation: Scale-out or Scale-up?

In the recent time, studies have been ongoing on the most economically viable route for microalgae bioprocess translation from laboratory to large-scale industrial production. Two key strategies that are readily available are the scale-out and scale-up options. The scale-out option involves replication of a singular well characterised module in parallel ensuring all engineering conditions are kept similar, and the final product pulled together into a common tank for downstream processing. This is quite often applicable to single-use systems that are currently under development stage to the maximum working capacity of 2000 L as previously discussed in Section 0.

Over the years, scale-up criteria have been established for microbial bioprocessing from micro to industrial scale and these are quite similar to heterotrophic cultivation of microalgae as highlighted on Figure 1.7. Some of the listed parameters have been discussed in Section 1.3.1.

Phototrophic cultivation scale-up criteria differ significantly due to light requirement being critical to its operation. As highlighted in Figure 1.7, light intensity, path length and saturation are very key. In addition are $k_L a$ and mixing rate. For externally illuminated photobioreactor, photobioreactor surface area to liquid volume is another parameter that has been proposed for scale-up irrespective of photobioreactor geometry.
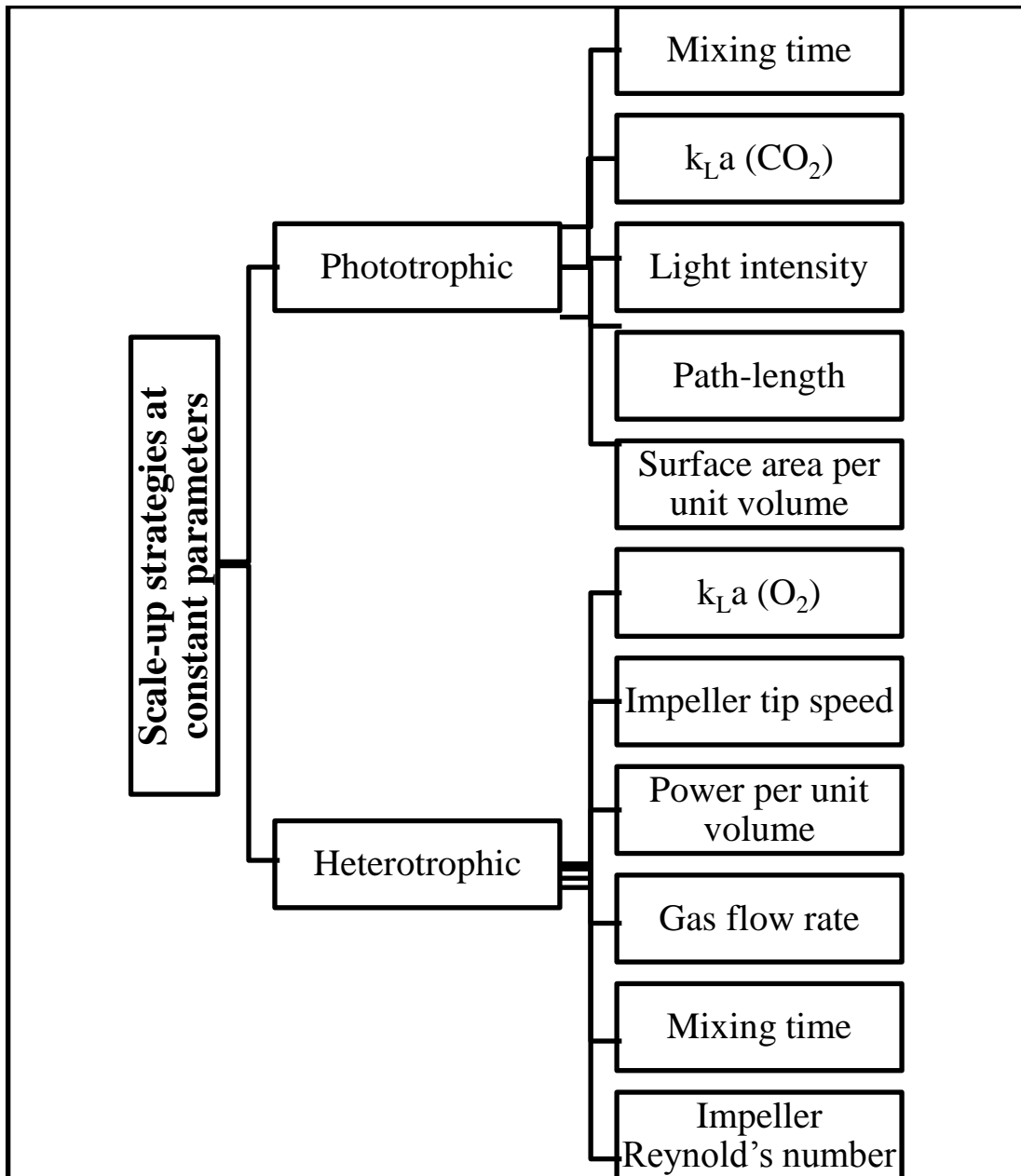
Figure 1.7: Classification of different engineering parameters for scale-up of microalgae cultivation either phototrophically or heterotrophically.

1.5   Aims and Objectives

The aim of this thesis is to establish a novel photobioreactor technology platform for early stage evaluation of microalgae cultivation under phototrophic conditions. The approach taken will demonstrate the utility of the platform for strain selection, optimisation and scale-up of culture conditions and also illustrate the wider application of the technology for heterotrophic cultivation of microalgae. Recent advances in microscale technologies as described in Section 1.2.4 are finding increasing application with microbial and mammalian systems. It is therefore timely to consider creating similar miniature photobioreactor technologies for microalgae cultivation. It is important that such miniature systems are well characterised in engineering terms (Section 1.3.1) in order to enable high-throughput parallel evaluation of culture conditions and their subsequent scale-up. To date there has been no publication in the scientific literature on miniature PBr technologies and just one describing the application of miniature bioreactors for heterotrophic cultivation of microalgae.

Within the context of this work, *C. sorokiniana* will be the main test strain used. The various bioreactor systems established will be evaluated in terms of cell growth kinetics and their relationship to the engineering conditions in each system. The work will also investigate the kinetics of various bioproducts formation including coloured pigment, total lipids and specific fatty acid methyl esters in relation to production of both biofuels (Section 1.1) and higher value products (Section 1.1.2). The specific objectives of the investigation are summarised below:

- The initial objective is to design and fabricate a novel prototype mPBr and then scale it out to a 24-well mPBr format. These systems will be characterised by studying the mixing efficiencies, oxygen transfer capabilities and liquid phase hydrodynamics. They will subsequently be used for the culture of *C. sorokiniana* to examine the impact of the engineering environment on growth and product formation and to demonstrate the utility of the platform for determination of optimal growth conditions. This work is presented in Chapter 3.

- Next a novel, orbitally shaken SUPBr platform will be developed and characterised for microalgae cultivation at laboratory scale. The engineering characterisation study will include visualisation of fluid flow and mixing behavior and quantitative evaluation of fluid flow regimes at different shaking frequencies. Again, the impact of this novel engineering environment will be investigated using *C. sorokiniana* as the test organism. This work will also consider criteria for the predictive scale-up of culture kinetics between the mPBr and the SUPBr. This work is presented in Chapter 4.

- The wider application of the miniature photobioreactor for heterotrophic cultivation of various microalgae strains will also be evaluated and scale-up criteria established from the mPBr to a conventional 7.5 L STR. This work is presented in Chapter 5.

- Finally, the wider implications of the findings will be considered and compared to data already published in the literature. Future developments will also be highlighted and appropriate recommendations made. This work is described in Chapter 6.

Chapter 2 describes the various bioreactor formats used, the strains used and their culture conditions as well as the various analytical techniques used for quantification of growth kinetics and bioproducts formation. The Appendices contain additional information on standard calibration curve, hydrodynamic studies in SUB and experimental set-up.

2.MATERIALS AND METHODS

2.1   Materials

2.1.1   Reagents and Suppliers

All reagents used in this work were obtained from Sigma-Aldrich (Dorest, UK), Fisher Scientific (Leicestershire, UK), VWR International Limited (Leicestershire, UK) and SLS Limited (Nottingham, UK) and were of 98% purity or greater. In addition, all gases used were supplied by BOC (London, UK) and were of the highest grade. Milli-Q and reverse osmosis (RO) water were used for all experiments.

2.1.2   Microalgae Source and Maintenance

The microalgae *Chlorella vulgaris, Chlorella protothecoides and Chlorella zofingiensis* were obtained from the culture collection of algae and protozoan (CCAP) (Scotland, UK). *Chlorella sorokiniana* was kindly provided by Dr. Saul Purton from the Institute of Structural and Molecular Biology, University College London. All strains were maintained on agar plates of different media compositions such as Tris-Acetate-Phosphate medium (TAP) (Kropats, 2007), *Euglena gracilis* medium (EG), three fold nitrogen bold basal medium containing vitamins (3N+BBM-V) as defined by the CCAP. All strains were streaked out on the three different media agar plates for short term (8-12 weeks) maintenance of cells and were incubated at 25 ℃ under 40 $\mu molm^{-2}s^{-1}$ light intensity. TAP media was adapted for *C. sorokiniana* and *C. prothothecoides* as reported in this work in the result Chapters. Nutrient agar slants stored at 4 ℃ in the dark were used for longer term maintenance of both strains (greater than 3 months).

2.1.3   Media Compositions

The media compositions used varied depending on experimental goals and the amount of individual constituents are detailed in Table 2-1. In general four different basal media were employed for C. sorokiniana cultivation: High Salt Medium (HSM), Bold Basal Medium (BBM), Tris-Base Phosphate Medium (TBP) and TAP.

Table 2-1: Media compositions used for cultivation of all *Chlorella* strains

Stock Solutions	Medium Components	TAP Media Concentration (gL^{-1})	Volume (mL) per Litre of Medium	TBP Media Concentration (gL^{-1})	Volume (mL) per Litre of Medium	HSM Media Concentration (gL^{-1})	Volume (mL) per Litre of Medium
5x Beijerinck's Solution	NH$_4$Cl	40.0	10.0	40.0	10.0	100.0	5
	CaCl$_2$ • 2H$_2$O	5.0		5.0		2.0	
	MgSO$_4$ • 2H$_2$O	10.0		10.0		4.0	
Phosphate Solution	K$_2$HPO$_4$ (anhydrous)	14.3	8.3	14.3	8.3	288.0	5
	KH$_2$PO$_4$ (anhydrous)	7.3		7.3		144.0	
Tris-Acetate	Tris-base	242.0	10.0	242.0	100.0	-	
	Glacial Acetic Acid (mL)	100.0		-		-	
Trace Elements Solution	EDTA-Na$_2$	50.0	1.0	50.0	1.0	50.0	1
	H$_3$BO$_3$ (boric acid)	11.1		11.1		11.1	
	ZnSO$_4$ • 7H$_2$O	22.0		22.0		22.0	
	MnCl$_2$ • 4H$_2$O	5.1		5.1		5.1	
	FeSO$_4$ • 7H$_2$O	5.0		5.0		5.0	
	CoCl$_2$ • 6H$_2$O	1.6		1.6		1.6	
	CuSO$_4$ • 5H$_2$O	1.6		1.6		1.6	
	(NH$_4$)$_6$Mo$_7$O$_{24}$• 4H$_2$O	1.1		1.1		1.1	
Enriched Media	Glucose	5 – 50		5 – 50			
RO Water			Up to 1 L		Up to 1 L		Up to 1 L

2.2   Novel (Orbitally Shaken) Miniature Photobioreactor Designs

2.2.1   Design of Miniature Photobioreactor (mPBr) Prototype

The miniature photobioreactor (mPBr) prototype was designed to be geometrically similar to a single well from a conventional, pyramidal base 24–well microtitre plate. A transparent Perspex was chosen for construction due to its optical and mechanical properties such as; light transmittance of > 92% with minimal light diffractions and intensity loss, refractive index of 1.92, tensile strength of > 62 MPa, and softening temperature of > 110 °C (Bayplastics Datasheets, 2014). The light path across the well is 16.5 mm similar to a maximum liquid height of 17 mm as shown in Figure 2.1. The well wall thickness was 2 mm and the typical working volume was 4 mL.

Mixing was achieved using an incubator shaker (Infors HT, Switzerland) equipped with temperature, humidity and CO_2 sensors coupled to a control unit. CO_2 levels were controlled by mixing air with 100% CO_2 from a cylinder. The mPBr was mounted on the shaking platform using a sticky mat (Infors HT, Switzerland). The orbital shaking diameter was 25 mm for all experiments with shaking frequency varied between 250 to 400 rpm. Each well was illuminated by a cool white LED attached to one of the sides. The total surface area available for light absorption was 272.3 mm^2. Light intensity from the LED was 160 $\mu molm^{-2}s^{-1}$ and was constant for all cultures.

Gas mass transfer was achieved in two ways. The first was head space aeration with CO_2 transfer into the liquid phase achieved through mixing by orbital shaking of the platform. A thin semipermeable membrane (VWR International Ltd, Leicestershire, UK) that allows air passage without microbial contamination was used as a seal on the wells with incubator headspace providing the required CO_2 for cultivation.
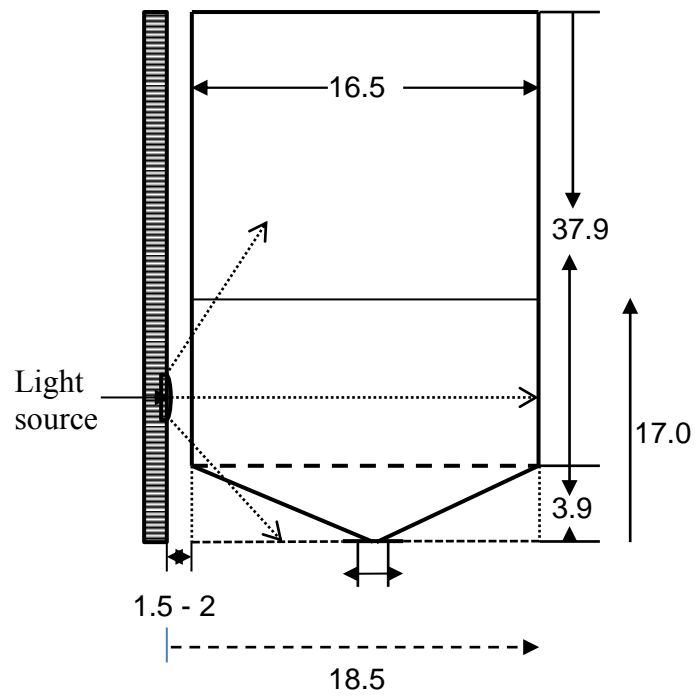
Figure 2.1: Diagram showing geometry and dimensions of a single unit from the prototype mPBr. All measurements are in mm.
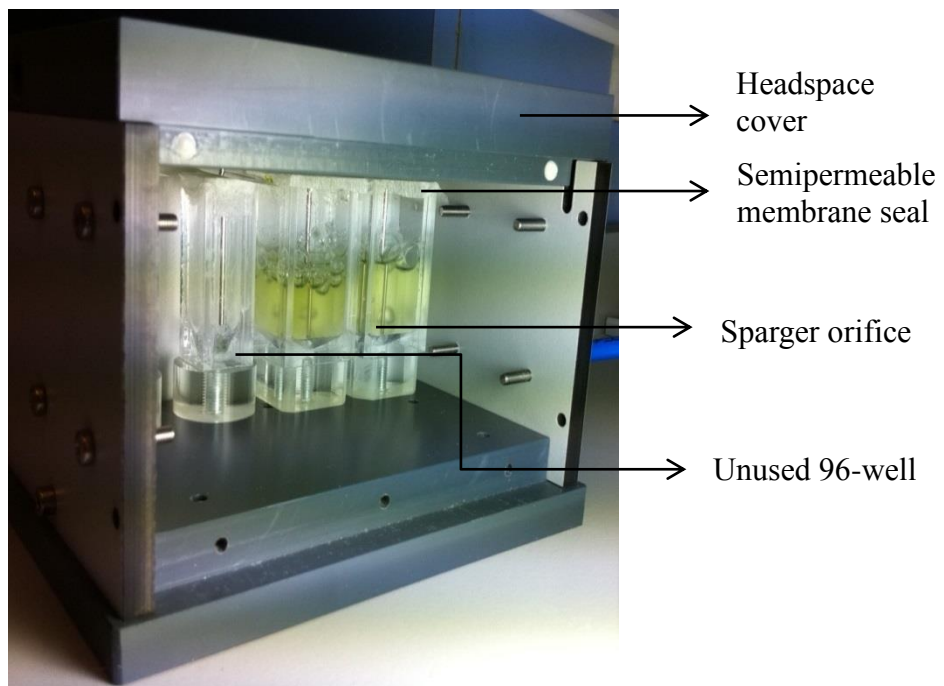
Figure 2.2: Photograph of the prototype twin-well mPBr with air sparger and semipermeable membrane seal.

Alternatively, each well of the mPBr was equipped with a stainless steel tube having a 4.90 mm internal diameter orifice that sparges CO_2 into the liquid phase at the base of the well. When used, the gas flow rate is manually controlled by a rotameter (Fisher Scientific, UK) over the range 0 – 200 mLmin^{-1}. Air was supplied from a cylinder with pre-defined CO_2 content. As shown in Figure 2.2, the individual mPBr wells were not equipped with pH or optical density (OD) probes with these parameters having to be measured offline. Temperature and relative humidity were measured and controlled within the shaking incubator chamber and were verified by control measurements.

2.2.2   Design of Novel Shaking Platform

A novel shaker was designed to house six, 24-well parallel mPBr plates with homogeneous light intensity across the shaking platform surface as shown in Figure 2.3. The high power warm white LEDs utilised had a variable wavelength from 450 – 620 nm and also provided variable light intensity of up to 2400 µmolm^{-2}s^{-1} at 5 cm distance. This distance allowed between the LED unit and the rotating platform ensures safe operation. Excess heat generated by the LED panel was removed by cooling water circulated around a refrigerated circulating water bath (Grant Instruments, Cambridge, UK). A Quantum Li-Cor light meter (Li-Cor Bioscience, Cambridge, UK) was used to monitor the light intensity throughout all experiments.

2.2.3   Scale-Out, Parallel 24–Well mPBr Design

In order to translate the engineering conditions in the twin-well mPBr to a parallel, 24-well mPBr, the light path-length and total surface area available for light absorption was kept constant. Using the shaking incubator platform described in Section 2.2.2, the light source was positioned below the wells compared to the side illumination described in the twin-well prototype. Three geometries of 24-well mPBr were employed having a pyramid base, a round base and a square base as shown in Figure 2.4. The square plates (with transparent base) had opaque walls, preventing well-to-well light diffraction, while the two other plate designs had translucent walls.
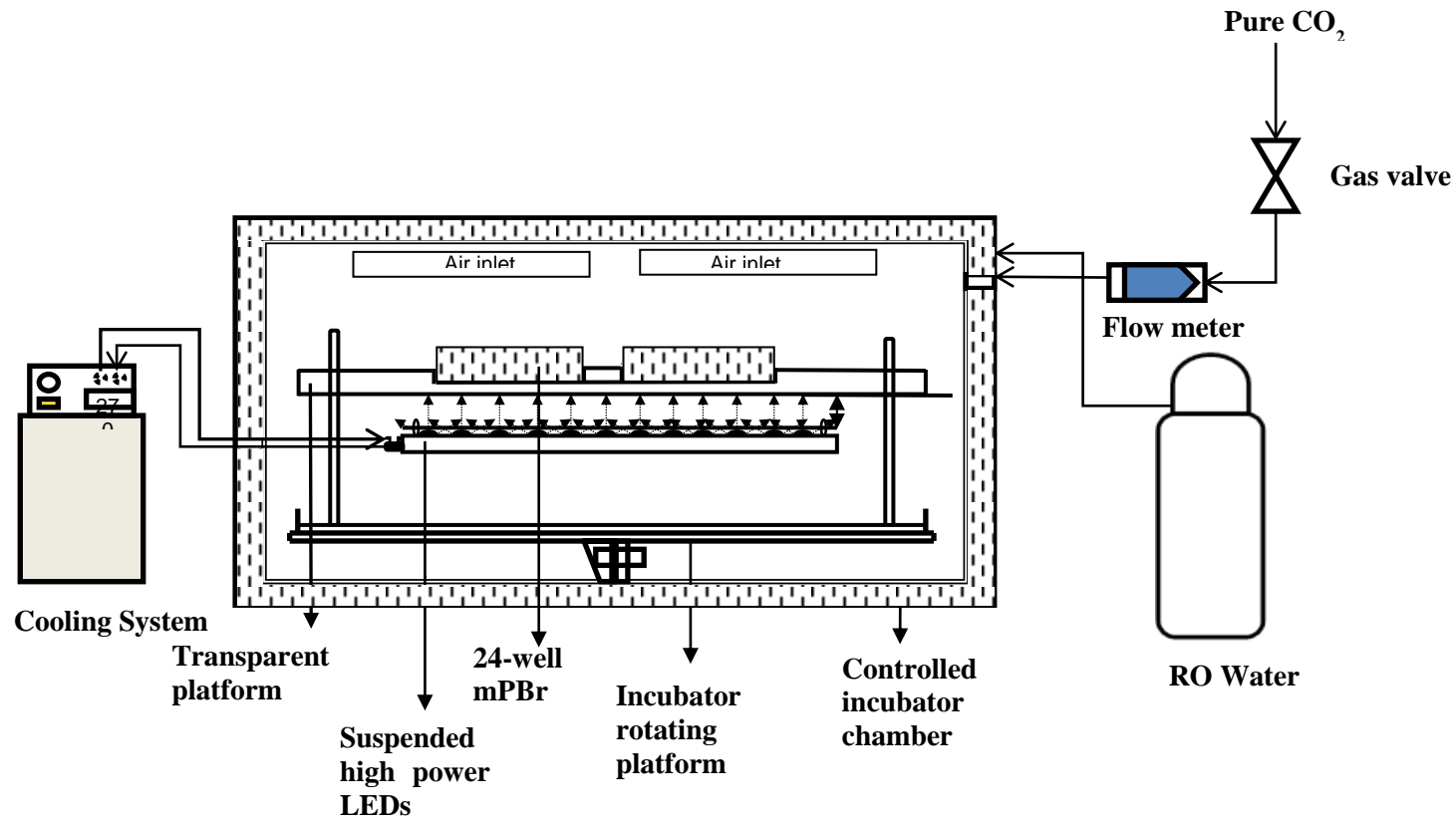
Figure 2.3: Experimental set-up showing the novel shaking platform for parallel, 24-well mPBr experiments. RO water was used for humidity control.
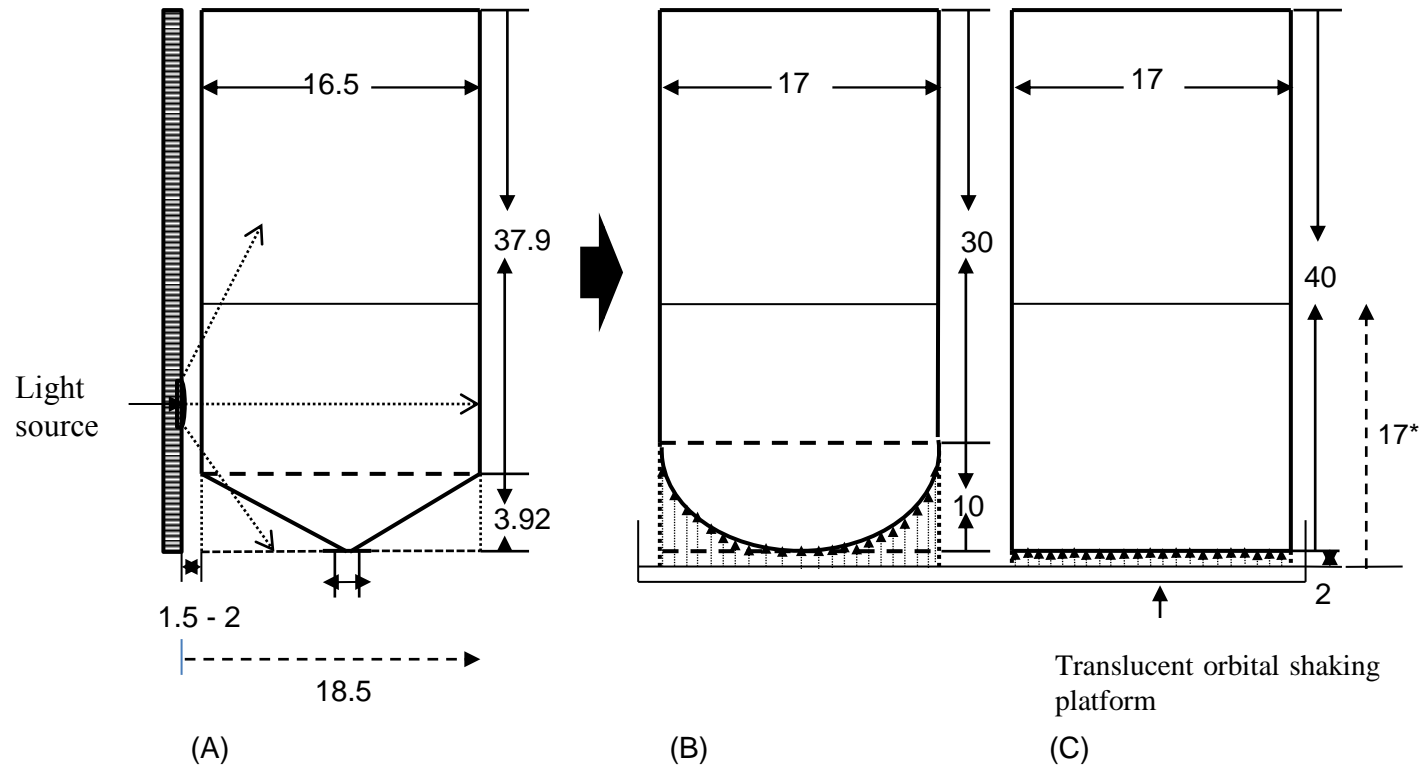
Figure 2.4: Schematic diagrams of the prototype mPBr and scale-out into the different 24-well mPBr geometries investigated: (A) pyramid base from prototype with side illumination, (B) round base having highest absorptive surface area with translucent walls, (C) square base having equal light path-length but least absorptive surface area with opaque walls. Arrows indicates distance from the source of light. All units in mm.

2.3 Single-Use (Orbitally Shaken) Lab Scale PBr

2.3.1 Platform Design and Experimental Set-up

The single-use photobioreactor (SUPBr) set-up was based on a standard 2 L CultiBag[TM] RM (Sartorius Stedim Biotech, Germany) made from flexible transparent three-layer polymeric material (Section 0). This was fixed on an orbitally shaken incubator platform (Infors, Switzerland) lit by high power LEDs as described in Section 2.2.2. The SUPBr with working volume of 0.5 − 1 L, was positioned perpendicularly to the clockwise orbital shaking as shown in Figure 2.5. The CultiBag[TM] was held in place at each end using a custom-made clamping arrangement as shown in Figure 2.6. The SUPBr had an illuminated surface area (A_{SUPBr}) uninflated of 0.15 m^2, with average height of 172 mm when inflated without liquid. Shaking frequencies were varied between 40 - 220 rpm at shaking diameters of 12.5, 25.0 and 50.0 mm.

2.3.2 SUPBr Control

The SUPBr was aerated by a continuous flow of gas through the headspace above the liquid. Well controlled air flow meters (Fisher Scientific, UK) and pressure valve regulators (Norgen pressure gauge, UK) were used to control the gas exchange in and out of the SUPBr. A pre-mixed gas comprising 2% CO_2 in air was piped into the SUPBr and the headspace gas exchange was kept at a constant 2 mLmin^{-1} throughout the experiment. The heating jacket was used to prevent filter blockage due to condensation. Other growth conditions such as temperature, light intensity and shaking frequencies were controlled within the incubator as described in Section 2.2.2.
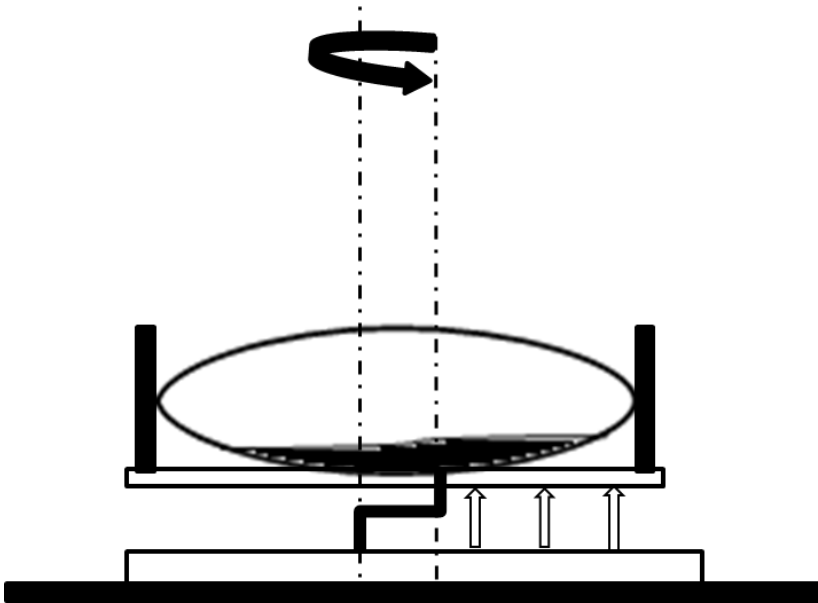
Figure 2.5: Schematic illustration of the orbitally shaken SUPBr platform. Arrows indicate the approximately constant distance from light source compared to rocked single-use bioreactor configurations used for mammalian cell culture.

Heating jacket

Gas exchange ports and tubing

SUPBr platform clamp edge

High power LED
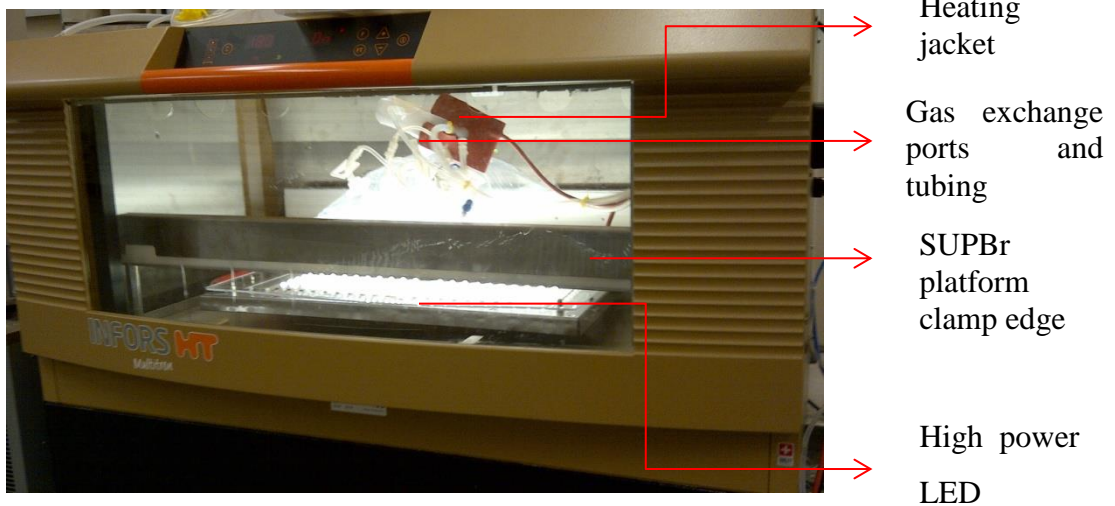
Figure 2.6: Photograph of the SUPBr mounted within the photo-incubator shaker set-up showing the SUPBr on a rotary shaking platform.

2.4 Engineering Characterisation of Photobioreactors and Bioreactors

2.4.1 Quantification of Oxygen Mass Transfer Rates and k_La

Oxygen mass transfer coefficient, k_La, values in orbitally shaken bioreactors (shake flasks and 24 SRW plates) and stirred tank bioreactors were determined using the dynamic gassing out technique (Betts et al., 2013). Prior to each experiment, a fluorescence-based oxygen micro-sensor probe (Presens, Germany) was calibrated between 0% (using 1% v/v sodium thiosulphate dissolved in RO water) and 100% air. All experiments were carried out at a constant temperature of 28 ^{o}C at varying shaking frequency and stirrer speed (100 - 950 rpm). Aeration rate for the 7.5 L stirred tank bioreactor was 1 - 2 vvm using atmospheric air. In all the bioreactors, the volumetric oxygen mass transfer coefficient, k_La, was determined from the measured dissolved oxygen-time profiles (Figure 2.7). The Micro TX3 software attached to the sensor contains an algorithm for averaging percentage dissolved oxygen readings over four repeat readings per time period. The percentage oxygen saturation plotted against time was fitted on semi-log graph and the gradient equals to k_La. A similar technique could be performed for measuring the rate of CO_2 transfer subjective to using an appropriate probe. In order to account for the probe response time for oxygen, Equation 2.1 (Dunn and Einsele, 1975) was used,

$$C_p = \frac{1}{t_m - \tau_p} \left[t_m \exp\left(\frac{-t}{t_m}\right) - \tau_p \exp\left(\frac{-t}{\tau_p}\right) \right] \qquad\qquad 2.1$$

where, C_p is the normalised dissolved oxygen concentration measured by the probe at time t, t_m equals k_La^{-1} and τ_p is the probe response time. All gassing out experiments were performed in triplicates.
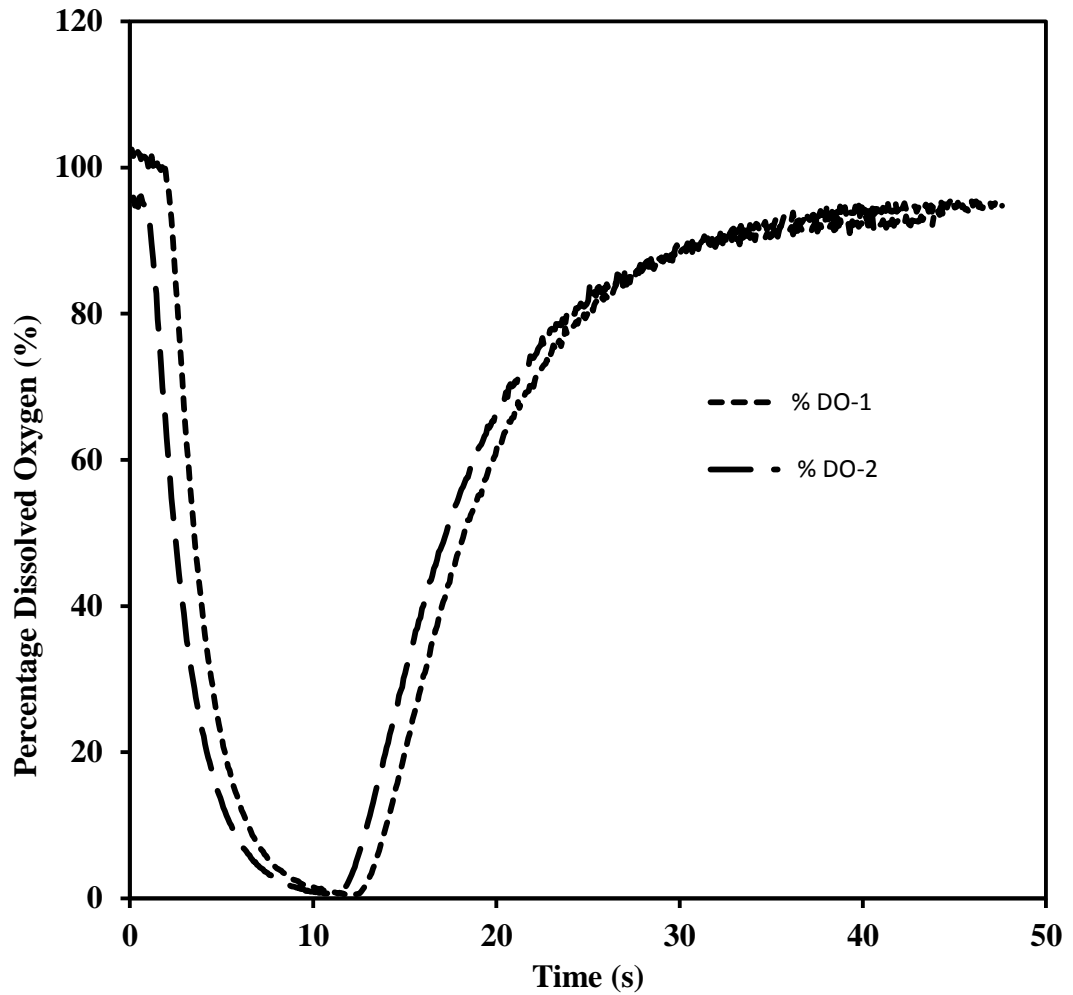
Figure 2.7: Typical dissolved oxygen–time profile for bioreactor k_La quantification. Data were obtained in a 250 mL shake flask bioreactor operated at a shaking frequency of 180 rpm and filled with 100 mL RO water. Curves represent two repeats under idnetical conditions.

2.4.2 Quantification of Evaporation Rates

The average evaporation rate across the parallel, 24-well SUPBr was determined by two methods: the first was by direct measurement of changes in mass and the second by OD measurement of a blue dye solution at 630 nm (Super Cook, Leeds, UK; at an initial concentration of 0.002%, v/v). To determine the evaporation rate in the 24-well mPBr, an individual well was filled with dye stock solution (4 mL fill volume), sealed with semipermeable membrane and shaken in the photo-incubator system at 32 °C, relative humidity 85% and 300 rpm at a diameter of 25 mm for 5 days. Light intensity conditions used for actual culture conditions were mimicked. The OD was determined for individual well and plates by transferring 1 mL of sample to a standard 1 mL acrylic cuvette and the absorbance measured using a spectrophotometer (Ultrospec 1100, Amersham Biosciences, UK). Measurements were blanked against 1 mL of RO water. Likewise, the weights of the plates were measured and evaporation rate calculated as shown in Equation 2.2,

$$\% \text{ evaporation} = \frac{W_{Initial} - W_{final}}{W_{Initial}} \times 100 \qquad\qquad 2.2$$

where $W_{initial}$ and W_{final} are the total mass of the fluid in all the wells before and after five days of incubation. Values presented here are based on triplicate measurements.

2.4.3 Mixing Time Quantification

The liquid phase mixing time, t_m, for all the systems used was determined by a standard pH-tracer method using a micro-pH probe (VWR International, UK). The probe position and height in the system was kept constant for all the experiments. The pH probe delivered an automated steady digital signal at a high frequency through a computer software program interfaced with a pH meter (Mettler Toledo, UK). Different concentrations of HCl and Sodium hydroxide (NaOH) (Sigma, UK), 0.025, 1 and 5 M were prepared and the fluid pH at the start was adjusted between pH 6.5 – 7.5. At the start of each experiment, the glass micro-pH probe was calibrated using standard buffers. For mixing time measurements as shown in Figure 2.8, pH fluctuations were recorded continuously after injecting 0.5% v/v of total working volume of known concentration of acid or base.

69
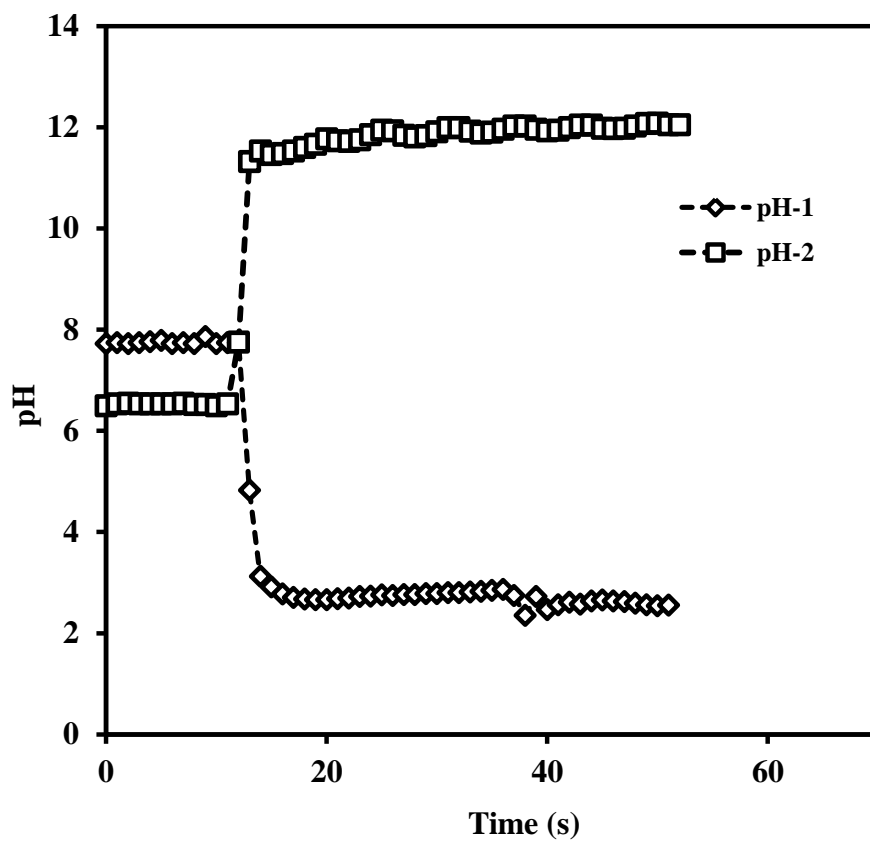
Figure 2.8: Typical pH–time profile for mixing time quantification. Data were obtained in a 2 L single-use bioreactor operated at a shaking frequency of 180 rpm and filled with 500 mL RO water. Curves represent two repeats at same conditions of adding acid and base respectively. For all conditions investigated the experiments were repeated four times.

The pH equilibration time was also detected using the pH-tracer programme by measuring pH change with time until it reached a steady value. All experimental runs were carried out in triplicate.

2.4.4   Visualisation of Fluid Hydrodynamics in the SUPBr

Investigation of fluid hydrodynamics in the orbitally shaken SUPBr was achieved using a DVR Fastcam (Photron, California, USA). This was mounted directly above the CultiBag at an inclination angle of 30 – 60 ° and the resolution was set at 640 x 480 pixels for all experiments. Two halogen red lamps (National Instruments, UK) were used to provide additional light for improved brightness and clearer focus. The camera was set to capture images at 125 fps over a period of 5 min, for each of the experimental runs. The images captured were stored for analysis using ImageJ software (http://rsbweb.nih.gov/ij/). Each experimental run was carried out by adding a food dye (2% v/v of the total working volume of RO water used) with an approximate injection time of 3 s (Figure 2.9).

2.4.5   Quantification of In-phase and Out-of-phase Phenomenon

 In-phase and out-of-phase flow phenomena were determined in the 2 L SUPBr using a different model of digital camera (Digital camera finepix, JX200, China) positioned perpendicularly to the longitudinal side of the SUPBr. The working fill volume (V_f) of 0.5 and the maximum liquid heights attained in the SUPBr were captured and processed as images using ImageJ software and normalised according to Equation 2.3. The normalised heights were thereafter plotted against corresponding shaking frequencies (f_o) at constant shaking diameter (d_o) (Figure 2.10).

$$H_N = \frac{H - H_o}{H_o}$$
$$\text{2.3}$$

where, H_o is the initial height of the fluid in the bag at no shaking and H is the maximum height gained at a given shaking frequency.

High speed camera

Flash

CPU-Monitor

SU-photobioreactor

Rotary platform

Shaker
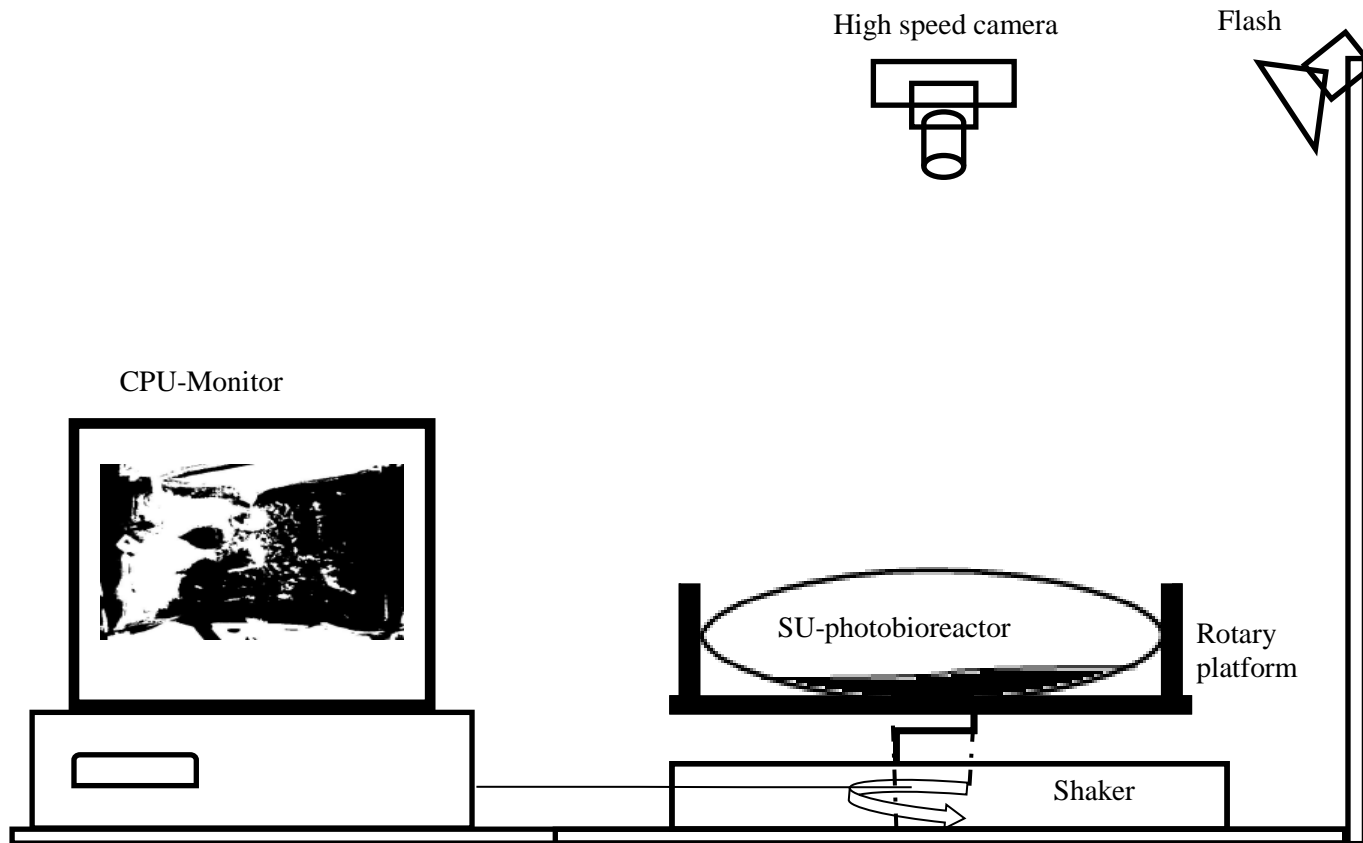
Figure 2.9: Experimental set-up for visualisation of fluid hydrodynamics and mixing time quantification.
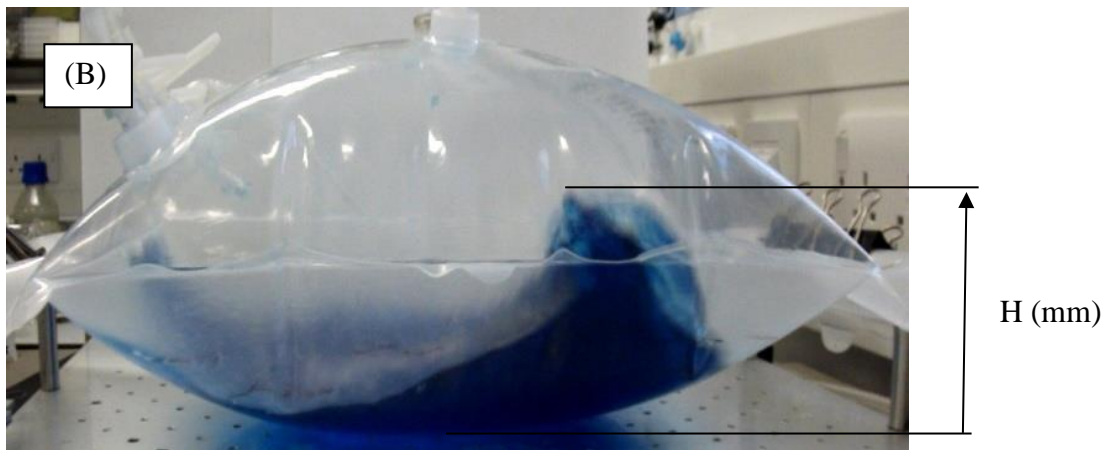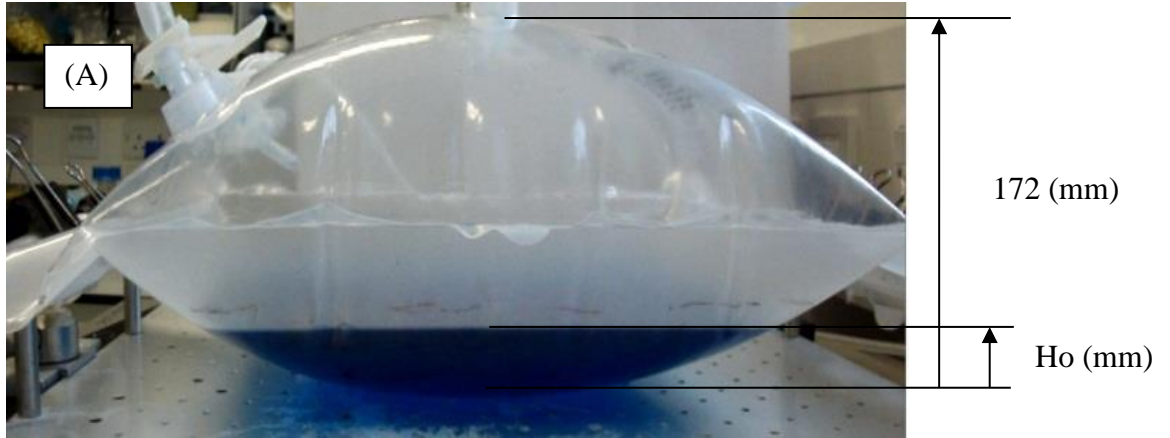
Figure 2.10: Example images from experiments used to explore in-phase and out-of-phase mixing in the SUPBr. (A) Showing the single-use photobioreactor before mixing commences and (B) image of liquid hydrodynamics and height attained at the experimental conditions: f_s = 130, V_f = 0.5 and d_o = 25 mm. H_o and H represents the height attained by the liquid before and during shaking respectively.

2.5 Phototrophic Cultivation Methods

2.5.1 Inoculum Preparation

The seed culture was inoculated from a *C. sorokiniana* stock maintained on nutrient agar slant at 4 °C into 50 mL TBP medium using 250 mL Erlenmeyer flasks. A Kuhner incubator shaker (Kuhner AG, Switzerland) operated at 180 rpm, 28 ± 3 °C, and with a light intensity of 55 $\mu molm^{-2}s^{-1}$ for 6 - 8 days was used for the cultivation. This was then repeated under the same conditions and allowed to grow for 4 days using 10% v/v inoculum before being used for bioreactor inoculation.

2.5.2 Cultivation in mPBr

The mPBr (prototype and 24-well) were aseptically filled with 4 mL working volume of medium and inoculated with ~ 5% v/v inoculum prepared as described in Section 2.5.1. Light intensity for the 24-well mPBr was varied while for the prototype mPBr it was kept constant. The CO_2 level was maintained between 2 – 20% in air. All experiments were carried out in batch mode with three replicates. Samples (400 μL) were withdrawn at 8 – 12 hr interval and stored at – 20 °C for analysis.

2.5.3 Cultivation in SUPBr

The 2 L SUPBr was aseptically filled with working fill volume fraction of 0.25 or 0.5 and inoculated with ~ 5% v/v inoculum prepared as described in Section 2.5.3. The SUPBr was illuminated at a fixed light intensity of 180 ± 20 $\mu molm^{-2}s^{-1}$ and aerated using enriched air with 2% CO_2 at a flow rate of 0.2 $Lmin^{-1}$. All experiments were carried out in batch mode at least in duplicate. Samples (4 mL) were withdrawn at 8 hr intervals and stored at – 20 °C for analysis.

2.6 Bioreactor Set-up for Heterotrophic Cultivation

2.6.1 Microwell Bioreactor

24-well standard round bottom plates (Sartorius Stedim Biotech, Germany) were used for the cultivation of the strain at microscale with total working volume of 4 mL (Figure 2.11 (A)). Mixing was ensured by an orbitally shaken incubator platform (Infors, Switzerland) depicted schematically in Figure 2.6. In order to ensure good gas transfer a semipermeable membrane was used as the seal and all the operations were performed under sterile conditions. Shaking frequencies were varied for both characterisation studies (Section 2.4.1) and culture kinetics (Section 2.5.2).

2.6.2 Shake Flask Bioreactor

For all the experiments, 250 mL Erlenmeyer shake flasks were used with total working volume of 100 mL (Figure 2.11 (B)). A similar experimental methodology was employed as described for 24-well microwell plates with a semipermeable membrane seal.

2.6.3 7.5 L Stirred Bioreactor

A New Brunswick 7.5 L bioreactor was used for scale-up of heterotrophic algal cultivations. The bioreactor aspect ratio H_T/D_T and the D_i/D_T are 1.8 and 0.3 respectively (Figure 2.11 (C)). The bioreactor was filled with minimal salt media as described in Table 2-1 to a final working volume of 4 L. Calibration of pH was performed using standard buffers at pH 4 and 7. This was subsequently followed by dissolved oxygen tension (DOT) probe calibration using 0% nitrogen gas and 100% gaseous air. The probes were placed in dedicated ports within the bioreactor and the vessel sterilised by autoclaving at 121 °C for 15 min. Once sterilisation was complete and the vessel had cooled, the probes were checked and where necessary re-calibrated. Glucose solution which had been filter sterilised through a 0.2 micron Stericup (Millipore, Wartford, UK) was added to the vessel aseptically and the bioreactor was allowed to run for 15 – 20 min prior to inoculation.
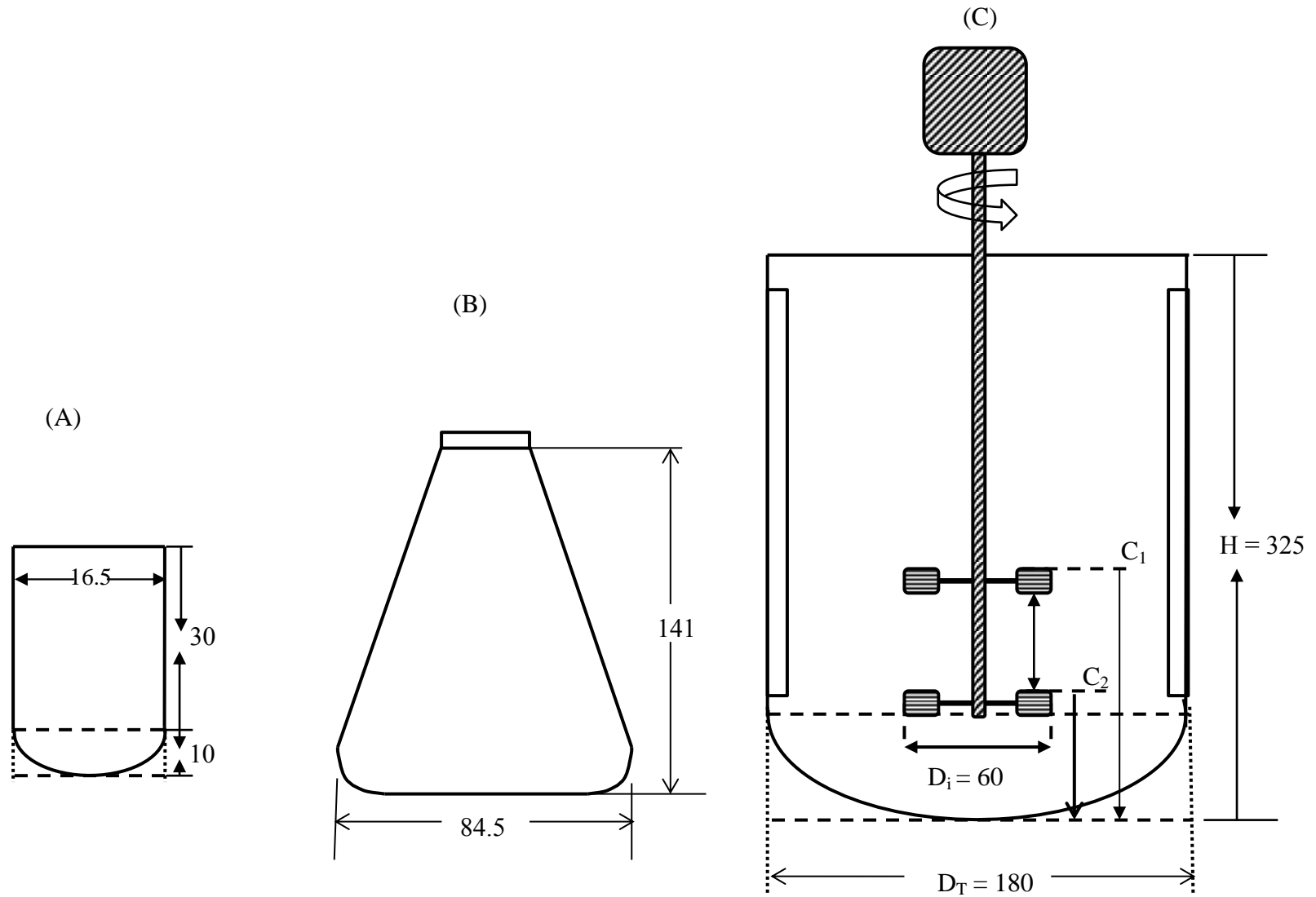
Figure 2.11: Schematic diagram of bioreactor geometries used for heterotrophic algae cultivation: (A) single well from a 24-well microtitre plate (B) 250 mL Erlenmeyer shake flask (C) 7.5 L Brunswick stirred tank bioreactor. All measurements were taken in mm. Where C_1 and C_2 are 100 and 44 mm.

2.7 Heterotrophic Cultivation of Microalgae

2.7.1 Seed Culture Preparation

C. sorokiniana streaked and incubated on a TAP medium agar plate at ambient room temperature under low light intensity of $40 - 60$ µmolsm^{-2}s^{-1} for 5 days was used as inoculum. The seed culture was inoculated from the plate into 50 mL TBP medium enriched with 10 gL^{-1} glucose using 250 mL Erlenmeyer flasks. The flasks were incubated in a Khuner incubator shaker operated at 180 rpm, and 28 °C for 4 days. This was then used as seed culture for subsequent fermentation at 10% v/v inoculum. Media compositions are as described in Table 2-1.

2.7.2 Algae Cultivation Kinetics in 24-Well and Shake Flask Bioreactors

The 24-well plates and the 250 mL shake flasks were filled with 100 mL working volume of media (prepared as described in Section 2.1.3) and the starting concentration adjusted appropriately (~ 5% v/v inoculum). The two systems were sealed with semipermeable membrane. The plates and flasks were positioned on the incubator shaker and the required growth conditions adjusted appropriately, temperature at 28 ºC and the shaking diameter at 25 mm. All the experiments were carried out in batch mode. Samples were withdrawn at 8 - 12 hr interval and stored at $- 20$ °C for analysis.

2.7.3 Algae Cultivation Kinetics in 7.5 L Stirred Tank Bioreactor

The 7.5 L New Brunswick stirred tank bioreactor was used with a working volume of 4 L. 3.5 L of sterile TBP media enriched with 10 gL^{-1} glucose solution was added to the bioreactor and inoculated from the seed culture. The starting OD of the inoculated media in the bioreactors was adjusted appropriately and the air flow rate kept at 1 vvm. The bioreactor was operated at a temperature of 28 °C. The DOT, and the stirrer speed were cascaded to keep the DOT above 30%. The pH values and OD measurements were determined from samples withdrawn at 12 hr intervals. Samples were stored at $- 20$ °C for further downstream analysis. All experiments were performed at least in duplicate.

2.8   Cell Disruption Methods

2.8.1   Freeze Drying

Culture broth collected at the end of the cultivation was centrifuged at 10,000 rpm, 4 °C for 10 min using a Heraeus Fresco 17 centrifuge (Thermo Scientific, UK). The supernatants were dispensed and the pellets washed twice with distilled water. The pellets were then prepared for freeze drying by dipping into liquid nitrogen for 2 min or stored in − 80 °C overnight and immediately transferred into an Edwards high vacuum freeze dryer (Crawley, England) for lyophilisation. The weights of the lyophilised cells were measured prior to further lipid analysis.

2.8.2   Batch Homogenisation

Batch cell disruption operations were performed using an APV Manton-Gaulin Lab 40 homogeniser (APV International, West Sussex, UK). The homogeniser has a maximum capacity of 40 mL per batch with minimum feed volume of 35 mL. Disruption operations were performed at 500, 750 and 1000 bar. 1 - 3 passes were carried out at each pressure. The lipid release and impact of homogenisation conditions on cells were evaluated immediately. All experiments were carried out in duplicates.

2.8.3   Focused Acoustic Ultrasonication

For small-scale lipid quantification, cells were disrupted by an adaptive focused acoustic (AFA) method using a Covaris E210 (Woburn, MA). Different volumes of microalga broth samples in borosilicate glass tubes were placed on a sample rack onto the Covaris' degassed water bath (5 L, Milli-Q water) which was maintained at 8 °C. Cells disruptions were done at 20% duty cycle and 1000 cycles per burst. Other parameters used are presented in Table 2-2 (Perez-Pardo et al., 2011). All experiments were repeated in duplicate or triplicates.

Table 2-2: Parameters and the variable ranges used for sonication experiments.

Parameter	Variable range	Unit
Acoustic power (intensity)	60 (3), 100 (6), >130 (10)	W
Sonication time	1, 2, 4, 8, 12	min
Sample volume	2, 4, 6, 8	mL
Sample concentration (mL broth per 8 mL sample, dilution with cell broth supernatant)	0, 0.5, 1, 2, 4, 6, 8	mL

2.9   Analytical Methods

2.9.1   Biomass Quantification and Growth Rate Calculation

The biomass concentration was determined by measurement of OD at 750 nm using a spectrophotometer (Ultrospec 1100, Amersham Biosciences, UK). The dry cell weight was determined using a pre-dried 15 mm diameter Whatman fibre glass filter paper (GE Healthcare, UK) and then dried to constant weight after sample addition. The calibration curve was generated (Appendix Figure I.1) and used for the conversion of the OD readings to mass. The specific growth rate (μ) during exponential phase was determined according to the following Equation 2.4 (Kumar and Das, 2012).

$$\mu = \frac{InX_2 - InX_1}{t_2 - t_1} \qquad\qquad 2.4$$

where, X_2 and X_1 are the dry cell weight concentration in gL^{-1} at time t_2 and t_1 (s) respectively.

2.9.2 Glucose, Ammonium and Green Pigment Quantification

A known volume of sample was centrifuged at 10000 rpm for 10 min, 900 µL of the clear supernatant was aspirated into a new centrifuge tube and the glucose and ammonium concentrations measured using a Nova Bioprofile Analyzer 400 (Nova Biomedicals, Cheshire, UK). The pellet from the centrifuged sample was then re-suspended in a solution of 90% v/v acetone (Fisher scientific, UK) and dimethyl sulfoxide (Sigma, UK) in the ratio 3:2 v/v (Anderson, 2005), and thereafter allowed to stand for 2 hr in sealed container kept in the dark. The sample was subsequently centrifuged under the same conditions and the OD 750nm of the supernatant measured using a 1 cm path length quartz cuvette. Concentrations of the different pigments were calculated according to Equations 2.5 – 2.7 (Jeffrey and Humphrey, 1975; Strickland and Parsons, 1972)

$$C_{chl-a} = [11.6(OD_{665} - OD_{750}) - 1.31(OD_{645} - OD_{750}) - 0.14(OD_{630} - OD_{750})]V_2 I^{-1}(V_1)^{-1}$$

$$2.5$$

$$C_{chl-b} = 20.7(OD_{645} - OD_{750} - 4.34(OD_{665} - OD_{750}) - 4.42(OD_{630} - OD_{750})]V_2 I^{-1}(V_1)^{-1}$$

$$2.6$$

$$C_{PPC} = [4.42(OD_{480} - OD_{750})]V_2 I^{-1}(V_1)^{-1}$$

$$2.7$$

where, V_1 is the sample volume (1 mL), V_2 is the volume of the extraction solvent (1 mL). All samples were repeated in three replicates.

2.9.3 Total Lipid Determination

Lipids were extracted using the modified Bligh and Dyer (1959) method. A mixture of chloroform–methanol (2:1, v/v) were added into the dried cell pellets and left overnight for 16 – 18 hr in sealed vials to prevent evaporation and also kept in fume cupboard for safety. These were further separated into chloroform and aqueous methanol layers by addition of methanol and water to give a final solvent ratio of chloroform:methanol:water of 1:1:0.9. The mix was then centrifuged at 4000 g for 20 min and the organic phase separated and evaporated to dryness under nitrogen. Total lipids were measured gravimetrically and stored at - 20 °C under nitrogen gas to prevent lipid oxidation or used directly for subsequent analysis.

2.9.4 Modified Sulpho-Vanillin Method

Lipid yield was analysed using the sulpho-phospho-vanillin method (Cheng et al., 2011). The sonicated samples were each transferred to a Falcon tube. Chloroform-methanol solution mix in the ratio 2:1 v/v was added to each Falcon tube with a volume equivalent to the sonicated sample in the tube. The Falcon tubes were vortexed for 2 minutes and allowed to stand for 20 minutes. This was followed by centrifugation for 10 minutes at 4000 rpm. For the lipid assay, 100 μL from the bottom phase of the centrifuged samples was carefully pipetted into a 96-microwell glass plate and the volatile organic solvent was allowed to evaporate. 100 μL concentrated H_2SO_4 was then added to each well and incubated at 70 °C and 400 rpm for 20 minutes in a thermomixer comfort MTP (Eppendorf, Germany). Rapid cooling of the plate was achieved by placing on wet ice for 2 minutes and the absorbance measured at 540 nm using Safire2 microplate reader incorporated with Magellan data analysis software (Tecan, Switzerland). 50 μL of prepared phospho-vanillin reagent was thereafter added to each well and a reaction time of 10 minutes was allowed. 100 μL of each well was then transferred to a new well and the absorbance measured at 540 nm. A standard triolein curve was developed for calibration as shown in Appendix Figure I.2.

2.9.5 Fatty Acid Methyl Ester (FAME) Analysis

FAME were prepared by direct trans-methylation of lipid extracts in dichloromethane with trimethyl sulfonium hydroxide (TMSH). The FAME were

analysed by using an auto-system XL capillary gas chromatograph (Perkin Elmer Inc., USA) equipped with a flame ionization detector (FID) and an omegawax 250 capillary column (30 m^3, 0.25 mm) (Sigma-Aldrich, UK). Nitrogen was used as carrier gas. Initial column temperature was set at 50 °C (2 min.), which was subsequently raised to 230 °C at 4 °C min^{-1}. The injector was kept as 250 °C with an injection volume of 2 μL under split less mode. The FID temperature was set at 260 °C. Individual FAMEs were identified by comparing their retention times and chromatogram size with the standards and quantified by developing standard calibration plot from mix of standard peaks (Sigma-Aldrich, UK) comprising of thirty seven standards (Xu et al., 2011). Standard calibration plot for selected FAME are shown in Appendix Figure I.3.

2.9.6 Calculation of Photosynthetic Efficiency and Biomass Yield on Irradiance

Calculation of photosynthetic efficiency (PE) was performed using Equation 2.8 according to Soletto et al., (2008) and Morita et al., (2002),

$$PE(\%) = \frac{r_G H_G}{IPAR} \qquad\qquad 2.8$$

where, r_G is the maximum daily biomass growth (gd^{-1}) and H_G = 22.9 kJgDW^{-1} the enthalpy of dry cell biomass. IPAR was obtained by multiplying photosynthetic active radiation (PAR) with illuminated surface area (m^2). A conversion factor of 18.78 kJsd^{-1} for cool white fluorescent lamps was assumed for LED (Janssen et al., 2003). Determination of biomass yield on light energy expressed as dry weight produced per amount of quanta (photons) absorbed in the PAR range ($Y_{x,E}$) was calculated according to Janssen et al., (2003), with the efficiency of light utilisation for photo-autotrophic growth expressed according to Equation 2.9.

$$Y_{x,E} = \frac{C_x \mu V}{PFD_{in} \times Ax 3600 \times 10^{-6}} \qquad\qquad 2.9$$

where, C_x is the biomass density (gL^{-1}), μ is the specific growth rate (h^{-1}), V is the liquid volume in well (m^3), PFDin is the photo flux density incident on the wall of the wells (μmolm^{-2}s^{-1}) and A is the light incident total surface area.

2.9.7 Particle Size Analysis

The particle size distribution of non-disrupted and disrupted microalgae cells were performed by laser diffraction using a Mastersizer 2000 (Malvern Instruments Ltd, Malvern, UK) with a small volume sample dispersion unit at a detection range of 0.01 – 2000 µm. Samples were added drop-wise until the 'obscurance' was within the acceptable range of 10-15% and the refractive index set to 1.03. The output is size distribution in terms of particle volume percentage. d_{10} and d_{90} values (Andrea, 2010) were those given by the instrument. For d_{10} or d_{90} determination, measurements were made in triplicates.

3. DESIGN AND CHARACTERISATION OF A MINIATURE PHOTOBIOREACTOR

3.1 Introduction

3.1.1 Miniature Photobioreactor Development

Microalgae are ubiquitous groups of organisms and are being increasingly investigated for several applications (Muthuraj et al., 2014; Rupprecht, 2009). Examples of the various types of product that can be produced in algae were summarised previously in Section 1.1.1. and include pharmaceuticals, nutraceutics, intermediate precursors, pigment, food supplements and biofuels component (Harun et al., 2010). Culture performance can be optimised for biomass, lipid, pigment or protein production depending on the particular application. Such optimisation experiments are currently performed in illuminated shake flasks and other laboratory scale photobioreactors as described in Section 1.2.4 (James et al., 2011; Pradhan et al., 2012; Rodolfi et al., 2009; Seletzky et al., 2007). This places limitations on the number of experimental variables that can be investigated in parallel.

Microwell based culture devices have now found widespread use for rapid and early stage assessment of culture conditions for microbial and mammalian cells. A number of these high-throughput systems have been characterised and reported in the literature (Barrett et al., 2010; Betts and Baganz, 2006; Hermann et al., 2003; Kumar et al., 2004; Micheletti et al., 2006; Micheletti and Lye, 2006).

Characterisation of the engineering environment within orbitally shaken microwell systems has shown the importance of shaking frequency, culture volume and well geometry on the overall performance (Marques et al., 2010; Zhang et al., 2008) while

---

†The majority of the results in this Chapter have been accepted for publication as: E.O. Ojo, H. Auta, F. Baganz, and G. J. Lye (2015). Design and parallelisation of a miniature photobioreactor platform for microalgal culture evaluation and optimisation. *Biochemical Engineering Journal.*

progressive improvements have been made in terms of aeration and control of environmental parameters (Betts et al., 2014; Lye et al., 2003; Zhou et al., 2009; Zimmermann et al., 2003).

Recently the use of a 24-well microplate for heterotrophic cultivation of microalgae was reported (Hillig et al., 2013). There remains, however, the need for a small-scale, high-throughput platform for the phototrophic culture of microalgae if the full range of their biological diversity is to be explored and their commercial potential evaluated. However, many of these strains are yet to be assessed for their optimal productivity and economic viability. The establishment of a small-scale, photobioreactor system would enable the early stage high-throughput evaluation and optimisation of many interrelated culture parameters.

3.1.2   Aim and Objectives

As outlined in Section 1.5 the aim of this Chapter is to design a novel twin-well prototype mPBr and perform adequate engineering characterisation to enable scale-out into a multiwell mPBr format. These studies build on past work on the application of microscale systems to heterotrophic culture of mammalian, bacteria and recently published microalgae cells (Barrett et al., 2010; Betts et al., 2014; Hillig et al., 2013). Use of this system for phototrophic cultivation is expected to reduce bioprocess development time and cost, thus improving economic viability of microalgae bioprocess development cost. The specific objectives of this Chapter are to:

- design and evaluate a prototype twin-well mPBr system mounted on an orbital shaking platform in an environmentally controlled incubator.

- perform detailed engineering characterisation of the mPBr and demonstrate scale-out from twin-well to 24-well mPBr.

- investigate culture reproducibility and performance in the 24-well mPBr and illustrate the potential of the system for optimisation of culture conditions.

- evaluate the impact of culture conditions on biomass, pigment and lipid productivity and also assess FAME compositions at selected conditions.

3.2   Miniature Photobioreactor (mPBr) Design and Operation

A mPBr design for phototrophic microalgae cultivation has not been described in the literature despite previous miniature bioreactor studies with bacterial, mammalian cells and heterotrophic cultivation of microalgae (Betts et al., 2014; Hillig et al., 2013; Isett et al., 2007). Consequently a novel prototype twin-well mPBr was designed to mimic a conventional 24-well microwell bioreactor as shown in Figure 3.1 and described in Section 2.2. Figure 3.2 gives additional details on different well geometries and dimensions. In order to facilitate subsequent scale-out of the twin-well mPBr, maintenance of key design parameters such as light transmittance and mixing efficiency were considered. Fluid mixing was achieved in the twin-well mPBr by orbital shaking up to a maximum frequency of 400 rpm at 25 mm shaking diameter. The maximum working volume in each well was limited to 4 mL to prevent splashing.

The light path-length across the well diameter was kept below 2 cm to ensure light penetration into the medium. In order to ensure efficient light dispersion and scale-out to the 24-well mPBr design, the positions of LEDs on the illuminated side were decided based on the solid angles of reflection, maximum path length and the liquid height in the wells as shown in Figure 3.1

To facilitate scale-out and parallel operation using conventional transparent and translucent 24-well plates, a novel shaker incubator with a Perspex shaking platform (on which the 24-well plates were mounted) was designed as shown in Figure 2.3. Initial light diffusivity tests performed during orbital shaking at a 5 cm distance from the fixed LED light source indicated no significant variation across the platform surface (results not shown). Light intensities quoted were measured directly at the base of the wells for all subsequent experiments.

Similarly, an initial contamination test was investigated with the use of semipermeable membrane with sterile RO water. Culture monitored for 5-days under typical experimental conditions showed no signs of contamination.
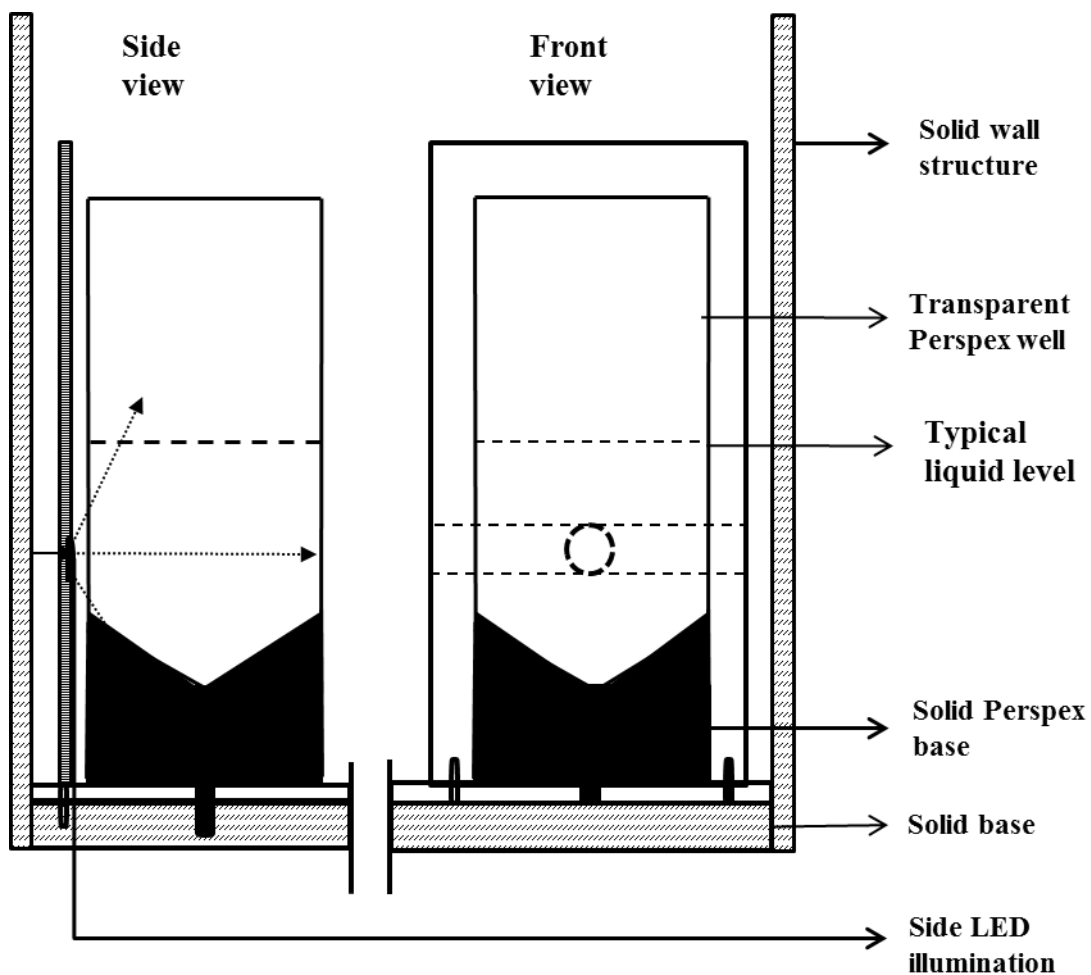
Figure 3.1: Schematic diagram of experimental set-up for the prototype twin-well mPBr lit from the side. A photograph of the actual twin-well mPBr is shown in Figure 2.2.
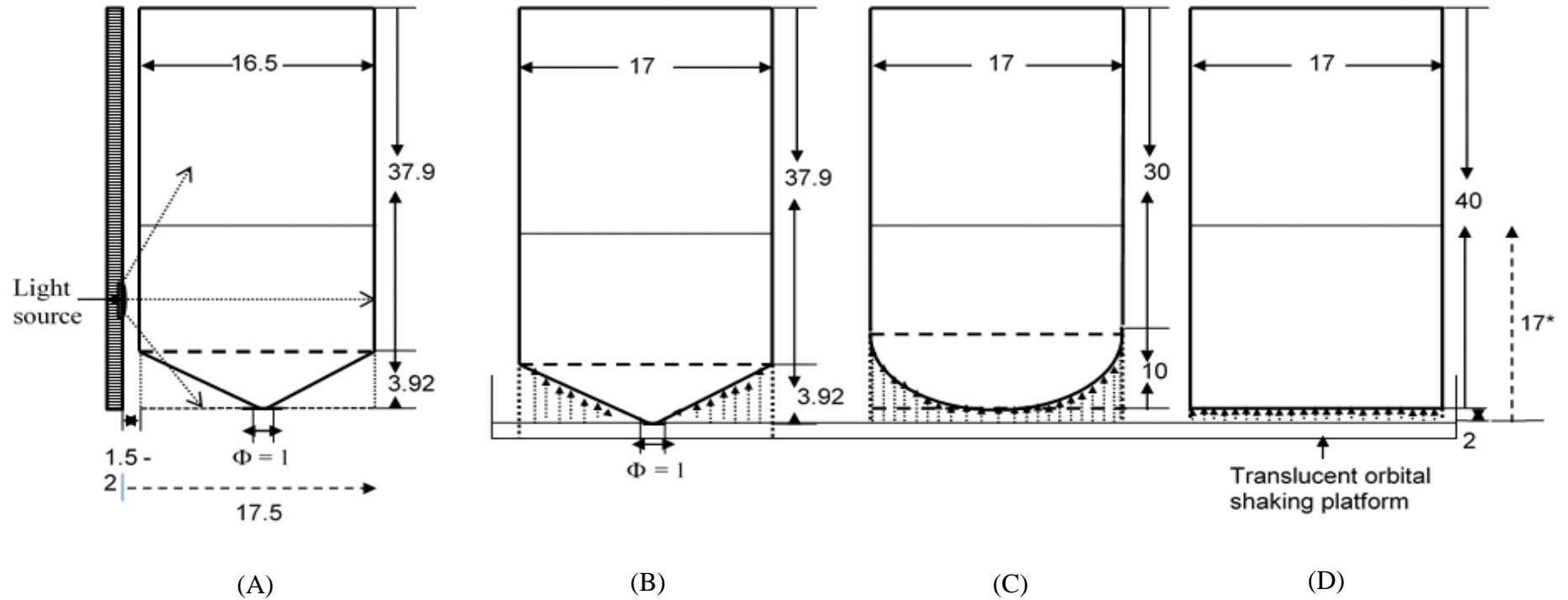
Figure 3.2: Comparison of mPBr designs for the purpose of identifying the impact of geometry on mixing and light absorption by microalgae. (A) prototype pyramid bottom mPBr (B) a single well from a scale-out 24-well pyramid bottom shaken mPBr (C) 24-well round bottom shaken mPBr (D) 24-well flat bottom shaken mPBr. All dimensions in mm.

3.2.1 Liquid Phase Hydrodynamics

Shaking frequency and well geometry are known to influence energy dissipation, fluid motion and mixing in shaken microwells (Micheletti et al., 2006). Here, fluid motion in the wells was visualised using a high speed camera as shown in

Figure **3.3**. In general shaking induced deformation of the fluid surface and created a vortex that moved around the walls of the well in-phase (Buchs et al., 2001) with the orbital motion of the platform. The depth of the vortex and hence the gas-liquid surface area available for gas mass transfer increased with increasing shaking frequency. At the highest shaking frequency studied the vortex reached the base of the well. These observations are similar to the fluid flow predicted in a 96-well plate using Computational Fluid Dynamics, CFD (Zhang et al., 2008).

3.3 Engineering Environment in the Incubator

3.3.1 Quantification of Oxygen Transfer Capability

Understanding how $k_L a$ in the 24-well mPBr varies with shaking frequency and well geometry is necessary for comparing the different bioreactor designs and to inform options for mPBr scale-out or scale-up (Gill et al., 2008b). As described in Section 2.4.1, obtained values of $k_L a$ calculated using Equation 2.1 are plotted against shaking frequency as shown in Figure 3.4. It can be seen that $k_L a$ values increased with an increase in shaking frequency which correlates directly with the increase in gas-liquid surface area for mass transfer noted previously. In contrast, the well geometry had no significant impact on $k_L a$ values at the liquid fill volume and over the range of shaking frequencies investigated. The $k_L a$ values obtained were found to be in the range reported for a similar 24-well bioreactor for experimental conditions of 300 rpm, shaking diameter of 25 mm and 2.5 mL working volume (Duetz, 2007; Duetz and Witholt, 2004; Hermann et al., 2003).

(A)

(B)
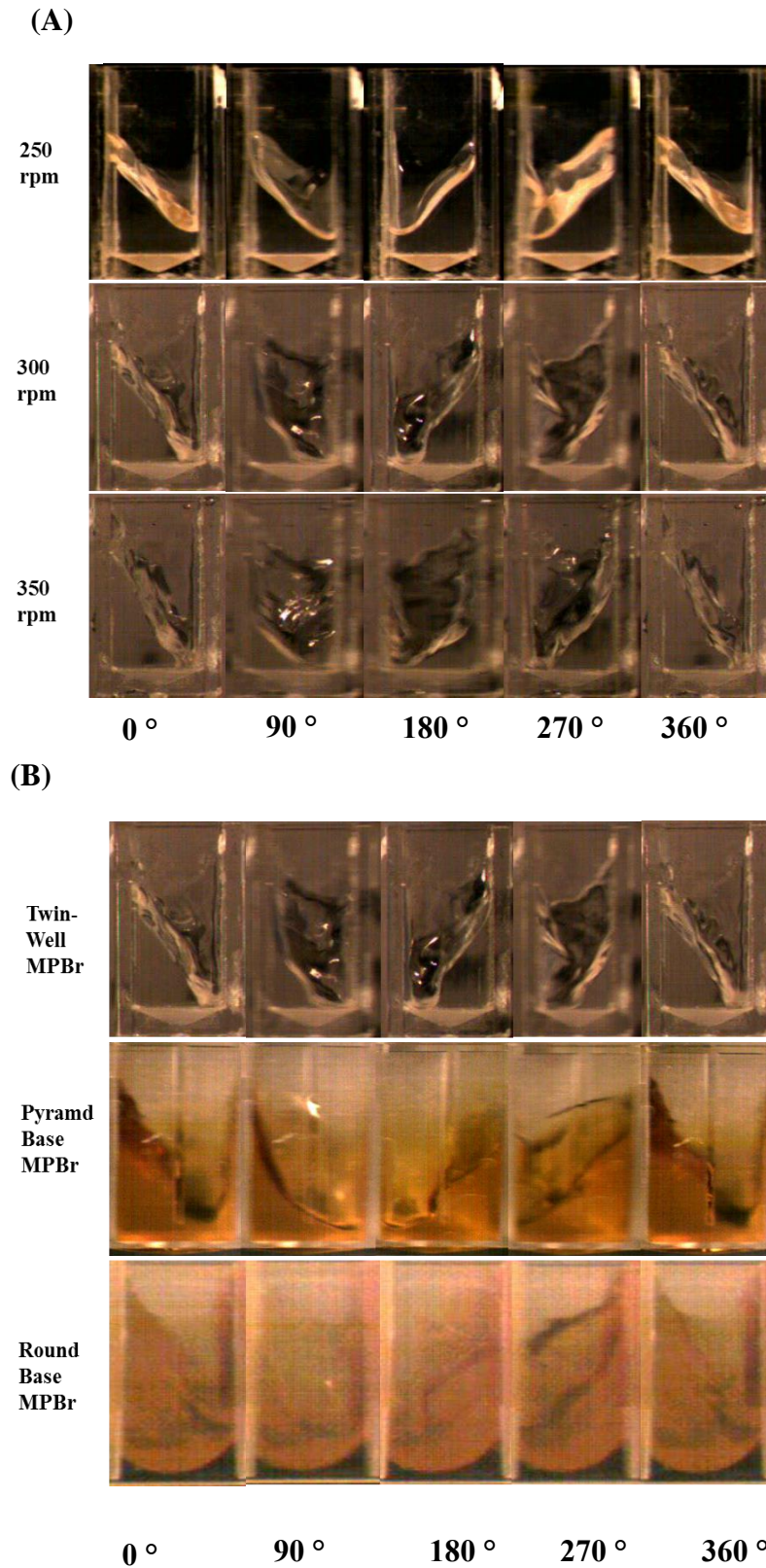
Figure 3.3: Visualisation of fluid hydrodynamics with angle of rotation (A) in the pyramid base 24-well mPBr at different shaking frequencies and (B) in the different mPBr geometries at 300 rpm. Experiments performed as described in Section 2.4.4.

3.3.2 Evaporation Studies

Extended culture times pose the challenge of evaporation on small-scale system used as bioreactor intended for mammalian cell and microalgae culture at elevated temperature. Minimization of evaporation effects in microtitre plate have been studied (Zimmermann et al., 2003) and some of the effects identified on culture performance have been associated with increase in broth osmolality, metabolite concentrations and cell specific productivity as observed in studies on mammalian cell culture (Betts et al., 2014; Silk et al., 2010).

Generally rate of evaporation increased with increase in temperature, however, increase in relative humidity (RH) reduces evaporation rate until the maximum percentage relative humidity was reached. At maximum 90% RH and culture temperature of 32 °C, variation in light intensity had no significant impact on evaporation. At 380 $\mu molm^{-2}s^{-1}$, chosen as optimal light intensity, the culture periods lasted for about 3.5 days which resulted in approximately 8–10% evaporative losses as depicted in Figure 3.5. This is considered to have no significant impact on the specific productivity during fed-batch culture. Overall evaporation rate was seen to be consistent across all the wells and plates. The gravimetric approach described in Section 2.4.2 was adopted. At the maximum RH of 90%, a condensation effect was observed at the operating temperature of 30 °C.
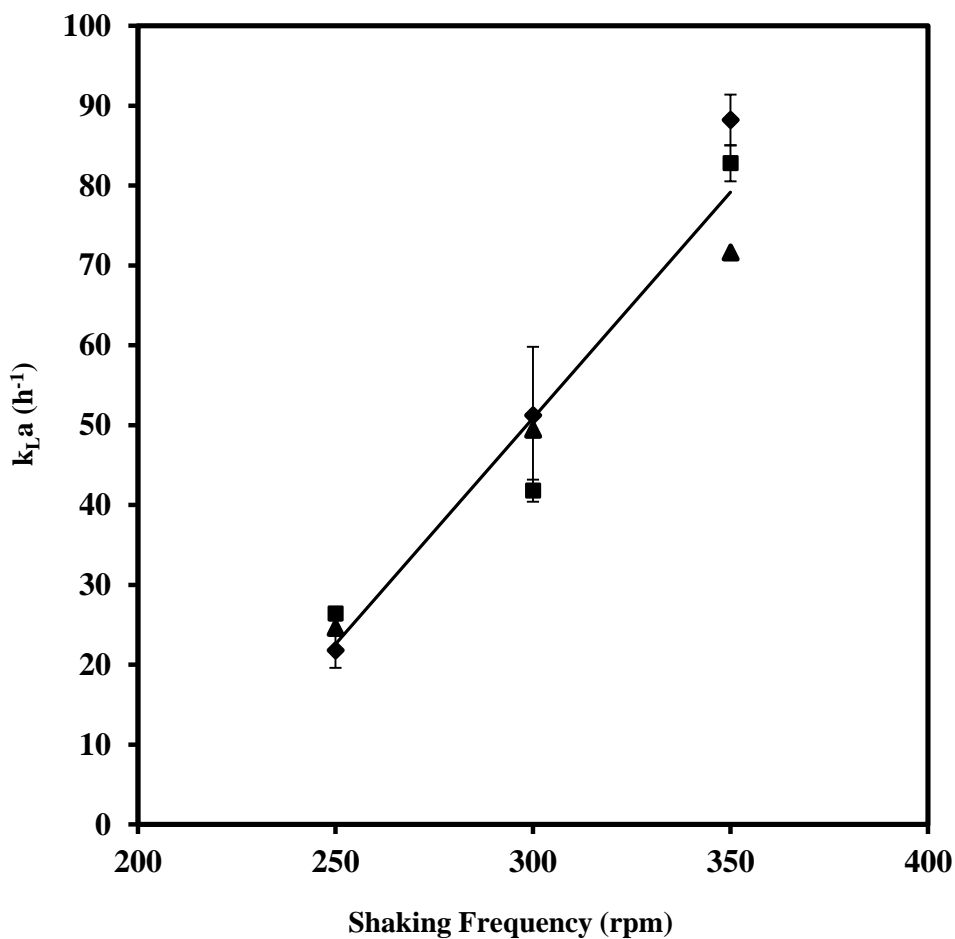
Figure 3.4: Characterisation of oxygen mass transfer at increased shaking frequency. Experimental conditions: N = 300 rpm; do = 25 mm; 32 °C; 5 days duration, 85% RH; RO water. Error bars represent one standard deviation about the mean (n=3). Solid line fitted by linear regression. Experiments performed as described in Section 2.4.1.
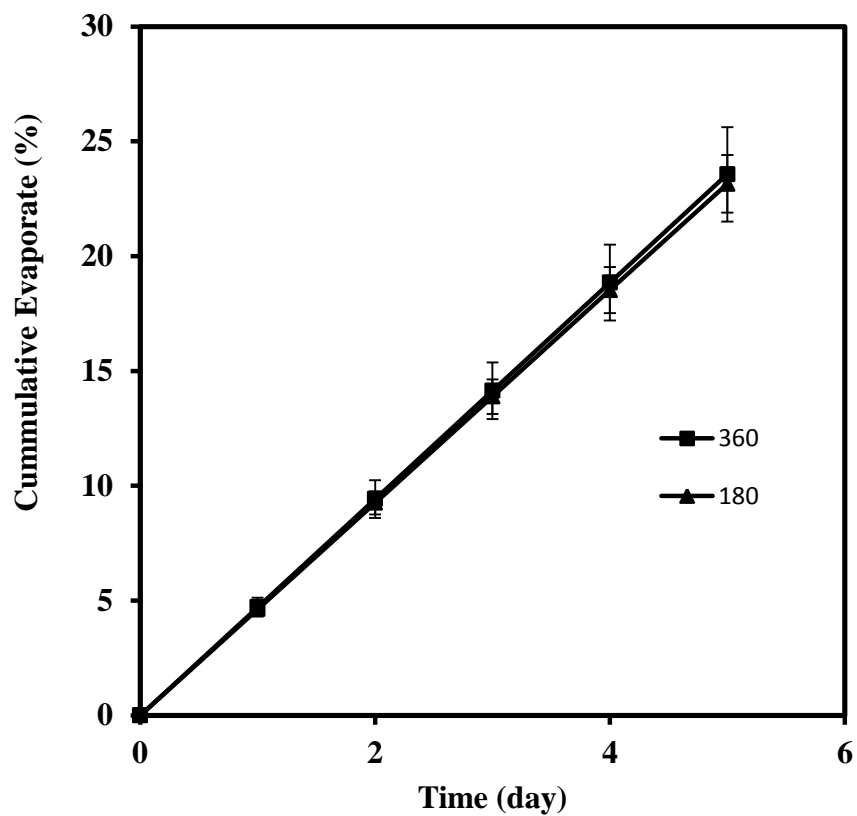
Figure 3.5: Determination of a percentage evaporation at different light intensity in the 24-well mPBr. Error bars represents one standard deviation about the mean (n=3). Solid lines fitted by linear regression. Experiments performed as described in Section 2.4.2.

3.4 mPBr Microalgae Culture Kinetics

3.4.1 Batch Cultivation in Prototype MPBr

Initial studies in the twin-well mPBr for batch cultivation of *C. sorokiniana* focused on optimisation of TBP media composition and environmental conditions as shown in Table 3-1. The first cultures at low tris-base concentrations of $20-60$ mM yielded low biomass concentrations of approximately 1 gL^{-1}. Similar results were reported using standard TAP medium without acetate by Kumar & Das (2012). The progressive decline in pH measured during the cultures resulted in decreased biomass growth and also caused chlorophyll bleaching due to broth acidification (Kumar and Das, 2012).

Media recipes and buffer concentrations were subsequently investigated, modified and optimised as indicated in Table 3-1. A self-buffering medium was formulated with 0.2 M tris-base; this also eliminated the need for the tris-acetate thus removing a potential source of inorganic carbon from the media. Further variation of the culture conditions such as an increase in temperature to 35 °C resulted in an almost two-fold increase in final biomass concentration (Table 3-1). Evaluation of different media formulations as described in Table 2-1 shows TBP to have produce the highest biomass concentration.

Variation of the shaking frequency led to further increases in biomass concentration up to nearly 6.0 gL^{-1} (Figure 3.6) representing a 6-fold improvement over the initial conditions. The approximate doubling in the growth rate and biomass yield seen when increasing the shaking frequency from 250 to 300 rpm matches the increase seen in the corresponding $k_L a$ values (Figure 3.4). Using the optimised medium formulated, the culture pH was also maintained relatively constant throughout both cultures between pH 6-7. The highest biomass concentration achieved here is comparable with the data of Cuaresma et al., (2009) for culture of *C. sorokiniana* in a flat plate photobioreactor.

Table 3-1: Optimisation of TBP media compositions using the prototype miniature photobioreactor. Experiments performed as described Section 2.5.2.

Temp. (°C)	Shaking Frequency (rpm)	Tris-Base Conc. (mM)	Photo-period (L/D) (hr)	% CO_2	Biomass Conc. (gL^{-1})
28	250	20	24:0	Atm.	0.85
28	250	60	24:0	Atm.	0.98
28	250	200	24:0	Atm.	1.27
28	250	200	18:6	2	0.98
35	250	200	24:0	2	2.85
35	300	200	24:0	2	5.87

Atm. = atmospheric air
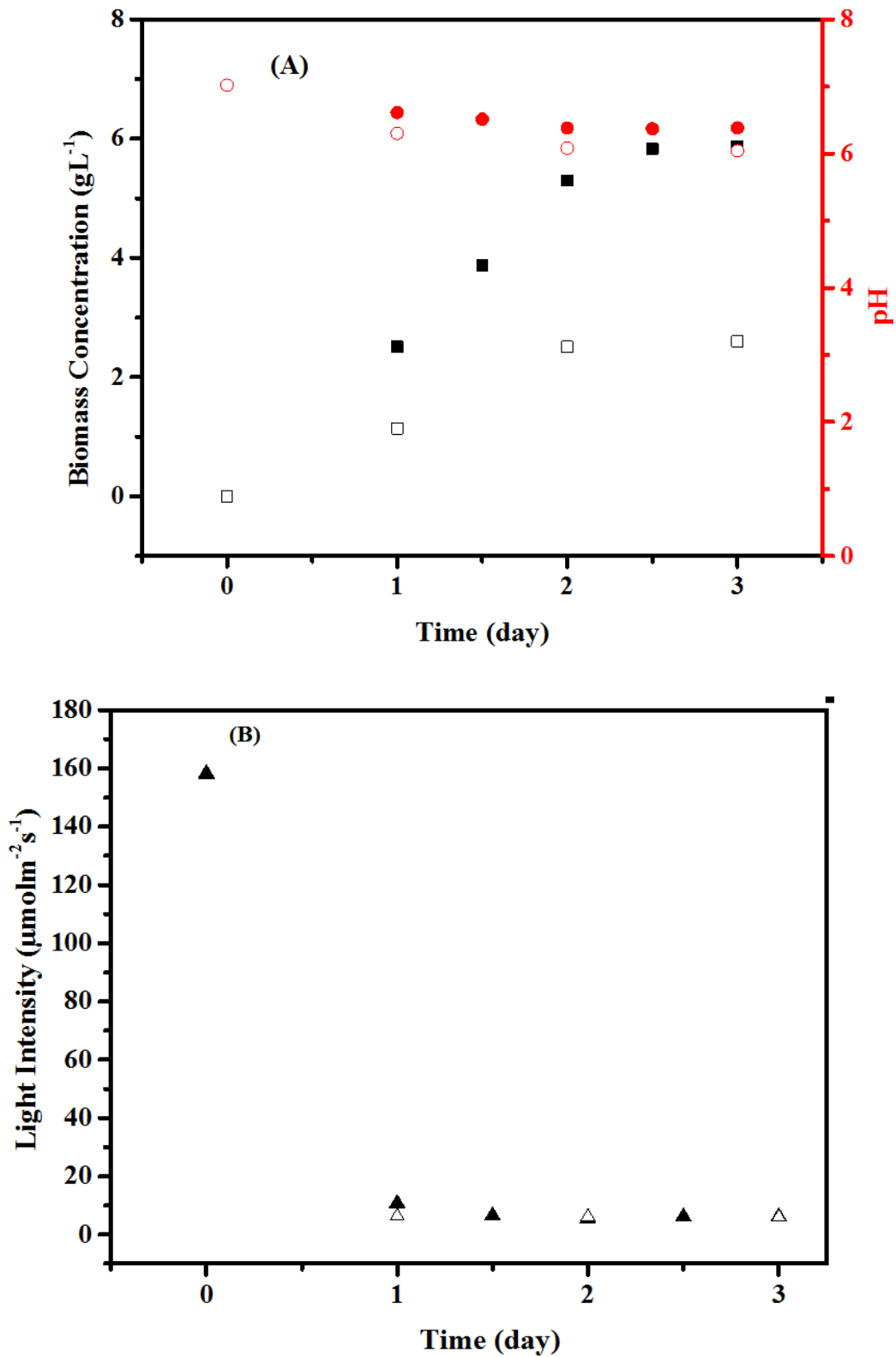
Figure 3.6: Effect of shaking frequency on the batch culture kinetics of *C. sorokiniana* in the twin-well mPBr. (A) (■, ■) biomass concentration, and (●, ●) pH. (B) (▲, ▲) light intensity. Where open and closed legend represent 250 and 300 rpm respectively. Experimental conditions: $V_f = 4$ mL; LI = 160 $\mu mol m^{-2} s^{-1}$; 32 °C; 85% RH. Experiments performed as described in Section 2.5.2.

3.4.2 Scale-out from Prototype mPBr to 24–well mPBr

Scale-out of the twin-well mPBr format into conventional multiwell plate designs was next assessed in order to facilitate greater parallelisation and hence increased experimental throughput. Such considerations are important for use of the mPBr in early stage strain selection and media optimisation applications. Important parameters impacting on scale-out operation include light intensity, fluid hydrodynamics and mixing and the surface areas available for light absorption and gas-liquid mass transfer. For the 24-well mPBr, the light path-length measured from the platform surface was taken as the reference light source and was matched to the light path length in the twin-well mPBr. As shown in Figure 3.7 (A), by maintaining the light path length and illuminated surface area approximately constant in wells of the same design (pyramid-shaped base) then similar rates and extents of cell growth were obtained and similar pH values recorded (data not shown).

For the scaled-out mPBr various 24-well plate geometries are available as shown in Figure 3.2. The dimensions of all the square edges in the upper parts of the wells are practically the same, yet the total surface area available for light absorption at the base in the wells differed depending on the base geometry (round, pyramid or flat/square). Figure 3.7 (B) shows the impact of base geometry on culture performance at a fixed light intensity of 240 $\mu molm^{-2}s^{-1}$.

These results show that polypropylene, translucent-walled round and pyramid-shaped base wells yielded similar biomass concentration. In contrast, the square flat-base mPBr, which had opaque walls   exhibited an approximately 22% reduction in final biomass concentration. Data on chlorophyll concentration in each of the cultures (not shown) indicated an approximately 56% higher chlorophyll concentration in the flat-based mPBr wells.

These results suggest that in cases, when screening for increased pigment production is required, the opaque-walled, square flat-based plates are the most suitable design while when investigating algal growth kinetics and biomass yields, the round and pyramid-based mPBr designs are most appropriate.
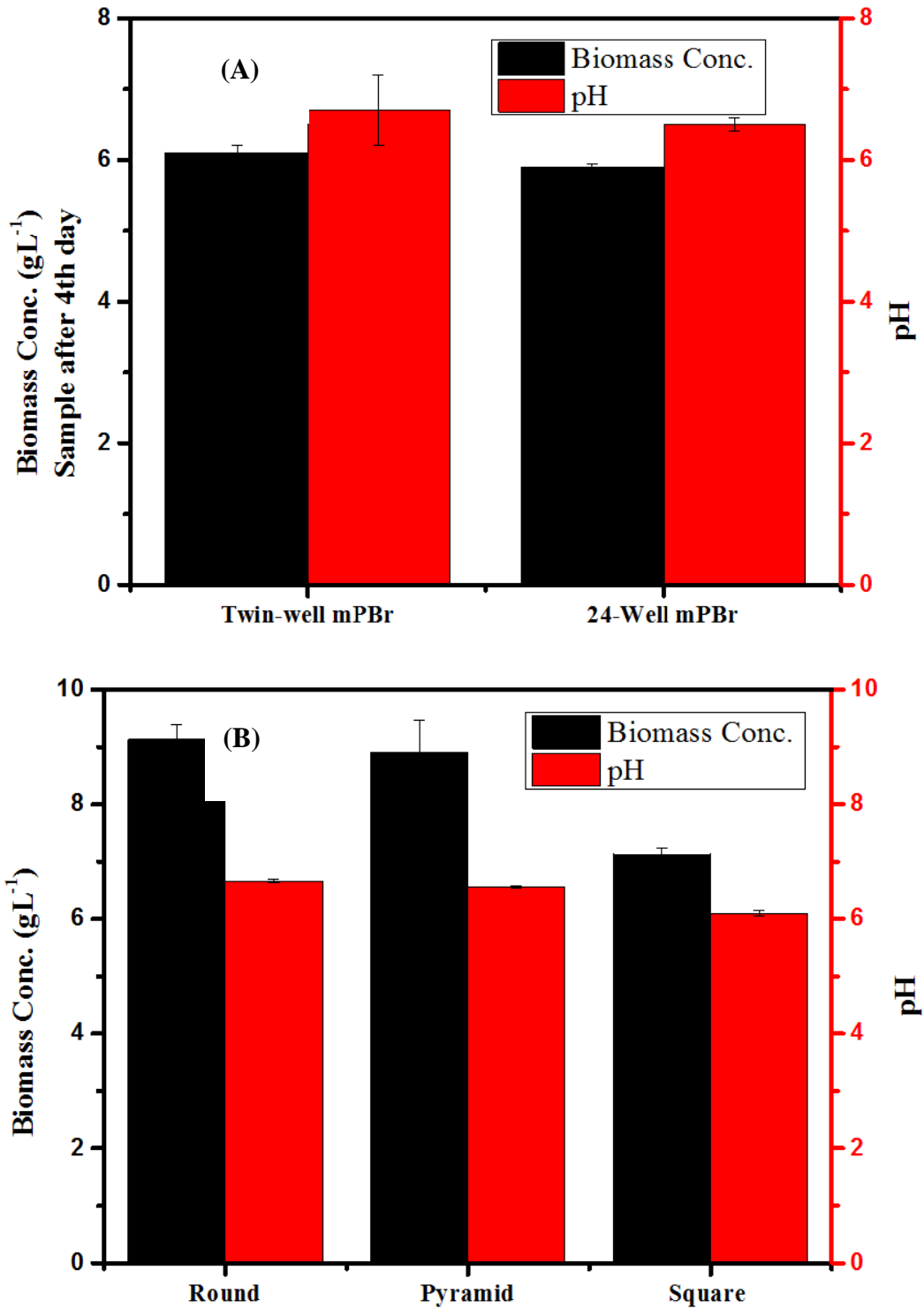
Figure 3.7: Comparison of batch culture kinetics of *C.sorokiniana* in different mPBr configurations: (A) Twin-well mPBr and 24-well mPBr under identical conditions. Experimental conditions: 4 mL fill volume; LI = 160 $\mu molm^{-2}s^{-1}$; 32 °C; 2% CO_2; 90% RH and N_f = 300 rpm. (B) Different geometries of 24-well mPBr at LI = 180 $\mu molm^{-2}s^{-1}$. Error bars represent one standard deviation about the mean (n=24 for 24-well mPBr and n=2 for twin-well mPBr). Experiments performed as described in Section 2.5.2 and 2.9.1.

3.4.3   Reproducibility of Parallel Microalgae Cultivation

An essential requirement of any parallel, multiwell platform is reproducible culture performance across individual wells under identical operating conditions. Figure 3.8 (A) shows biomass and chlorophyll concentration for parallel *C. sorokiniana* cultivation in the 24-well mPBr. The experiments were performed at two different sets of conditions of shaking frequency and light intensity. Comparison of overall biomass concentrations shows a two-fold increase at higher shaking frequency and light intensity (270 rpm, 180 μmolm^{-2}s^{-1}).

Generally, well-to-well evaluation of biomass concentration at the tested conditions showed good reproducibility across the 24-wells. Only in the outer wells of the mPBr plate, closest to the incubator door, were edge effects observed. So results from these wells are excluded from this analysis. Quantitative assessment of chlorophyll production in the wells on each row also yielded similar concentrations for chlorophylls a, b and C_{ppc} as shown in Figure 3.8 (B). In essence, use of the mPBr for parallel microalgae cultivation shows consistent and reproducible results.
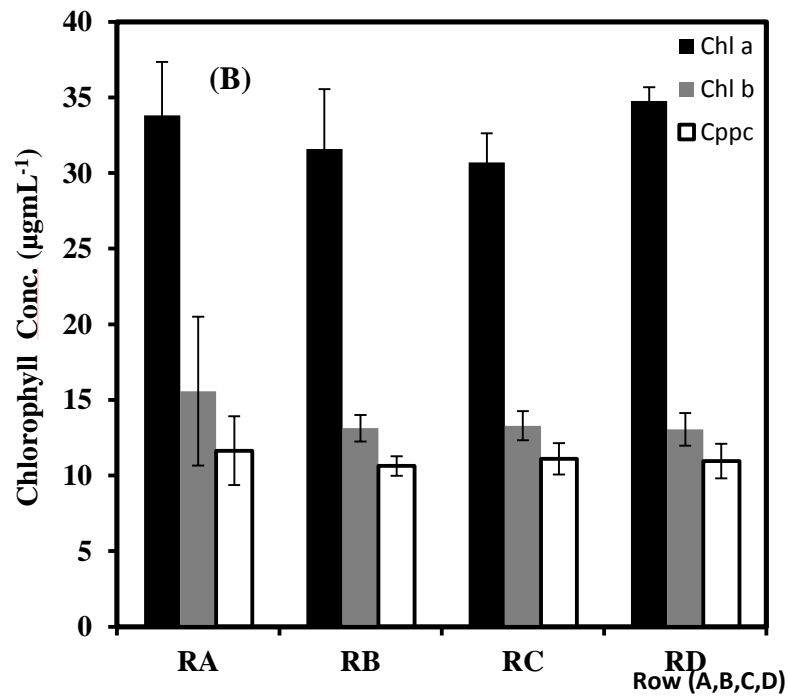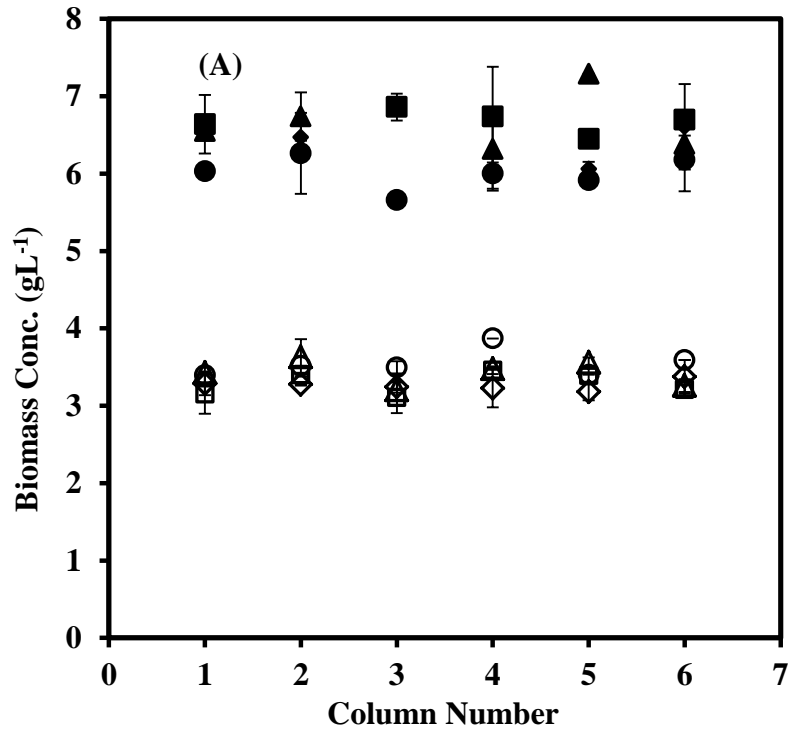
Figure 3.8: Evaluation of well-to-well performance on batch cultivation of *C. sorokiniana* in the 24-well mPBr. (A) Biomass concentration at condition 1: N_f = 270 rpm, LI = 180 $\mu molm^{-2}s^{-1}$, temperature 32 °C, 2% CO_2; condition 2: N_f = 250 rpm, LI = 160 $\mu molm^{-2}s^{-1}$, temperature 30 °C, 2% CO_2. (♦, ■, ▲, ●) and (◊, ■, ▲, ●) represents row A, B, C and D of the plate respectively. (B) chlorophyll concentration at condition 1. Error bars represent one standard deviation about the mean (n=24). Experiment performed as described in Section 2.5.2.

3.5 Optimisation Studies using mPBr

3.5.1 Effect of Light Intensity on Culture Kinetics and Chlorophyll

Phototrophic cultivation of *C. sorokiniana* depends largely on the intensity of light supplied and the rate of photosynthesis occurring in the cell (Cuaresma et al., 2009). Assessment of the effect of increasing light intensity on biomass productivity showed increases in biomass productivity up until 380 $\mu molm^{-2}s^{-1}$ after which no significant difference was observed. In general, as light intensity increases, specific growth rate increases slightly, while doubling time reduces as shown in Figure 3.9 (A). Optimal biomass productivities were achieved at 380 $\mu molm^{-2}s^{-1}$ above which an inhibitory effect due to excessive light saturation above the required threshold caused a reduction in cell productivity. Understanding the light thresholds for optimal biomass productivity is very important for implementing mPBr systems (Béchet et al., 2013).

An assessment of the effect of light intensity on chlorophyll production by *C. sorokiniana* in the mPBr shows reduction in Chl a concentration at higher light intensities. While no significant difference was observed in the Chl b and Cppc except at the highest light intensity tested where significant reduction in pigment productivity was observed as shown in Figure 3.9 (B). In the litreature it is generally believed that pigment bleaching is caused by two phenomena; light saturation above the threshold intensity and acidification of growth media due to uncontrolled pH. The highest concentration of Chl a observed at the lowest light intensity tested was thought to be due to limited rate of photon capture leading to reduced rate of biomass formation thus allowing more time for the photosystems to produce more pigments (Figure 3.9 (B)).

3.5.2 Effect of CO_2 Concentrations on Culture Kinetics and Total Lipids

The biomass productivity in photosynthetic culture does not only depend on the light availability but on the amount of carbon dioxide present in the culture broth for microalgae uptake. The effect of the percentage carbon dioxide concentration was evaluated on the culture of *C. sorokiniana* using the mPBr.
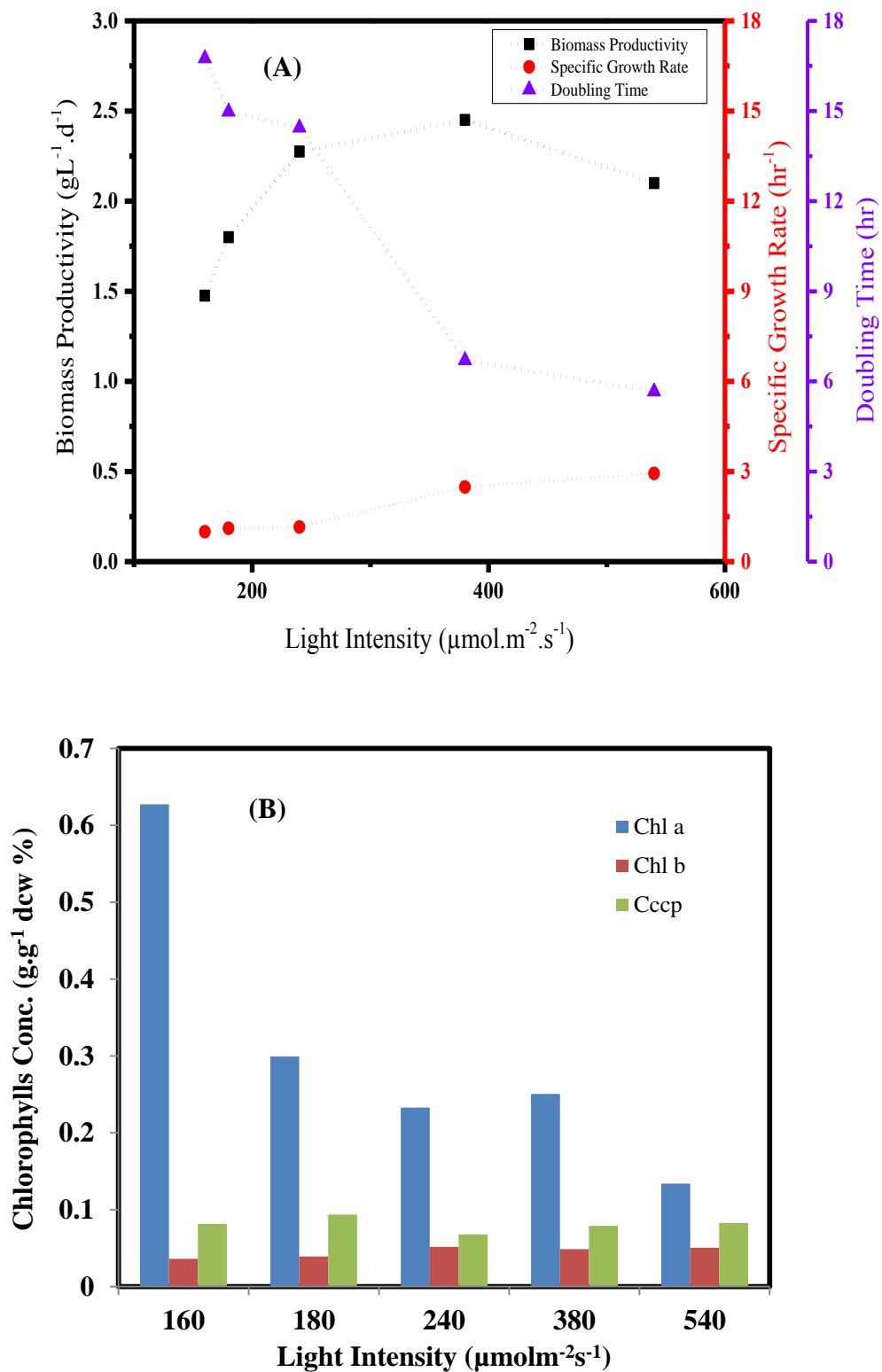
Figure 3.9: Effect of light intensity on culture kinetics of *C.sorokiniana*. (A) specific growth rate, doubling time and biomass productivity (B) chlorophyll concentration, chlorophyll a chlorophyll b Cppc. Experiment performed as described in Section 2.5.2.

As shown in **Error! Reference source not found.**, highest biomass productivity and specific growth rate was observed at 5% CO_2, while comparable performances were observed at all other percentage CO_2, however, atmospheric air achieved doubling time of 28 hr. Low level of CO_2 available for driving the metabolic activities required for cell divisions was thought to have led to elongated doubling time. This subsequently leads to reduced rate of photon capture and loss of more photon energy. Pigments concentration showed no significant variation across all percentage CO_2 tested (Figure 3.11 (A)). Likewise total lipids was maximum between 0-5% CO_2 and above this range, no significant difference was observed as shown in Figure 3.11 (B).

3.5.3   Effect of CO_2 Levels on Fatty Acid Composition

Analysis of FAME derived from *C. sorokiniana* lipid shows a high potential for biodiesel production. The unsaturated, especially the polyunsaturated FAMEs have lower melting temperatures which improve the low-temperature utilisation of biodiesel (Tang et al., 2011). Monounsaturated and saturated fatty acids with carbon chain length in the range C16–C20 were considered for comparison, since these groups have been identified previously as best suited for biofuel production (Chader et al., 2011; Li et al., 2013)**.**

For the different esters evaluated, results at 10% CO_2 enrichment showed the highest FAME concentrations for the most prevalent PUFA. For all the other CO_2 concentrations tested the FAME concentrations were not significantly different. FAME production under atmospheric air was lowest in all the tested fatty acid methyl esters except heptadecanoic acid (Figure 3.12). For the accumulation of high amounts of FAME, 5–20% CO_2 appears to be the best range although biomass productivity decreases at the higher CO_2 levels.
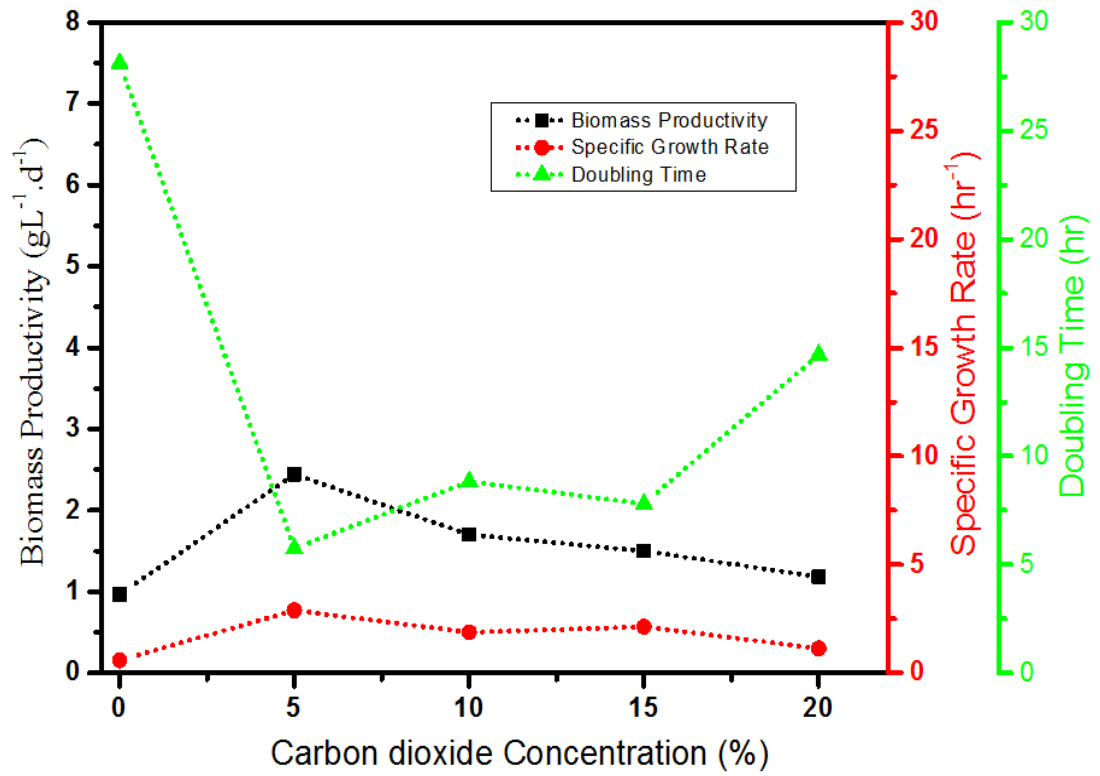
Figure 3.10: Effect of headspace CO_2 concentration on culture kinetics of *C. sorokiniana.* biomass productivity. As described in Section 2.
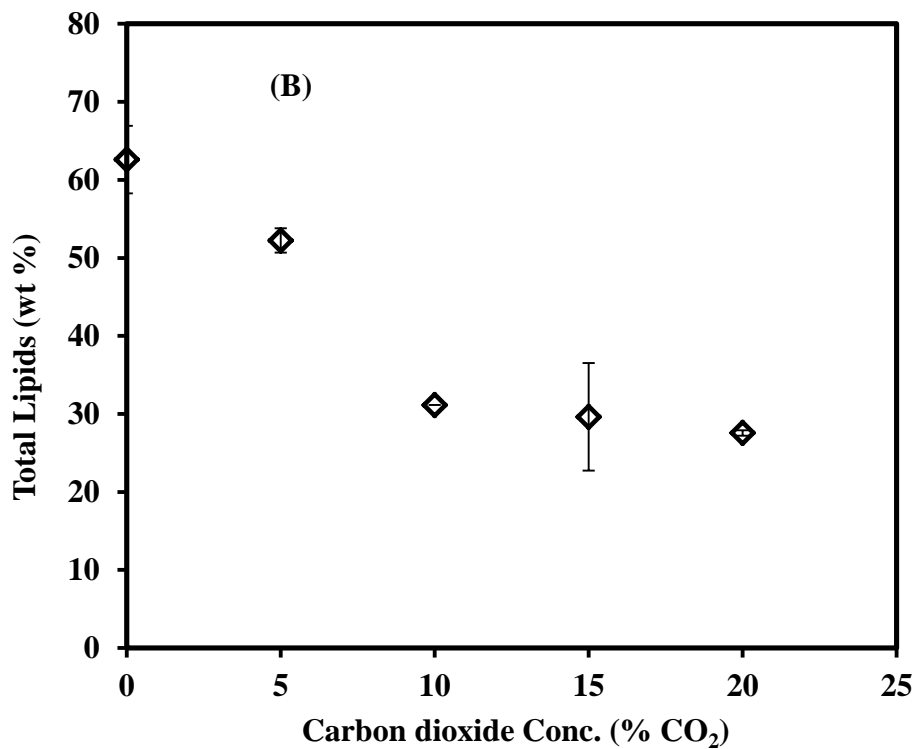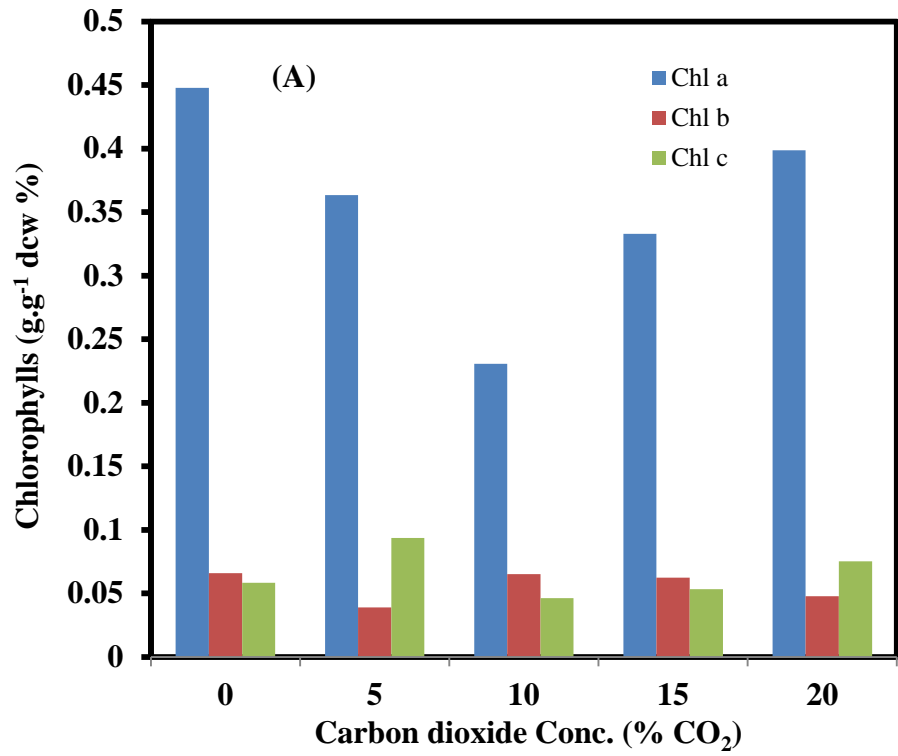
Figure 3.11: Effect of headspace CO_2 concentration on *C. sorokiniana* culture. (A) Chlorophyll concentration. (B) Percentage total lipids produced in at different shaking frequency. Error bars represent standard deviation about the mean (n=3). Experiment performed as described in Section 2.9.3.
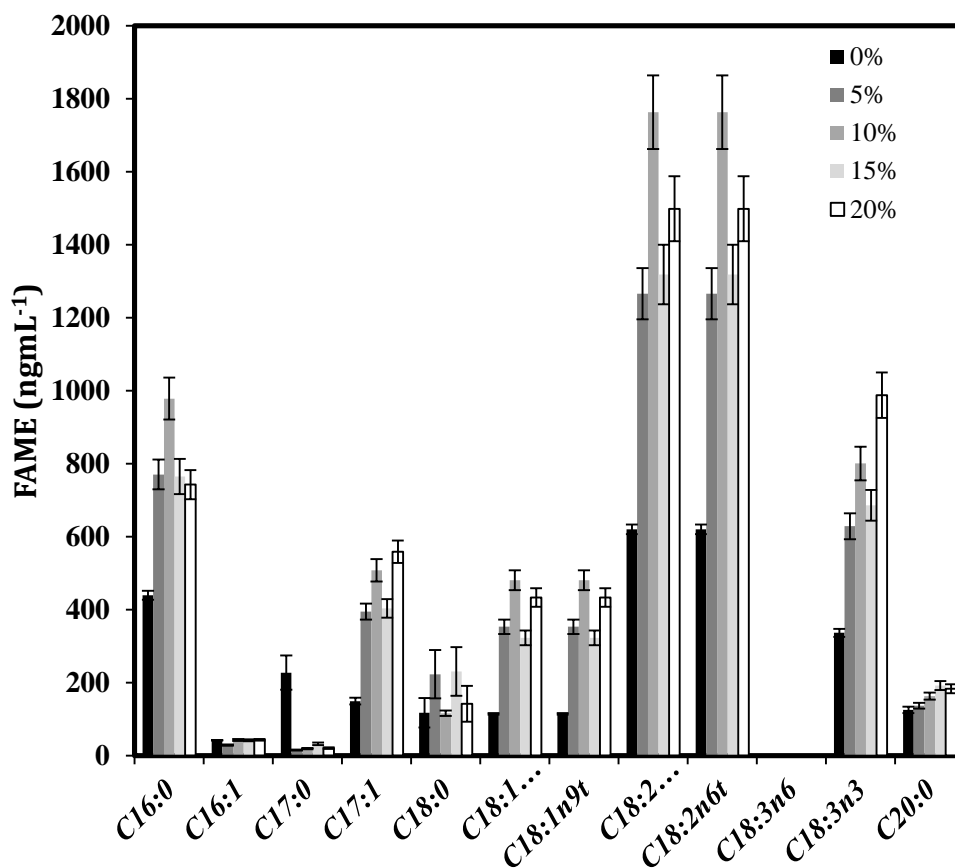
Figure 3.12: FAME ester derivatives of *C. sorokiniana*. Error bars represent one standard deviation about the mean (n=3). Experiment performed as described in Section 2.9.5. FAME samples taken from cells cultured as shown in Figure 3.10. FAME analysis performed as described in Section 2.9.3.

3.6   Summary

As described in Section 3.1.2, the aim of this Chapter was to design a novel, orbitally shaken miniature photobioreactor technology, suitable for early stage and parallel evaluation of microalgal cultivation conditions. This was achieved and the experimental system designed is shown in Figure 2.3. The geometries of the individual wells investigated are shown in Figure 3.2. In terms of the engineering environment within the mPBr, orbital shaking provides rapid mixing, effective gas-liquid mass transfer (Figure 3.4) and a relatively constant light intensity throughout each well (Figure 2.3). Oxygen mass transfer coefficients were in the range 20-90 h^{-1} and increased with orbital shaking frequency. Light intensity could be controlled between 100 – 1800 $\mu mol sm^{-2}s^{-1}$. The shaker incubator platform provides uniform control of light intensity, CO_2 levels, temperature and liquid evaporation across multiple plates (Figure 2.3).

The utility of the system was illustrated for investigation and optimisation of the culture conditions of *C. sorokiniana* (Table 3-1/Figure 3.10). It was shown that the medium formulation could be investigated in order to provide better control of culture pH, between pH 6-7 (Figure 3.5) and overall a 6-fold increase in biomass growth (Figure 3.7) was achieved compared to the starting literature conditions (Table 3-1). In order to further understand the robustness of the media reformulated to maintain a constant culture pH it would be interesting to repeat these experiments using higher cell density fed-batch culture approaches.

The cell densities achieved were comparable to those reported for *C. sorokiniana* on a similar medium in a flat plate photobioreactor (Cuaresma et al., 2009). In terms of practical application the mPBr shaker platform enables higher throughput evaluation of microalgae growth kinetics than current shake flask systems with an approximately 20-fold reduction in material requirements. Further research into micro-probes that could be incorporated into the microwell will further strengthen the high-throughput capabilities and ensure online data capture and potential control. In addition, utility of the small scale technology for phototrophic cultivation further provides insight into future developments in terms of geometry re-designs and automation capabilities. This equally implies the development of downstream

technologies which corresponds to the upstream and specifically for microalgae. Worth quantifying is the economic advantage the mPBr provides for early stage bioprocess development of microalgae for pharmaceutical, biofuel and other purposes.

The next Chapter addressed scale translation and the ability of the mPBr to accurately mimic culture conditions in larger scale photobioreactor designs. To facilitate this work the orbital shaking platform described in this Chapter will be redesigned in order to also accommodate a single-use culture bag for use as a novel photobioreactor as described in Section 2.3.

4. DESIGN OF AN ORBITALLY SHAKEN SINGLE-USE, PHOTOBIOREACTOR FOR SCALE-UP STUDIES

4.1 Introduction

4.1.1 Single-Use Bioreactor Technology

Single-use bioreactors (SUBs) have found increasing applications in recent years (Hillig et al., 2014b; Zhang et al., 2009). SUBs are typically made from polyethylene or polyester multi-layer films and are provided pre-sterilised by gamma irradiation (Singh, 1999) with working volumes in the range 1 - 2000 L (Brecht, 2009). The original SUBs operated on a slowly rocked platform designed to induce a wave-type motion in the culture fluid promoting mixing and gas mass transfer. The main applications include early stage mammalian cell culture process development and inoculum generation (Kalmbach et al., 2011; Oncül et al., 2009). The most recent SUB designs resemble conventional stirred tank bioreactors (Figure 1.5) and are now commonly used for therapeutic antibody and vaccine production.

For phototropic microalgae cultivation under contained conditions, most modern photobioreactors (PBr) are based on air lift designs with light being supplied externally or radiated internally as described in Section 1.2.3. In addition to the requirements for good mixing and gas mass transfer, adequate light must be supplied to enable efficient photosynthesis. Since the penetration of light into a culture fluid follows an exponential decay function, it is desirable to have short light paths at constant distance from the light source as described in Section 1.2.2.1. In this regard orbital shaking of a single-use photobioreactor (SUPBr) bag could provide a number of advantages as illustrated in Figure 4.1 (A&B) since a shorter and more constant light path length is maintained.

4.1.2   Aim and Objectives

As outlined in Section 1.5, the aim of this Chapter is to design and evaluate a novel, orbitally shaken single-use photobioreactor technology for phototrophic microalgae cultivation. The shaken SUPBr is considered a useful tool for early stage algae cultivation increasing experimental throughput and reducing operating costs by overcoming the need for bioreactor cleaning and sterilisation (Lehmann et al., 2013; Singh, 1999). In particular, interest was focused on the engineering characterisation of this novel SUB and how the hydrodynamic environment impacts on fluid mixing and algal growth. These studies build on a number of recent works, that have addressed fluid mixing in a range of orbitally shaken or rocked SUBs of different geometries and scales (Betts et al., 2006; Kalmbach et al., 2011; Micheletti et al., 2006; Oncül et al., 2009; Tan et al., 2011; Tissot et al., 2010). The specific objectives of this Chapter are to:

- demonstrate the utility of the single-use CultiBag^{TM} as a potential photobioreactor on a shaken orbital platform.

- characterise the novel SUPBr design over a range of operating conditions and set points.

- quantify the impact of fluid hydrodynamics on key engineering characteristics of the SUPBr including mixing and gas-liquid mass transfer.

- establish optimal culture condition for microalgae cultivation.

- establish predictive scale-up criteria from mPBr discussed in Chapter 3 and the SUPBr established in this Chapter.
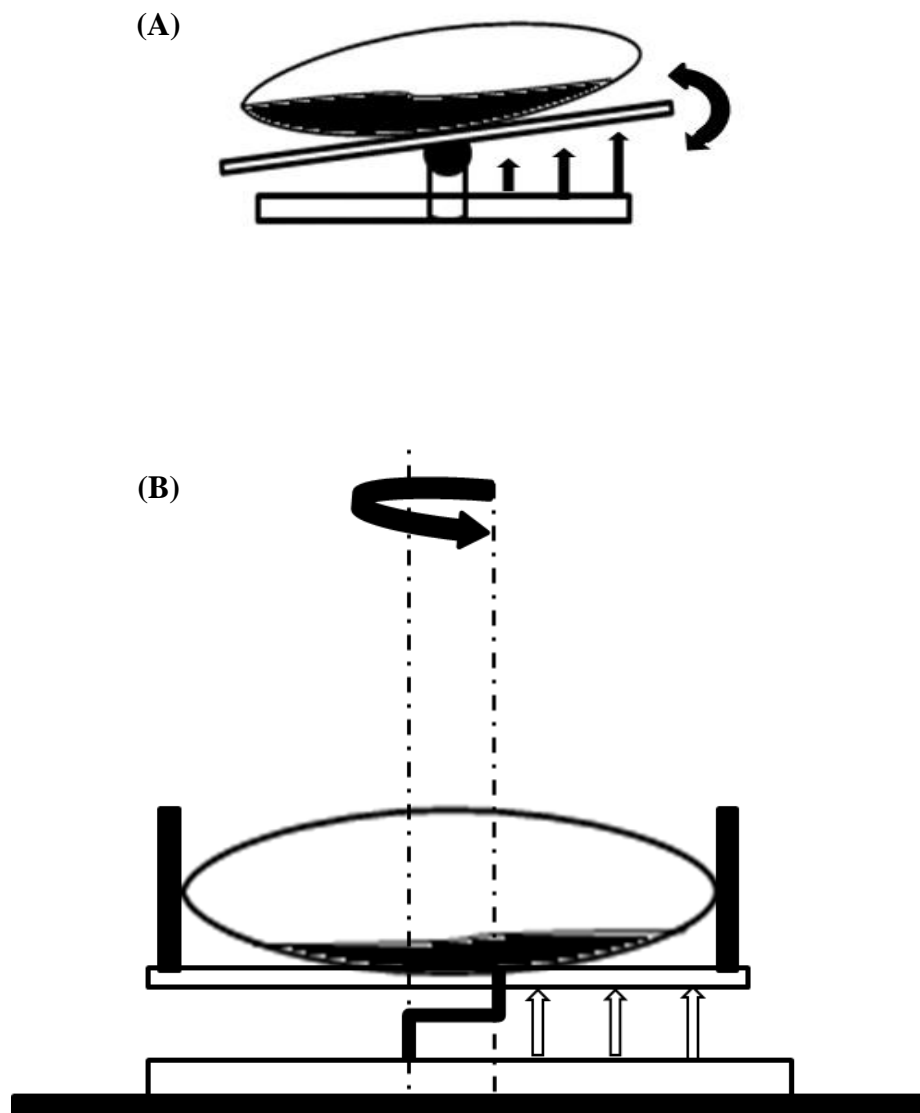
Figure 4.1: Comparison of (A) a rocked, wave-generating platform and (B) an orbitally shaken platform for single-use photobioreactor agitation. Arrows indicate the more uniform and consistent light path length achieved using orbital shaking. Experimental set-up as described in Section 2.3.1.

4.2   Visualisation of Fluid Motion in the SUPBr

The fluid hydrodynamics of a rectangular single-use bioreactor, mounted on an orbitally shaken platform, have not previously been investigated. Consequently, initial studies used a high speed video camera (Section 2.4.4) to record fluid motion following addition of a dye tracer once a pseudo steady-state flow pattern is established. Image J software was then used to process still images captured at different angles of rotation and to map-out the dispersion of the dye as illustrated in Figure 4.2. Prior to the analysis, the time taken to achieve homogenous dispersions with different sample injection volumes (5% of total volume) was established as shown in Appendix Figure II.4. At low shaking frequencies ($N < 90$ rpm), the fluid was observed to move in an orbital motion in time with the motion of the platform (Figure 4.2 (A)). The tracer dye indicated that the fluid flowed sequentially into each corner of the bag during a single orbital rotation gradually becoming more dispersed. This suggests an 'in-phase' fluid motion analogous to that seen in shaken conical flask and microwell bioreactors (Büchs et al., 2001).

At intermediate shaking frequencies ($N > 90$ rpm to $N < 180$ rpm) there was evidence of a transitional flow regime (Figure 4.2 (B)), where the fluid flowed between opposite sides of the SUPBr. At high shaking frequencies ($N \geq 180$ rpm) the Image J analysis indicated a centrally localised region of turbulent fluid (Figure 4.2 (C)). Here the coloured dye dispersed in multiple directions simultaneously irrespective of the angle of orbital rotation until it was evenly distributed throughout the entire volume of the fluid. This is similar to the 'out-of-phase' phenomena seen in other shaken bioreactor formats (Büchs et al., 2001; Büchs et al., 2007). During these experiments, it was noticed that the height attained by the liquid inside the SUPBr was strongly correlated with the shaking frequency and the observed fluid flow regime. This was subsequently used as a quantitative metric to explore the observed flow transitions in more detail.
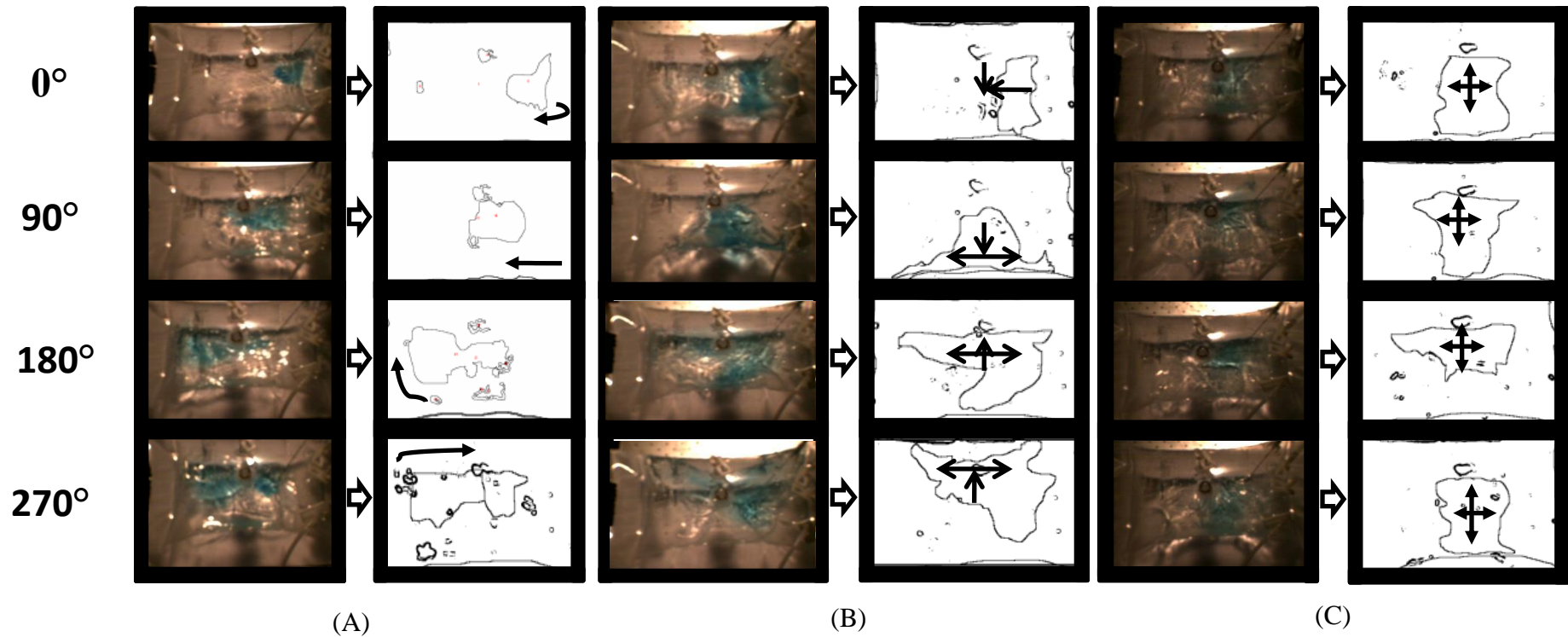
Figure 4.2: Visualisation of fluid hydrodynamics and schematic representation of dye dispersion in an orbitally shaken Biostat Cultibag^{TM} showing (A) in-phase fluid motion at N = 50 rpm (B) transitional fluid motion at N = 90 rpm and (C) out-of-phase fluid motion at N = 180 rpm. Arrows indicate generalised direction of liquid flow as observed in the continuous video footage. Experimental conditions: V_f = 0.25, do = 25 mm. Experiment performed as described in Section 2.4.4.

4.3 Determination of In-Phase and Out-of-Phase Operating Regimes

The fluid dynamics of orbitally shaken bioreactors of various geometries have previously been characterised by the movement of the fluid relative to the rotating shaken platform (Funke et al., 2009). In-phase conditions result in short mixing times and reduced hydrodynamic shear on the cells, while out-of-phase conditions are characterised by poor mixing and gas-liquid mass transfer (Büchs et al., 2001). In order to better understand these phenomena in the novel SUPBr, the maximum fluid height achieved during shaking was determined from the captured video images as shown in Figure 4.3 (A&B). The earlier visual observations indicated that the height achieved was a function of shaking frequency, shaking diameter and fluid fill volume. The measured heights were normalised as shown in Appendix Figure II.5 and plotted against shaking frequency as shown in Figure 4.3 (A&B) at different orbital diameters.

For both shaking diameters and the different fill volumes investigated, the data suggests an almost linear increase in the dimensionless height for shaking frequencies of 40 - 90 rpm. Immediately after 90 rpm the height attained decreases and attains a more or less constant level for the majority of the conditions studied. Superimposed on Figure 4.4 (A&B) are the boundaries for the in-phase, transitional and out-of-phase flow patterns described in Section 4.1.2. These clearly indicate that the range of shaking frequencies over which there is a linear increase in the normalised liquid height corresponds to the in-phase flow regime while out-of-phase conditions resulted in a more or less constant liquid height. It therefore becomes interesting to study the impact of these different flow regimes on fluid mixing and algal growth.

The influence of liquid height on light attenuations is shown in Figure 4.5. The liquid height is equivalent to the light path length. This data could provide useful insight for modeling the relationship between photosynthetic rate and light intensity in the SUPBr as previously discussed in Section 1.2.2.1.
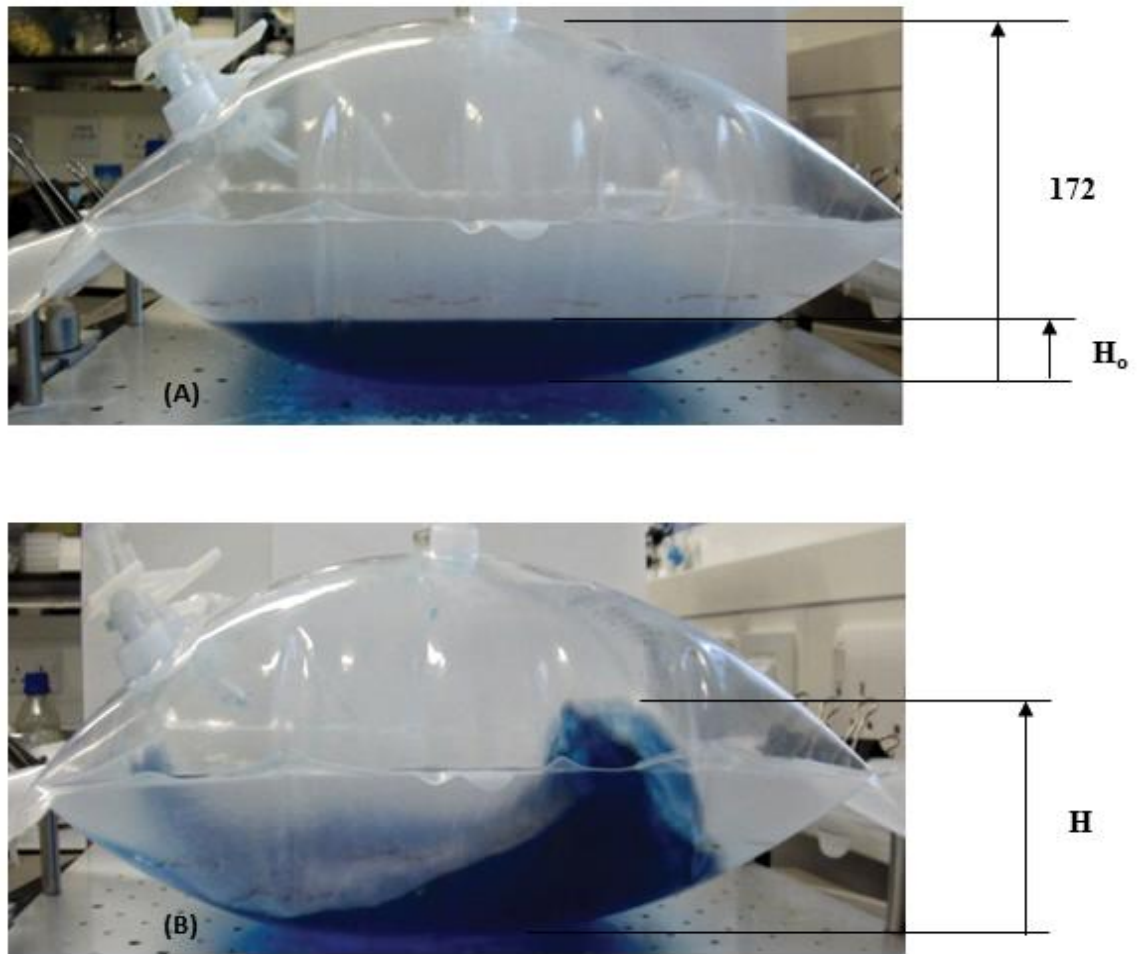
Figure 4.3: Example images showing (A) the single-use photobioreactor before orbital shaking commenced and (B) the fluid motion and liquid height attained under the experimental conditions: N = 220 rpm, V_f = 0.5 and d_o = 25 mm. H_o and H represent the height attained by the liquid before and after mixing commenced respectively. Experiment performed as described in Section 2.4.5.
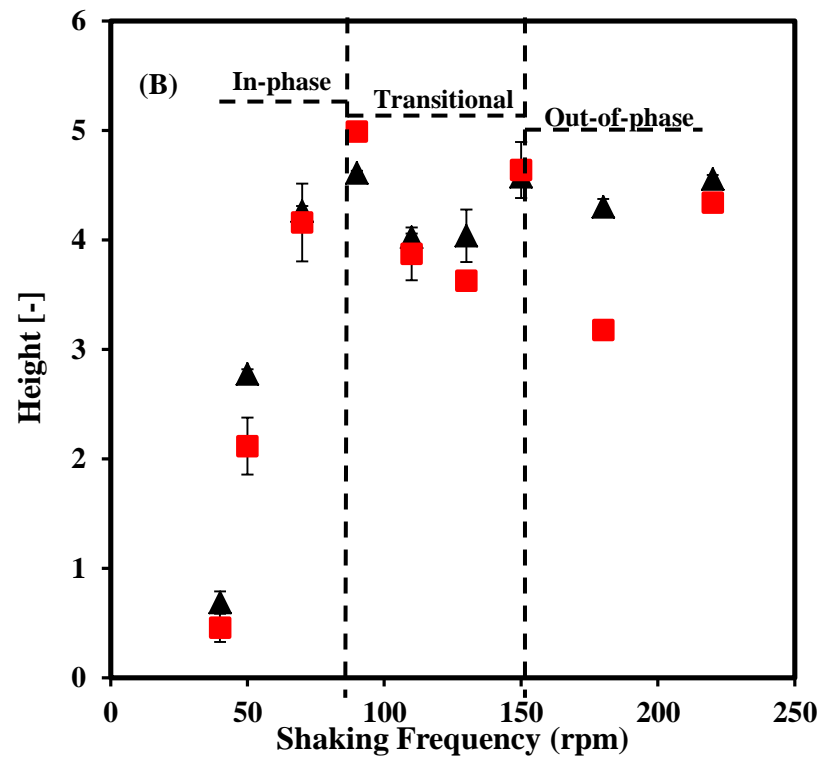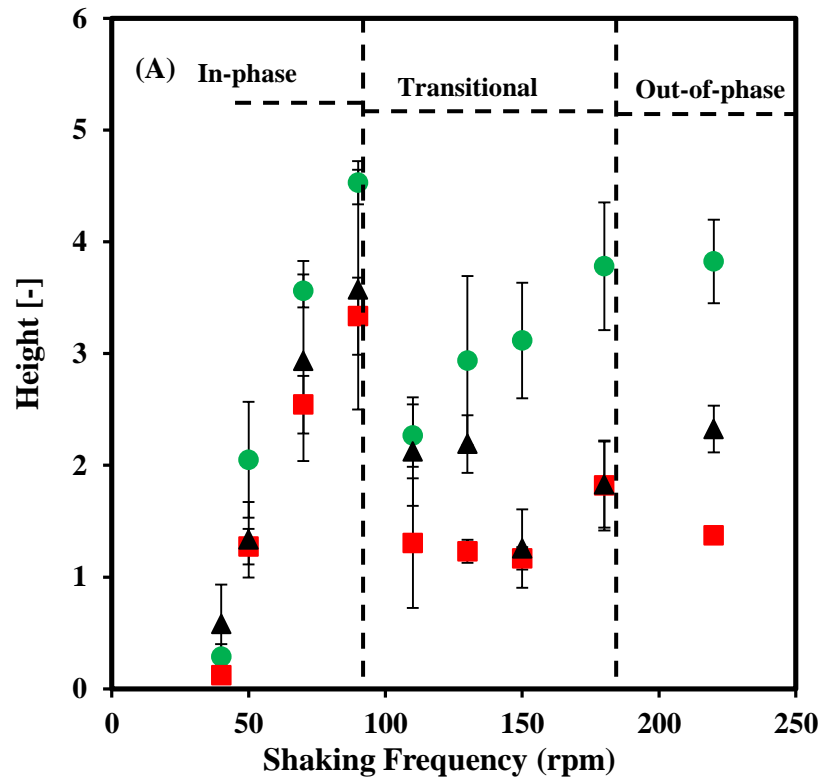
Figure 4.4: Effect of shaking frequency on fluid hydrodynamics in the single-use photobioreactor as determined by the maximum height attained by the shaken liquid (A) at $d_o = 25$ mm and (B) at $d_o = 50$ mm. Fill volume fractions (V_f) used are: (●) 0.5 (■) 0.25 (▲) 0.1. Error bars represent one standard deviation about the mean (n=3). Experiments performed as described in Section 2.4.5.
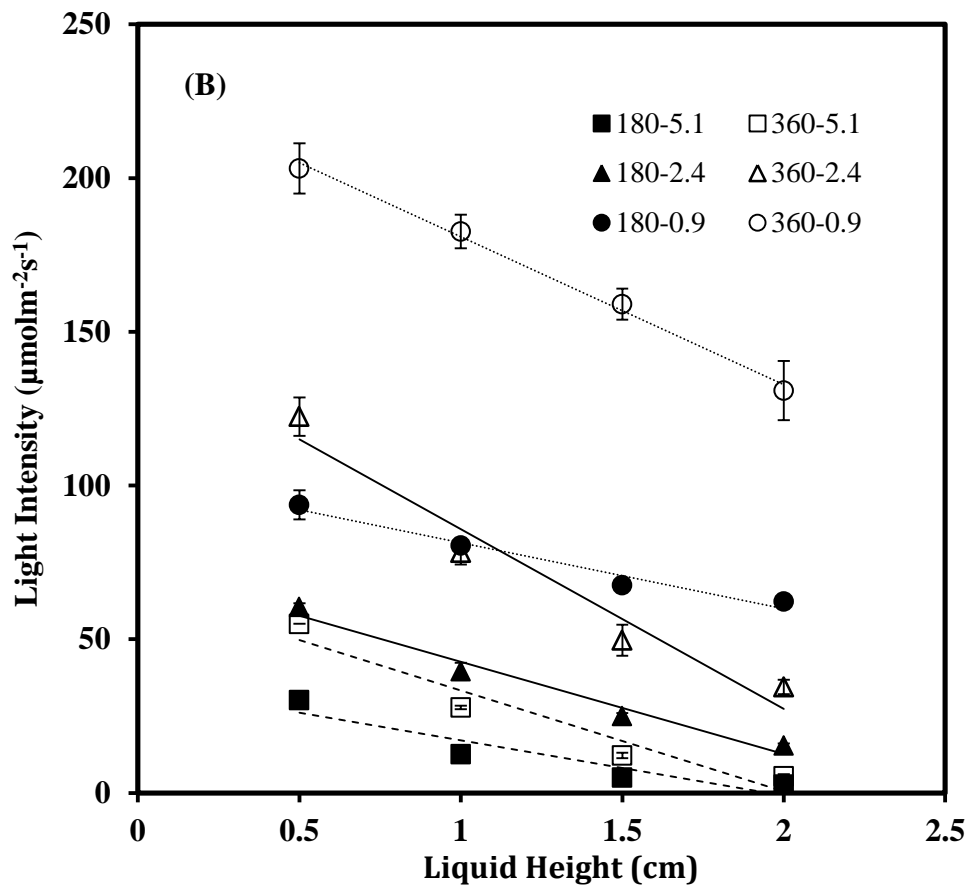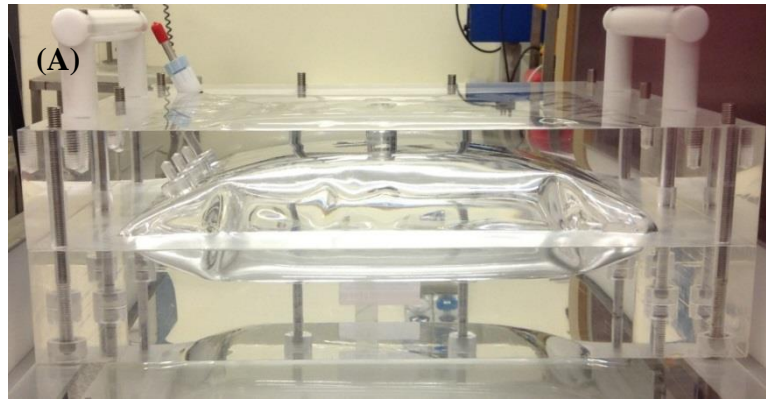
Figure 4.5: Effect of liquid height on light saturation in the SUPBr system. (A) Photograph of the solid mimic of 2 L CultiBag[TM] made from Perspex and (B) Light attenuation in the mimic SUPBr at varying broth height. Experimental conditions are: LI = 240 $\mu molm^{-2}s^{-1}$, N = 180 rpm, d_o = 25 mm. 0.5, 1, 1.5 and 2 cm liquid height is corresponds to 250, 500, 750 and 1000 mL liquid volume. All height measurements were taken from the center of the mimic SUPBr. Error bars represent one standard deviation about the mean (n=3). Experiment performed as described in Section 2.3.1.

4.4   Quantification of Fluid Mixing Time

Rapid fluid mixing is normally a pre-requisite for effective bioreactor operation. Effective mass and heat transfer is generally achieved in bioreactors with shorter mixing times (Micheletti et al., 2006; Tan et al., 2011) and mixing time itself has been found to be useful as a scale–up criterion in several bioreactor geometries (Betts et al., 2006). Prior to mixing time quantification, verification of the effect of injection port used and the volume and molar concentration of acid and base added were investigated. Based on the analysed data in Appendix Figure II.6, mixing time was observed to reduce with increases in injection volume of the acid. However, no significant difference was observed with the molar concentration (over the range 0.025-10 M) or injection ports used. Subsequently, mixing times were quantified using the optimised pH-tracer conditions, as described in Section 2.4.3, at varying shaking frequencies (40 - 220 rpm), fill volumes ($V_f = 0.1 - 0.5$) and orbital shaking diameters (12.5, 25 and 50 mm) as shown in Figure 4.6 (A&B).

 At the lowest shaking frequencies investigated ($\leq$50 rpm) the mixing time was extended, up to 230 s, in most cases. At shaking frequencies $\geq$50 rpm the mixing time was found to become rapid and approximately constant in the range of $15 - 30$ s for all the fill volumes investigated. Furthermore, comparisons of mixing times determined at different shaking diameters were similar with only slightly higher average values at the smaller shaking diameters. Probably the most interesting observation, however, was that at $\geq$50 rpm, mixing times were low and independent of whether the SUPBr was shaken under in-phase or out-of-phase operating conditions.

Similar mixing times were found using a more conventional wave mixing platform for 2 - 20 L bags based on computational fluids dynamics simulations (Oncül et al., 2009). In terms of selecting operating conditions in the SUPBr for algal cultivation, operation at shaking diameters of 25 or 50 mm and at lower fill volumes, i.e. 0.25, are recommended given the rapid mixing, large gas-liquid area per unit liquid volume for gas mass transfer and the reduced light path length for light penetration into densely growing cultures.
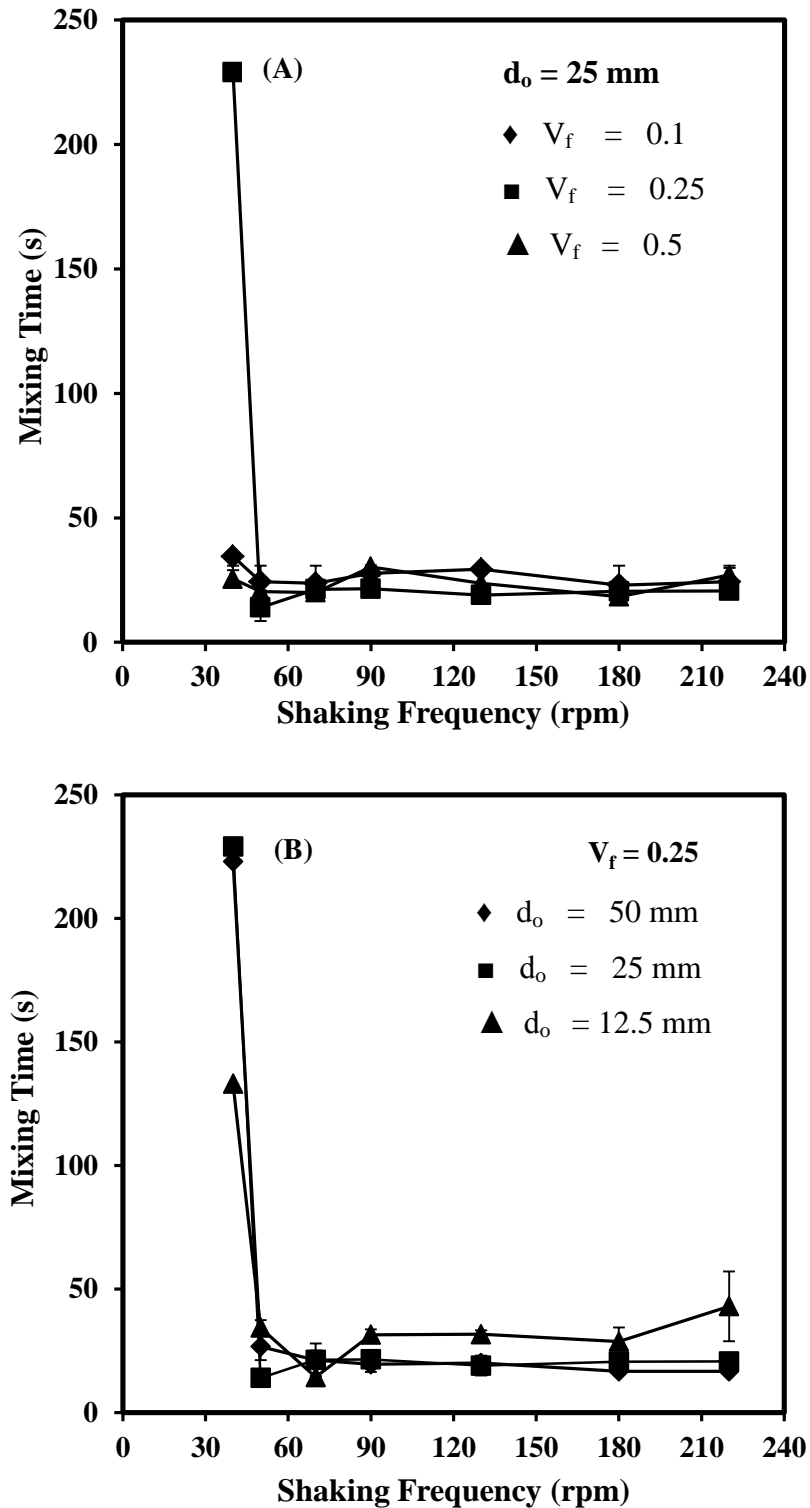
Figure 4.6: Effect of shaking frequency, fill volume (V_f) and orbital shaking diameter (d_o) on liquid mixing time in the SUPBr. (A) Mixing time (t_m) at $d_o = 25$ mm and varying fill volume, and (B) t_m at $V_f = 0.25$ with varying d_o. Error bars represent one standard deviation about the mean (n=3). Experiments performed as described in Section 2.4.3.

4.5 *C. sorokiniana* Growth Kinetics in the SUPBr

4.5.1 Effect of Operating Conditions on Growth Kinetics

The growth kinetics of *C. sorokiniana* were subsequently examined over a range of SUPBr operating conditions. *C. sorokiniana* was chosen because of its robustness and easy handling (Li et al., 2013). Cultures were performed at a constant light intensity of ~ 180 ± 20 $\mu molm^{-2}s^{-1}$ using air enriched with 2% v/v CO_2 as carbon source which was provided via head space surface aeration. The growth medium was modified, by replacing the tris-acetate with 0.2 M tris-base, in order to buffer the pH during culture between 7.04 – 5.80 (Kumar and Das, 2012). Early stationary phase cultures were used for inoculating the shaken SUPBr (Mattos et al., 2012) and nitrogen concentration was kept low to allow early production of lipid at the mid-exponential phase; a technique widely used to ensure high biomass yield and lipid production with a high linoleic acid concentration which is a key requirement for biodiesel production (Chader et al., 2011; Cordero et al., 2011).

Biomass concentration profiles at different shaking frequencies showed a short log phase during day one followed by a stationary phase after three days. Final biomass yield was 6.6 gL^{-1} at 180 rpm (Figure 4.7 (A)). Shaking frequencies above this tend not to have a significant influence on growth kinetics at constant light intensity and working volume. As shown in Figure 4.7 (B) the initial ammonium concentration (7 mM) was sufficient to support cell growth over day 1 – 2 and was depleted by day 2 – 3 after which lipid accumulation occurred. Figure 4.7 (B) also shows pH was maintained constant between 7.0 – 5.8.
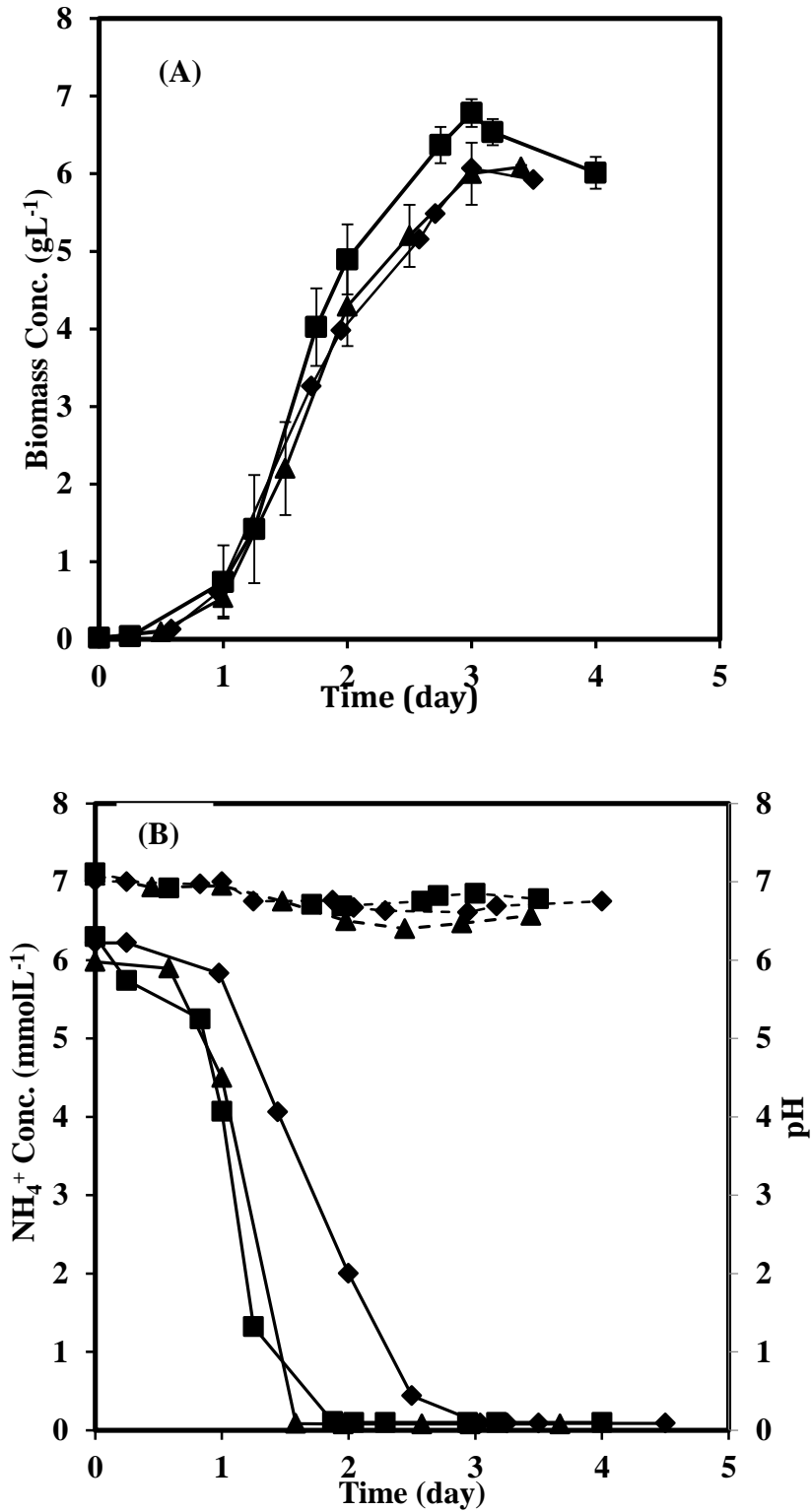
Figure 4.7: Impact of mixing time and fluid hydrodynamic on growth kinetics of *C. sorokiniana*. (A) Biomass concentration, (B) NH_4^+ utilisation and pH at $V_f = 0.25$ and different shaking frequencies: (▲) 70 rpm (♦) 90 rpm (■) 180 rpm ($V_f=0.5$). Error bars represent one standard deviation about the mean (n=2). Experiment performed as described in Section 2.5.3.

4.5.2   Effect of Fill Volume on Culture Kinetics

Fill volume was expected to have a significant influence on SUPBr performance due to increase in the liquid depth and reduction in surface area to volume ratio at higher fill volumes. As shown in Figure 4.8 (A), doubling the total liquid volume (V_f increases from 0.25 to 0.5) led to a decrease in algal growth rate and yield resulting in a calculated decrease in biomass productivity of approximately 35 - 40%. Other effects at increased cell density include cell shadowing that can lead to reduced cell growth rate (Cuaresma et al., 2009). The decreased biomass growth rate also corresponded to a decreased rate of nitrogen utilisation. With the nitrogen source becoming limiting in the batch experiments, increased lipid productivity was observed corresponding decreases in biomass and chlorophyll productivities. At all the conditions investigated, maximum chlorophyll concentration varies between 20 – 25 mgL^{-1}.

However, the rate of chlorophyll formation was lower at higher fill volume (Figure 4.8 B). The percentage total lipid formation across the various shaking frequencies range between 18 - 28% (as shown in Figure 4.8 C), comparable to results obtained by Wan et al. (2011) where, *C. sorokiniana* was cultured mixotrophically with zero initial glucose concentration. Nitrogen deprivation has been reported to improve the lipid content (Hsieh and Wu, 2009) which was also confirmed by the result obtained in this work. The total lipids extracted from *C. sorokiniana* have been estimated to consist of approximately 93% of neutral lipids with the rest being polar lipids (Zheng et al., 2013).

Evaluation of different growth parameters as shown in Table 4-1 reveals that at constant fill volume and light intensity, no significant differences were observed in growth at different shaking frequencies up to 180 rpm. This agrees with the mixing time studies discussed previously in Section 4.4. However, operation at a higher frequency of 220 rpm resulted in a slight reduction of biomass concentration and PE. Doubling the fill volume at the optimum shaking frequency (180 rpm) resulted in significant reduction in all the growth parameters assessed. These results further show how important are light path length, surface area to volume ratio and fluid
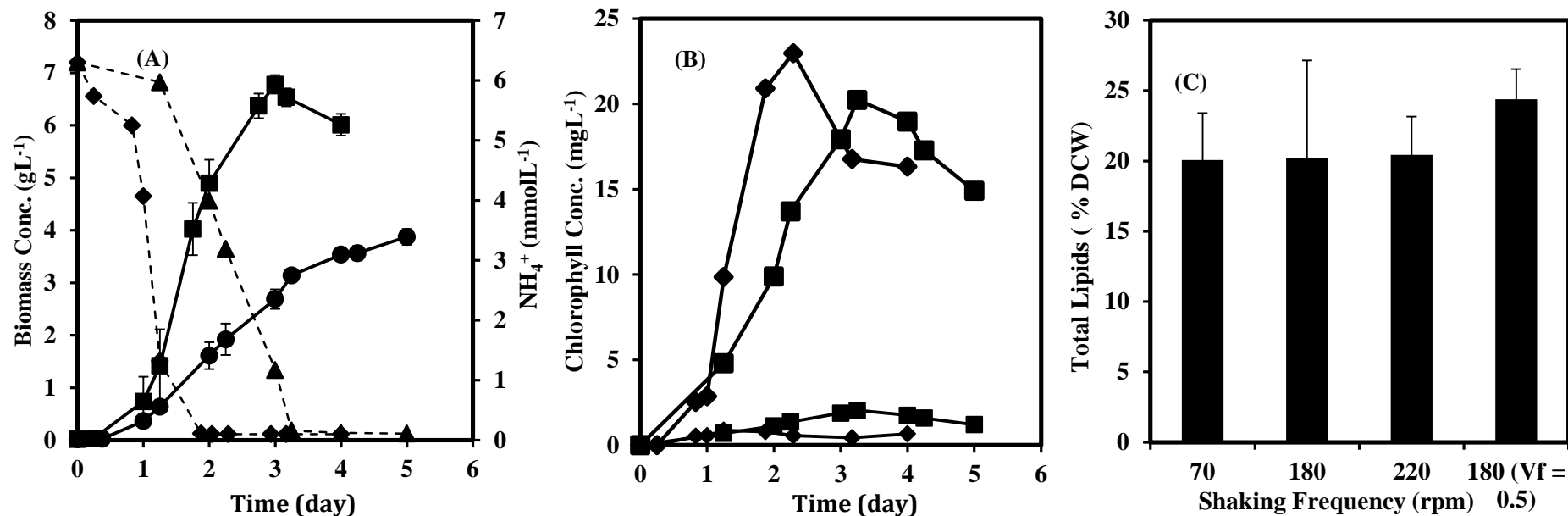
Figure 4.8: (A) Effect of fill volume on growth kinetics and Nitrogen consumption by *C. sorokiniana*. Biomass concentration at (●) V_f = 0.5 (■) V_f = 0.25. and Nitrogen uptake kinetics at (▲) V_f = 0.5 (♦) V_f = 0.25. (B) Effect of fill volume on Chlorophyll a production at (■)V_f = 0.5, (♦)V_f = 0.25) and carotenoids concentration at (■)V_f = 0.5, (♦)V_f = 0.25} at N = 180 rpm. (C) Effect of fill volume on total lipid produced per dry cell weight, DCW (gL^{-1}). Experiments performed at V_f = 0.25 unless otherwise indicated. Error bars represent one standard deviation about the mean (n=2). Experiment performed as described in Section 2.5.1 & 2.5.3.

Table 4-1: Summary of *C. sorokiniana* growth kinetics at different shaking frequencies and fill volumes in a 2 L orbitally shaken Biostat Cultibag^{TM} (180 μmolm^{-2}s^{-1}).

Growth Parameters	Fill Volume					
	$V_f = 0.25$					$V_f = 0.50$
	70 rpm	90 rpm	130 rpm	180 rpm	220 rpm	180 rpm
Specific growth rate (h^{-1})	0.05	0.05	0.09	0.11	0.12	0.02
Biomass conc. (gL^{-1})	6.0	6.1	6.1	6.6	6.2	4.1
Biomass productivity (gL^{-1}d^{-1})	2.0	2.0	2.0	2.3	2.1	0.8
Photosynthetic efficiency (%)	17.7	16.5	16.5	18.4	17.0	6.7
$Y_{x,E}$ (gmolphotons^{-1})	1.6	1.6	2.8	3.8	3.9	NA

hydrodynamics in SUPBr design. The biomass yield on photon absorption ($Y_{x,E}$) shows an increase with increasing shaking frequency and may be due to increased exposure of the cells to light.

Similar results were reported by Cordero et al. (2011), using Roux flasks laterally illuminated using a mercury halide lamp at varying luminous intensity. Comparison of the specific growth rate and biomass concentration varied between $0.05 - 0.13$ h^{-1}, and $6.0 - 9.0$ gL^{-1} respectively. Despite slight differences in some of the operating parameters used improved culture performance was observed in the SUPBr as shown in Table 4-2. In addition, studies showed that cultivation of *C. sorokiniana* in a flat panel photobioreactor under continuous conditions gave a biomass concentration of 5.7 gL^{-1} at the lowest dilution rate (Cuaresma et al., 2009). Comparing the SUPBr data with other optimised photobioreactors of different geometry suggests the SUPBr offers potential advantages in terms of biomass productivity, reduction in process time and reduced chances of contamination.

4.6   Scale-up from mPBr to SUPBr

Having established the mPBr technology in Chapter 3 and the larger SUPBr technology in this chapter, it becomes interesting to consider predictive scale translation between the two culture formats. Comparisons of culture performance between the mPBr and SUPBr were thus undertaken using the identified scale-up criteria previously discussed in Section 1.4. The selected scale-up parameters and their values are listed in Table 4-3. Based on these conditions culture kinetics of *C. sorokiniana* in the two culture system are as shown in Figure 4.9 (A-C). The results indicate similar growth rates and yields and comparable offline measurements for pH and ammonium depletion Figure 4.9 (B).

Table 4-2: Comparison of *C. sorokiniana* biomass production in different photobioreactor geometries (S/V = 470 m^{-1}, PE = 18.41 %).

PBr mixing technique	S/V (cm^{-1})	Irradiance (μmolm^{-1}s^{-2})	Percentage CO$_2$ (%)	PE (%)	Biomass concentration (gL^{-1})	References
Bubble column	0.57	100	5	NA	2.9	Kumar and Das, (2012)
Air lift	0.57	100	5	7.1	4.4	Kumar and Das, (2012)
Air lift	NA	300	2	NA	1.5	Chiu et al., (2008)
Air lift	NA	Solar radiation	5	NA	1.5-3.5	Ugwu et al., (2005)
Shaken SU	0.36	180	2	11.7	6.0 – 6.6	This study

NA= Not available; SU = single use

Table 4-3: Identified scale-up criteria for comparison of culture performance.

Engineering conditions	Light intensity (μmolm^{-2}s^{-1})	S:V (cm^{-1})	Path length (cm)	Flow regime	Carbon dioxide (%)
mPBr	180	1.1	1.7	Observed turbulence	2
SUPBr	180	1.2	1.5	Observed turbulence	2
Comments	Constant	Constant	Constant	Similar	Constant

Growth kinetics	Specific growth rate (h^{-1})	Biomass productivity (gL^{-1}d^{-1})	Chlorophyll productivity (mgL^{-1}d^{-1})	Biomass yield on light	Total lipids (% gg$_{dcw}$)
mPBr	0.1	2.1	8.0	8.7	NA
SUPBr	0.1	2.3	5.7	8.2	20
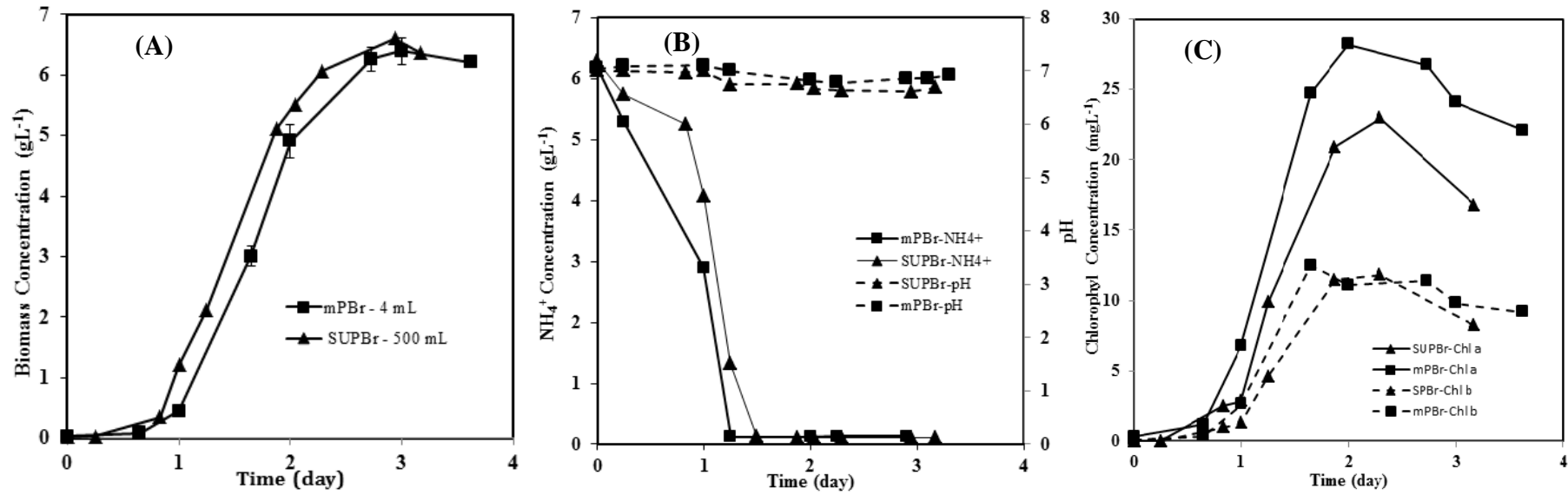
Figure 4.9: Comparable growth kinetics for scale translation of C. sorokiniana from 24-well mPBr (4 mL) to shaken SUPBr (0.5 L) at matched surface area to volume ratio, light intensity and path length. (A) Biomass concentration profiles (B) NH4+ concentration (C) Chlorophyll concentrations. Error bars represent one standard deviation about the mean (n = 3). Experiment performed as described in Section 2.5.

4.7   Fatty Acid Methyl Ester Composition

The lipid composition of the algae cultured under various conditions was also determined to ensure consistency. The different FAMEs analysed using GC-FID as described in Section 2.9.5, showed good reproducible chromatographs as shown in Appendix Figure II.7. The analysis were grouped based on the degree of saturation and unsaturation such as; saturated fatty acids (SFA), monounsaturated fatty acids (MUFA) and PUFA. For all the different culture conditions tested, palmitic acid methyl ester (PAME) was amongst the most prevalent. Approximately, $33 \pm 3.6\%$ PAME and $41.21 \pm 1.3\%$ SFA of the total identified FAME were produced as shown in Table 4-4. These results are comparable with those obtained by Lu et al., (2012) and Zheng et al., (2013) which are $36.1 - 42.8\%$ and 45.6% SFA respectively.

Work done by Cha et al., (2011), shows about two-fold increases in the SFA achieved under varied concentration of nitrate, with 86.3% of SFA produced at 0.18 mM nitrate concentration compared to the 7.5 mM ammonium salt employed in this study (Cha et al., 2011; Lu et al., 2012; Zheng et al., 2013). This could be indicative of the impact of nitrogen source and concentration on the SFA production. Nonetheless, this study shows that the total amount of SFA produced is independent of the fill volume and shaking frequency.

Unsaturated fatty acids correspond to ~ 60.6% of total FAME. These comprise of the MUFA and PUFA with individual percentage compositions in the range of $22.5 - 26.7\%$ and $30.5 - 38.2\%$ respectively across all conditions. FAME with C16 and C18 chain lengths have found more direct application to the biofuel industry than others. Estimation of the total percentage of C16 and C18 carbon chain length shows 98% of total FAME with PAMEs (C16:0) and linoleic acid methyl esters (C18:2n6c) forming the major constituents for biodiesel production. From the results shown (Table 4-4), the biodiesel component of the FAME increased with increasing frequency up to 180 rpm. This suggests that under higher shaken frequencies, higher fatty acids methyl esters used as biofuels are produced. On the contrary, the effect of fill volume did not have an effect on the percentage composition of the C16 – C18 components. Other FAME produced of pharmaceutical importance includes capric

Table 4-4: Impact of SUPBr operating conditions on FAME produced by *C. sorokiniana*. Error represents one standard deviation about the mean (n=3). FAME analysis performed as described in Section 2.9.5. Samples analysed from Figure 4.8.

Fatty Acids (wt % of identified FAME)	Structural formulae	Shaking frequency (rpm) ($V_f = 0.25$)			180 rpm ($V_f = 0.5$)
		70	180	220	
Butyric Acid	C4:0	0.54 ± 0.06	0.22 ± 0.14	0.42 ± 0.01	0.73 ± 0.02
Caprylic Acid	C8:0	0.13 ± 0.02	0.06 ± 0.00	0.10 ± 0.01	0.12 ± 0.00
Capric Acid	C10:0	8.51 ± 2.76	0.16 ± 0.10	1.62 ± 0.25	0.82 ± 0.06
Undecanoic Acid	C11:0	0.33 ± 0.05	0.22 ± 0.01	0.33 ± 0.03	0.48 ± 0.00
Lauric Acid	C12:0	0.11 ± 0.04	0.17 ± 0.15	0.09 ± 0.04	0.12 ± 0.00
Tridecanoic Acid	C13:0	1.80 ± 0.85	0.06 ± 0.00	0.29 ± 0.06	0.20 ± 0.02
Myristic Acid	C14:0	0.56 ± 0.05	0.56 ± 0.02	0.64 ± 0.05	0.83 ± 0.01
Myristoleic Acid	C14:1	0.34 ± 0.03	0.00 ± 0.00	0.33 ± 0.02	0.06 ± 0.00
Palmitic Acid	C16:0	27.18 ± 14.5	35.12 ± 1.42	33.80 ± 2.07	36.71 ± 0.71
Palmitoleic Acid	C16:1	3.39 ± 0.30	3.60 ± 0.15	4.42 ± 0.28	5.16 ± 0.11
Hepatdecanoic acid	C17:0	0.36 ± 0.03	0.33 ± 0.01	0.22 ± 0.01	0.22 ± 0.01
cis-10-Hepatdecanoic Acid	C17:1	3.79 ± 0.33	4.12 ± 0.20	4.32 ± 0.28	3.91 ± 0.09
Stearic Acid	C18:0	2.13 ± 0.18	2.26 ± 0.12	2.73 ± 0.16	2.80 ± 0.07
Oleic/Elaidic Acid	C18:1n9c-t	16.01 ± 1.34	14.77 ± 0.75	15.65 ± 0.91	17.58 ± 0.43
Linoleic Acid	C18:2n6c	30.02 ± 0.00	32.05 ± 1.62	28.22 ± 1.69	27.39 ± 0.61
Linolelaidic Acid	C18:2n6t	0.92 ± 0.27	0.15 ± 0.01	0.06 ± 0.00	0.20 ± 0.01
y-Linoleic Acid	C18:3n6	0.11 ± 0.02	4.57 ± 0.25	4.52 ± 0.28	2.94 ± 0.07
α-Linoleic Acid	C18:3n3	4.64 ± 0.42	1.40 ± 0.14	2.08 ± 0.11	0.00 ± 0.00
Arachidic Acid	C20:0	0.13 ± 0.00	0.34 ± 0.03	0.26 ± 0.02	0.00 ± 0.00
Active Biofuel Components	C16 - C18	88.54	98.34	96.02	96.92
Saturated Fatty Acids	SFA	41.80	39.50	40.49	43.04
Monounsaturated Fatty Acids	MUFA	23.52	22.48	24.72	26.71
Polyunsaturated Fatty Acids	PUFA	35.68	38.15	34.88	30.53
Unsaturated Fatty Acids (MUFA+PUFA)	UFA	59.20	60.64	59.60	57.24
Ratio of Unsaturated to Saturated Fatty Acids	UFA:SFA	1.42	1.54	1.47	1.33

acid, lauric acid, myristoleic acid, palmitoleic acids and stearic acid methyl esters (Devi, 2013). Eicopentasanoic acid methyl esters (EPA) are not produced at any of the tested conditions; this may be due to the absence of acetate in the medium which might be a key metabolic precursor for the production of FAME of higher carbon chain length of C20 and above

4.8   Summary

As described in Section 4.1.2, the aim of the Chapter was to design and evaluate a novel orbitally shaken single-use photobioreactor technology and this has been achieved. The orbital shaking platform described in Chapter 3 was modified to accommodate the larger (SUPBr) as shown in Appendix Figure II.8. The hydrodynamics of the systems were then investigated and the existence of an in-phase and out-of-phase shaking conditions were shown for the first time (Figure 4.4) in this photobioreactor geometry. The effect of the hydrodynamics on culture performance was also investigated (Figure 4.6) and indicated an insignificant impact on growth kinetics across the tested shaken frequencies.

During high density culture of microalgal, shadowing, partial dark zones and non-homogenous light distribution is often expected in this system (Chen et al., 2011). This is attributed to the unidirectional travel of light from the source. It was observed that from the liquid surface, light penetration reduces to almost zero as path-length and biomass concentration increases. This results in light intensity becoming limiting factor for growth under a batch or fed-batch cultivation. During high cell density culture, a step change in shaking frequency and light intensity may prevent growth termination due to limiting effects. Understanding of the particle residence time at the various mixing conditions may further help find optimal conditions between light intensity and shaking frequency.

Subsequently predictive scale translation of growth kinetics between the mPBr described in Chapter 3 and the SUPBr described here was investigated. Excellent agreement in growth rates and yields were found between the two bioreactor scales based on matched scale-up criteria (Figure 4.9 and Appendix Figure II.9). This represents a 125-fold scale translation suggesting the application of both devices as a platform technology for early stage phototrophic algal culture development.

The generic nature of the miniature bioreactor technology as a tool for algal bioprocess development is established in Chapter 5. This will explore heterotrophic culture of *C. sorokiniana and C. protothecoides* in the mPBr and subsequent scale-up of culture performance to conventional laboratory scale stirred tank bioreactors.

5. MINIATURE BIOREACTOR PLATFORM APPLICATION TO HETEROTROPHIC CULTIVATION OF MICROALGAE

5.1 Introduction

5.1.1 Heterotrophic Cultivation of Microalgae

As previously discussed in Section 1.1 microalgal biomass is finding increasing industrial application for human and animal consumption, for production of value added chemicals and as an alternative source of energy (Pulz and Gross, 2004). The metabolic versatility of microalgae has meant that in order to meet the increasing market demand, autotrophic, heterotrophic or mixotrophic cultivation strategies have been explored (Chisti, 2007; Scott et al., 2010; Stephens et al., 2010; Wijffels and Barbosa, 2010).

Certain strains of microalgae, such as *Chlorella, Dunaliella, Scenedemus, Botryococcus, Neochloris*, *Tetraselmis* and several others (Muhamed et al., 2011) possess the ability to switch between phototrophic and heterotrophic metabolism. Heterotrophic cultivation has been reported to have a number of advantages including higher biomass yield and volumetric productivity (Doucha and Lívanský, 2008; Ip and Chen, 2005; Orus et al., 1991). This is because different types of organic carbon substrates can be used and biomass synthesis proceeds at nearly maximum theoretical efficiency of $0.4 - 1.4$ CO_2/C (Perez-Garcia et al., 2011). Important products produced by microalgae cultured heterotrophically include lipids, polyunsaturated fatty acids, pigment, carotenoids and Lutein (Bumbak et al., 2011).

In terms of bioreactor design, the use of an organic source of carbon, such as glucose, for heterotrophic cultivation circumvents the need to provide light and CO_2

---

†The majority of the results in this Chapter have been submitted for publication as: E.O. Ojo, H. Auta, F. Baganz, and G. J. Lye (2015)**.** Parallel miniature bioreactor for optimisation of heterotrophic microalgae cultivation conditions and predictive scale-up to a laboratory scale stirred tank reactor. Biotechnology for Biofuels.

to the bioreactor in order to facilitate respiration (Huang et al., 2010; Perez-garcia et al., 2010). This means that conventional stirred tank bioreactors (STR) (Abdollahi and Dubljevic, 2012; Li et al., 2007b) and microwell based systems (Betts et al., 2014; Hillig et al., 2014b) can readily be applied for heterotrophic microalgae cultivation. The higher growth rates and biomass yields that can be achieved mean that the supply of oxygen to the culture will become critical, especially for high cell density and fed-batch cultivation processes.

5.1.2 Aim and Objectives

As outlined in Section 1.5, the aim of this Chapter is to explore the wider application of the mPBr platform established in Chapter 3 for the evaluation of heterotrophic microalgae cultivation. In particular the goal will be to further characterise the engineering environment in the shaken miniature photobioreactor (mPBr) and establish predictive scale-up criteria to a conventional laboratory scale stirred tank bioreactor.

The specific objectives of this Chapter are to:

- experimentally quantify k_La and mixing time in the 24-well mPBr, conventional shake flasks and a 7.5 L STR

- evaluate heterotrophic culture kinetics of *C. sorokiniana* in the 24-well mPBr under various growth conditions

- establish scale-up criteria for heterotrophic cultivation of *C. sorokiniana* in the three bioreactor systems

- demonstrate the scalability and reproducibility of culture kinetics and FAME production in the different geometries

5.2 Bioreactor Selection and Operation

As in previous studies with microbial systems (Elmahdi, 2003; Islam et al., 2008; Zhang et al., 2008) heterotrophic cultivation of *C. sorokiniana* in the 24-well mPBr will be compared with conventionally used shake flask systems and a standard 7.5 L STR as shown in Figure 2.11. The choice of the 24-well mPBr with square edges and round base was based on previous engineering characterisation studies with this well geometry (Barrett et al., 2010; Zhang et al., 2008). The square edges and the round base promote higher OTRs than in standard round wells by mimicking the effects of

baffles in the conventional stirred bioreactor as described in Section 2.6. The same shaker incubator used for phototrophic studies (Chapter 3) is used although without illumination in this case. While the shaken mPBr and flasks are not sparged, and hence do not have a dispersed gas phase as in the STR, it is expected that adequate OTRs can be achieved.

The shaking platform was designed to hold six 24-well mPBr and four 250 mL shake flasks as previously described in Sections 2.6.1 and 2.6.2. This allows multi-plate parallel cultivation and simultaneous evaluation of different growth parameters in the two different bioreactor formats. Semipermeable membranes were used to seal both the mPBr plates and the shake flasks to prevent evaporation while still allowing adequate transfer of oxygen during the extended cultivation periods required for microalgae. These membranes have also been found useful in bacteria and mammalian cell culture (Islam et al., 2008; Zanzotto et al., 2004; Zimmermann et al., 2003).

At temperatures above ambient, evaporation is a critical consideration in the design of microwell based cultivation systems as described previously in Chapter 3. However, operation of the shaker incubator at an elevated RH of 85%, along with use of the semipermeable membrane covers, showed a negligible loss of media over a cultivation period of five days. In order to accurately quantify cell growth kinetics in the 24-mPBr a sacrificial sampling method was used as described by Islam et al. (2008).

5.3   Bioreactor Mixing Time Quantification

Previous work on shaken microwell systems has shown the importance of adequate fluid mixing to promote solids suspension and good oxygen transfer (Barrett et al., 2010). Mixing time quantification has been performed using a variety of different physical and chemical methods (Vallejos et al., 2006). Here, for the shaken bioreactor systems, a pH-based technique has been used (Section 2.4.3) which records fluctuations in pH in response to added acid. A micro-fibre optical pH probe was attached firmly onto the wall of either the 24-well mPBr or shake flask to ensure continuous data capture via a connected pH meter as described in Section 2.4.3.

Measured mixing times were generally in the range of 10-20 s and were similar for both the 24-well mPBr and the shake flasks at shaking frequencies between 200 - 400 rpm. At the lower shaking frequency of 180 rpm for the shake flask the mixing time was found to be significantly higher, of the order of 145 s as shown in Figure 5.1 Visual observations showed that in this case there was an orbital flow of liquid around the cylindrical base of the flask without any significant axial flow and mixing occurring. Comparison of data for the orbitally shaken bioreactor geometries with the STR showed that the mixing time in the STR was in general approximately 55% lower. This data could provide some insight into the hydrodynamics and energy transfer rate across the different bioreactor geometries and hence and their ultimate impact on culture kinetics.

Engineering characterisation of several novel bioreactor systems has shown mixing time to be an important criteria for evaluating the relationship between mixing dynamics and gas-liquid mass transfer. Oxygen transfer (further discussed in Section 1.4) in non-sparged microwells occurs via the gas-liquid interface at the fluid surface. It is dependent on the shaking frequency, liquid fill volume, microwell geometry and microplate seal type employed. This equally holds true for shake flasks system. In a sparged STR, however, the fluid hydrodynamics will be different with mixing achieved by mechanical agitation with an impeller. Here, impeller rotational speed and design, and ratio of liquid height to impeller height and number, will be the main determinants of mixing time and oxygen transfer.

5.4   Bioreactor Oxygen Mass Transfer Coefficient ($k_L a$)

Irrespective of bioreactor scale and geometry, for efficient heterotrophic cultivation of microalgae the oxygen transfer capability of the bioreactor will be critical. $k_L a$ has previously been identified and utilised as a suitable criteria for scale-up between small-scale shaken bioreactor formats and STRs (Islam et al., 2008). Based on the gassing out method described in Section 2.4.1 experimental $k_L a$ values were determined using Equation 2.1 and plotted against shaking /stirring frequency as shown in Figure 5.2 for the three different bioreactor geometries. The maximum $k_L a$ was determined to be 95 h^{-1} in the 24-well mPBr. Comparison of $k_L a$ values in the
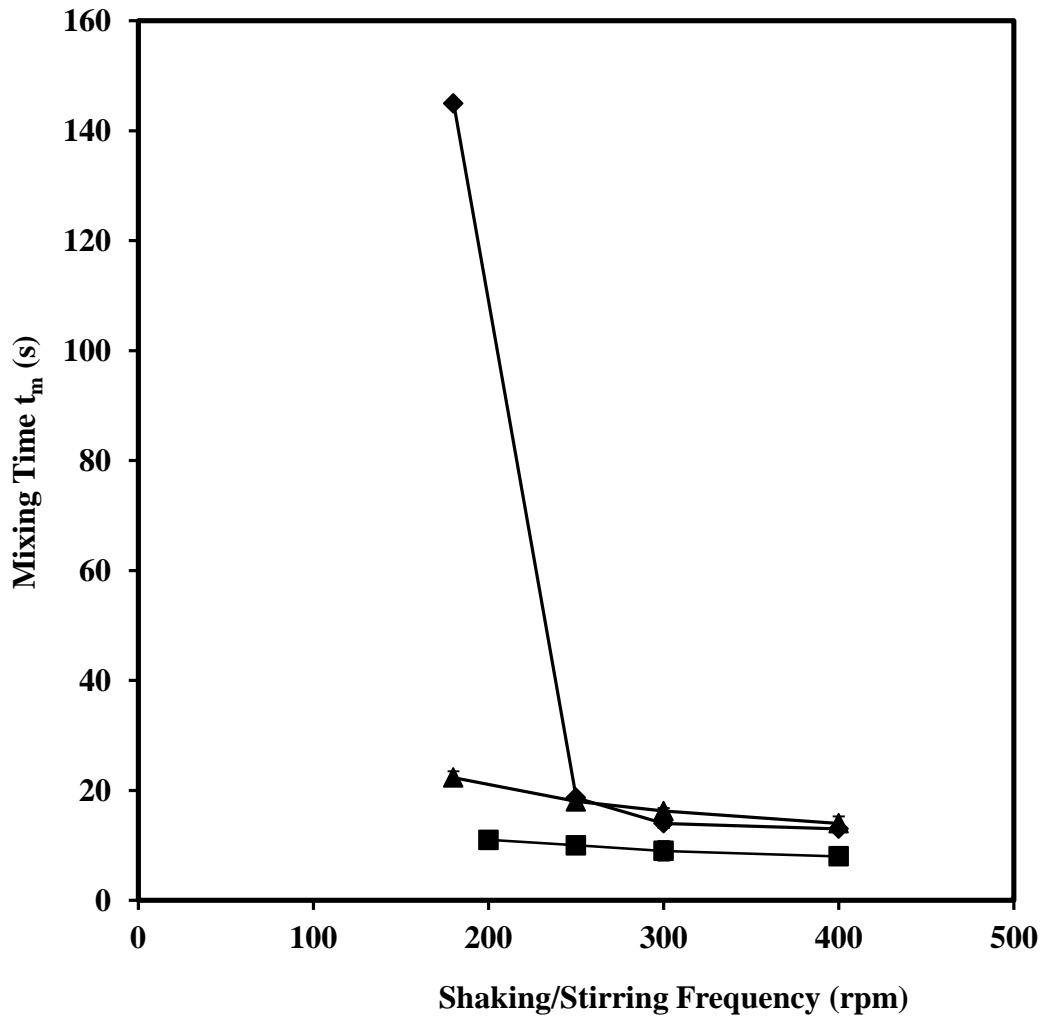
Figure 5.1: Effect of bioreactor geometry on mixing time at different shaking/stirring frequencies: (▲) 24-well mPBr (♦) shake flask (■) 7.5 L STR. Experimental conditions: d_o = 25 mm; V_f = 4 mL, 100 mL and 4 L respectively. Error bars represent one standard deviation about the mean (n=3). Experiments performed as described in Section 2.4.3.

three bioreactor systems shows a similar trend with k_La values increasing with increasing shaking / stirring frequency. In the case of the STR previous reports have shown that stirrer frequency has a more significant effect on k_La than increases in aeration (Gill et al., 2008).

Based on the data shown in Figure 5.2, two sets of operating conditions were identified for subsequent scale-up studies (Section 2.7) with *C. sorokiniana* aimed at matching growth performance in the mPBr and STR formats (shake flasks was used as a control). As indicated on the plot with circles, the chosen operating conditions are as follows:

> **High k_La (35-40 h^{-1}):** These conditions were achieved at a shaking/stirring frequency of 300 rpm in all formats. Here the k_La was matched between the mPBr and STR, although k_La for shake flasks was lower at 21 h^{-1}. Based on the data in Figure 5.1 the corresponding mixing times are comparable and in the range 10-18 s.
>
> **Low k_La (10-18 h^{-1}):** These conditions are achieved at a shaking/stirring frequency of 180 rpm in STR and 250 rpm in mPBr. Based on the data in Figure 5.1 the corresponding mixing times are comparable and in the range 10 – 22 s.

5.5   Heterotrophic *C. sorokiniana* Cultivation in the mPBr

Heterotrophic cultivation of microalgae in the 24-well mPBr comes with specific requirements such as the need for evaporation control, enabling sufficient oxygen transfer and efficient mixing. The extended time required to run a batch culture at temperatures higher than 25 ℃ can make evaporation significant, impacting negatively on biomass concentration determination by OD measurement (Section 2.7). As mentioned previously, evaporative losses can be minimized over a typical 5-day culture period by operation of the shaking incubator at a relative humidity of over 85%. Initial assessment of culture performance of *C. sorokiniana* using the 24-well mPBr at different shaking frequencies showed an increase in biomass concentration with increase in shaking frequency. An increase in the shaking frequency from 250 to 300 rpm resulted in approximately 25% increase in biomass productivity (Figure 5.4 (A) and Figure 5.5 (A)).
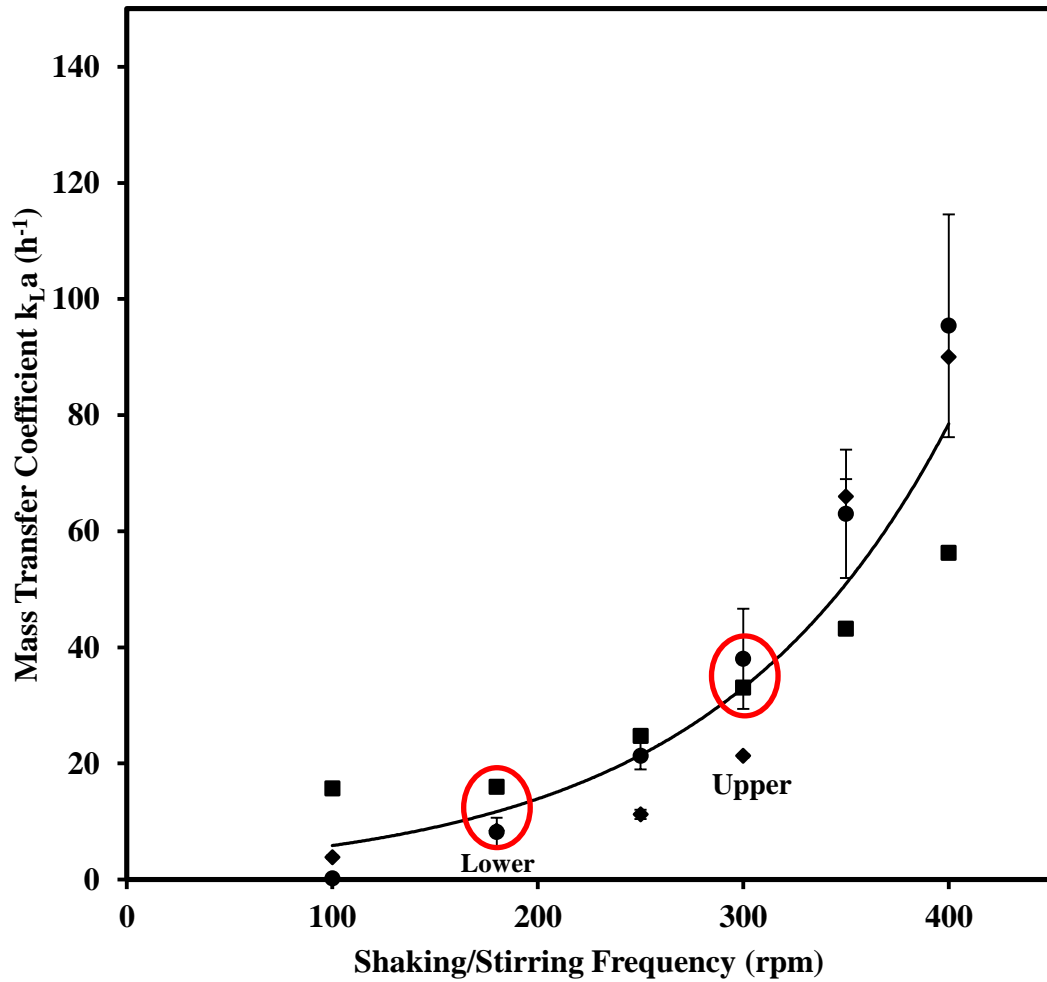
Figure 5.2: Bioreactors oxygen mass transfer coefficient (k_La) as a function of shaking/stirring frequency: (●) 24-well mPBr; (♦) shake flask; (■) 7.5 L STR. Experimental conditions: $d_o = 25$ mm; $V_f = 4$ mL, 100 mL and 4 L respectively. Error bars represent one standard deviation about the mean (n=3). Experiments performed as described in Section 2.4.1.

The highest biomass concentrations achieved were 3.5 and 4.7 gL^{-1} respectively. The position of the 24-well mPBr plates on the shaking platform (as described in Section 2.6) was also investigated and showed no significant impact on the culture performance as demonstrated in Figure 5.3 (A). However, edge effects were noticed on the rows in the 24-well mPBr closest to the incubator opening and were not included in subsequent experiments. Further evaluation of chlorophyll production, as shown in Figure 5.3 (B), across each row on the 24-well plate shows no significant difference.

To demonstrate the potential of the mPBr for heterotrophic media optimisation studies, a comparative analysis of *C. sorokiniana* growth was next undertaken in three selected media formulations: TBP, bold basal media (BBM) and HSM. The compositions of these media are described in Table 2-1. Table 5-1 summarises the growth kinetic parameters determined from these experiments.

The results indicate that the TBP medium achieved in the highest biomass concentration and highest biomass productivity due, in part, to the tightest control of pH during the culture. BBM, on the other hand, had the highest biomass yield on glucose. HSM shows the worst performance due to sudden decrease in pH after 2 days of culture limiting further cell growth. Zheng et al., (2013) reported an increase in pH of *C. sorokiniana* cultured in Kuhl medium from pH 6 to 9 with poor growth observed at pH of 9. Depending on the media composition, the most favoured pH for growth of *C. sorokiniana* varies between pH 5 - 7 for acidic media and 7 − 9 for basic media, with pH values beyond these ranges becoming inhibitory. In order not to reduce the glucose uptake rate (Tanner, 2000; Zheng et al., 2013), it is imperative to keep the external medium pH above 5 because lower values cause a drop in the intracellular pH from 7.3 to 6.3 as observed in *C. saccaharophila* (Gehl and Colman, 1985).
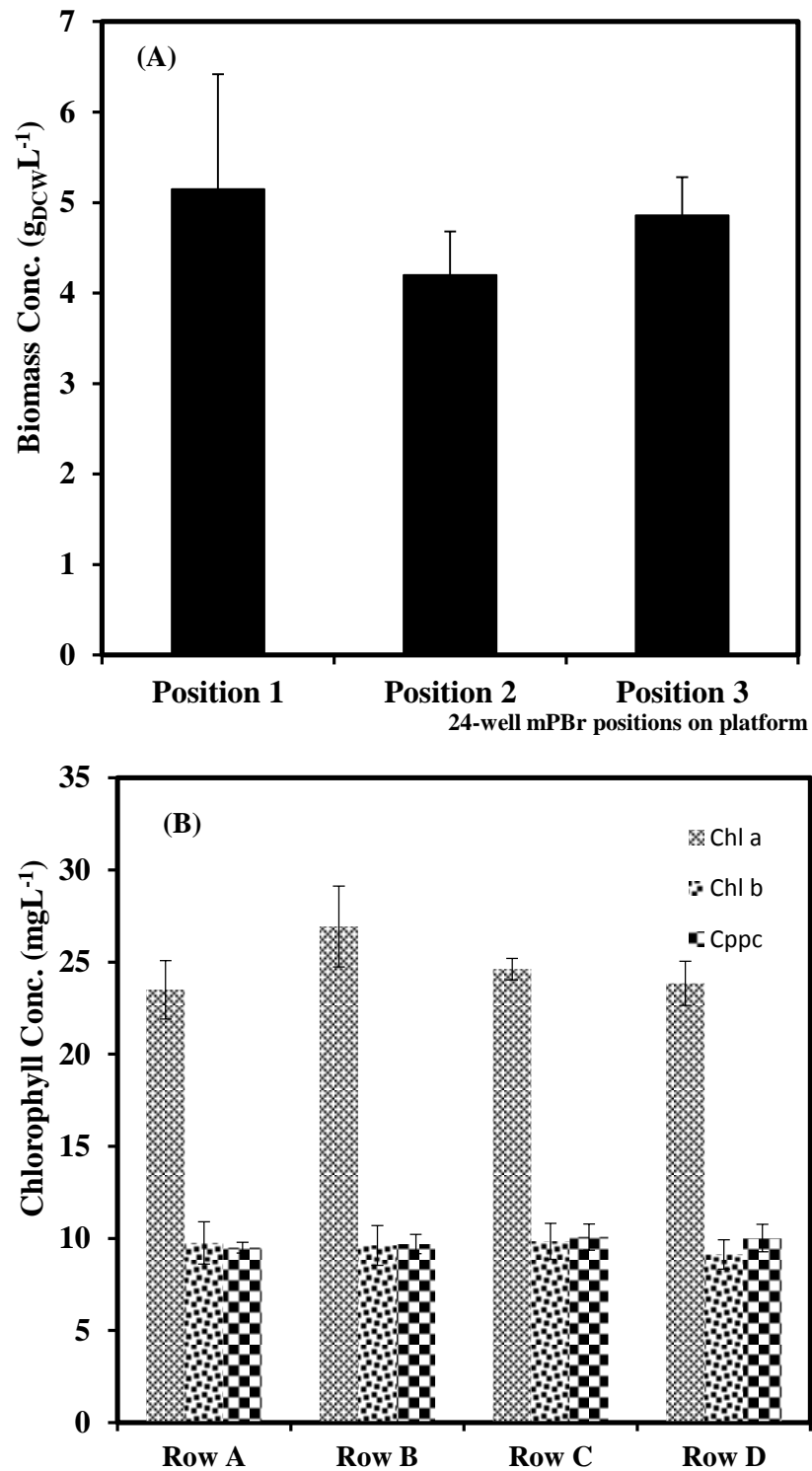
Figure 5.3: Evaluation of plate-to-plate and well-to-well performance for batch culture of *C. sorokiniana* in the 24–well mPBr: (A) biomass concentration across 24 wells mPBr at three different plate positions on the shaken platform; (B) pigment concentration across rows on an individual 24–well mPBr plate. Error bars represent one standard deviation about the mean (n=2). Experiments performed as described in Section 2.7.2.

Table 5-1: Heterotrophic growth kinetics of *C. sorokiniana* in the 24-well mPBr using different culture media. Experiments performed as described in Section 2.6 Media formulations as described in Table 2.1.

			Growth parameters			
Media	X_{final} (gL^{-1})	μ (d^{-1})	Productivity (gL^{-1}d^{-1})	pH range	Yx,s (gg^{-1})	Yx,N (gmmol^{-1})
TBP	4.93	2.58	1.23	7.04 - 6.65	0.97	0.66
BBM	4.08	1.70	1.02	7.03 - 7.54	1.48	nd
HSM	1.33	1.33	0.33	7.01 - 3.17	0.46	0.30

TBP-Tris-base Phosphate Medium, BBM – Bold Basal Medium, HSM - High Salt Medium, Yx,s – Biomass yield on substrate, Yx,N – Biomass yield on nitrogen (nd – not determined)

For subsequent scale-up experiments, the TBP medium was selected due to the enhanced growth performance and the use of an ammonium salt as the source of nitrogen. This allows improved buffering of the medium pH by increasing the amount of tris-base to 0.2 mL^{-1} (as described in the previous medium optimisation study in Section 3.5) without affecting growth or glucose assimilation. Furthermore, *C. sorokiniana* is known to produce a higher biomass yield per gram of nitrogen consumed with ammonium compared to other nitrogen sources such as nitrates and yeast extracts (Zheng et al., 2013).

5.6   Scale Translation of Heterotrophic Cultures

The use of $k_L a$ as a basis for scale translation was investigated for heterotrophic cultivation of *C. sorokiniana* in the three bioreactors formats described in Section 2.4. The shaking/stirring frequency was based on the operating conditions corresponding to the low and high $k_L a$ values defined in Section 5.4. In the case of the STR at high $k_L a$ conditions, the stirring frequency was initially set at 180 rpm but was cascaded up to 250 rpm in order to maintain a constant dissolve oxygen tension DOT of 40%.

At low $k_L a$ conditions, batch culture of both *C. sorokiniana* and *C. protothecoides* was investigated as shown in Figure 5.4. In the case of *C. sorokiniana* a longer lag-phase was observed in the 24-well mPBr (Figure 5.4 (A)) compared to both shake flask and STR formats. This led to a lower final biomass concentration of 3.46 gL^{-1}, compared to 3.85 gL^{-1} in the other bioreactor formats. *C. protothecoides* exhibited similar growth pattern to that observed with *C. sorokiniana* with lower growth in the 24-well mPBr as shown in Figure 5.4 (B). However, the final biomass concentration achieved of 16.4 gL^{-1} was significantly higher than with *C. sorokiniana*.

Table 5-2 summarises the calculated kinetic parameters and yields for the two strains grown in the three different bioreactor formats, In terms of final biomass concentration, that for *C. protothecoides* was 75% higher than *C. sorokiniana* due to better adaptation of cell metabolism to organic carbon utilisation. This strain has also been evaluated for biodiesel production from laboratory to commercial scale (Li et al., 2007b; Li et al., 2008; Miao and Wu, 2006). In previously reported studies,
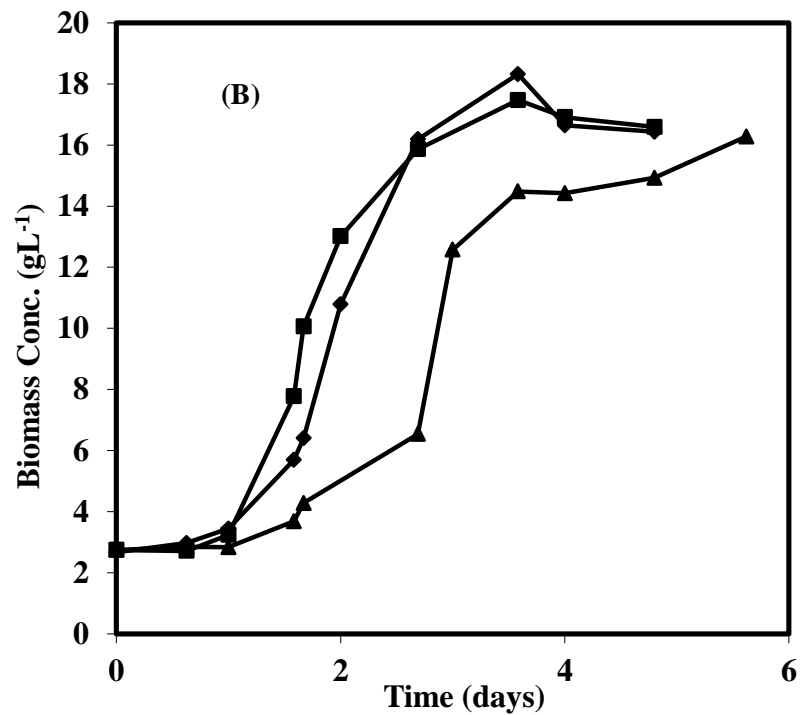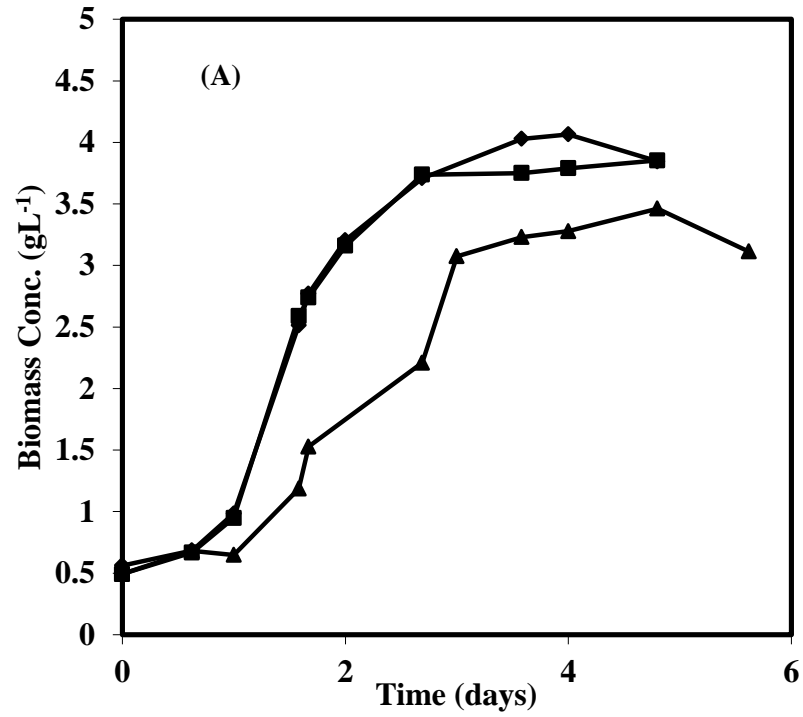
Figure 5.4: Comparison of biomass growth kinetics during batch culture of different microalgal strains at low $k_L a$ conditions: (A) *C. sorokiniana* and (B) *C. protothecoides*. Conditions in (▲) 24-well mPBr; (■) 250 mL - shake flasks and (♦) 7.5 L STR are: V_f = 4 mL, 100 mL and 4 L respectively. Error bars represent one standard deviation about the mean (n=3). Experiments performed as described in Section 2.7.

Table 5-2: Comparison of heterotrophic growth kinetics for *C. sorokiniana* and *C. protothecoides* at low k_La conditions. Cultures performed at matched k_La as described in Section 2.7 (na: not applicable).

Low k_La Conditions	*C. sorokiniana*			*C. protothecoides*		
	24-Well mPBr	**Shake Flask**	**7.5 L Bioreactor**	**24-Well mPBr**	**Shake Flasks**	**7.5 L Bioreactor**
Shaking frequency/agitation (rpm)	250	180	180	250	180	180
Air flow rate (vvm)	na	na	1	na	na	1
Culture Performance						
μ_{max} (d^{-1})	0.78	0.81	0.78	0.75	0.94	0.92
X_{final} (gL^{-1})	3.11	3.85	3.85	16.26	16.59	16.43
$Y_{x/sNH4}$ (gg^{-1})	0.45	0.56	0.56	2.35	2.39	2.37
$Y_{x/sglucose}$ (gg^{-1})	0.68	0.76	0.76	3.56	3.63	3.75

Sheyn et al., (2010) obtained an average biomass concentration of $10 - 20$ gL^{-1} using four different strains of *C. protothecoides,* Likewise, Xu et al., (2006) obtained 15.5 gL^{-1} biomass concentration cultured for 184 h on glucose. The other calculated growth parameters highlighted in Table 5-2 show similar growth kinetics between the shake flask and STR formats but lower final biomass concentrations and growth rates in the mPBr (for both strains). While the k_La values were matched between the three bioreactor formats visual observation suggested that the fluid mixing was less intense in mPBr than in the other systems.

Given the poor fluid hydrodynamics observed in the mPBr at the low k_La conditions (250 rpm) the growth of *C. sorokiniana* in the three bioreactor formats was also evaluated at the high k_La conditions (300 rpm). Here visual observation suggested enhanced fluid flow and increased turbulence in the mPBr at the higher shaking frequency which is in accordance with literature studies on microwell fluid hydrodynamics (Büchs et al., 2001; Zhang et al., 2008). At these high k_La conditions growth in the mPBr and STR showed similar final biomass concentration of approximately 5 gL^{-1} over a growth period of 5 days (Figure 5.5 (A)). The final biomass concentration in the shake flask was slightly lower most probably due to it exhibiting the lowest k_La under these conditions (Figure 5.2). Further growth kinetic parameters are summarised in Table 5-3 and again show a good match in terms of growth rate, yield and substrate utilisation between the mPBr and STR formats. Figure 5.5 (B) and Figure 5.6 shows comparable glucose utilisation and pH profiles.

The impact of the engineering environment and bioreactor geometry on the cell size distribution during the high k_La cultures was also evaluated as described in Section 2.9.7 (cultures at higher rpm values were not investigated due to vibration of the incubator shaker at higher shaking frequencies). At conditions of high k_La, the measured cumulative particle size distribution shows similar particle size across the three different geometries as shown in Figure 5.7. These results indicate that bioreactor geometry and fluid hydrodynamics had no effect on cell size nor caused any form of cell disruption.

146
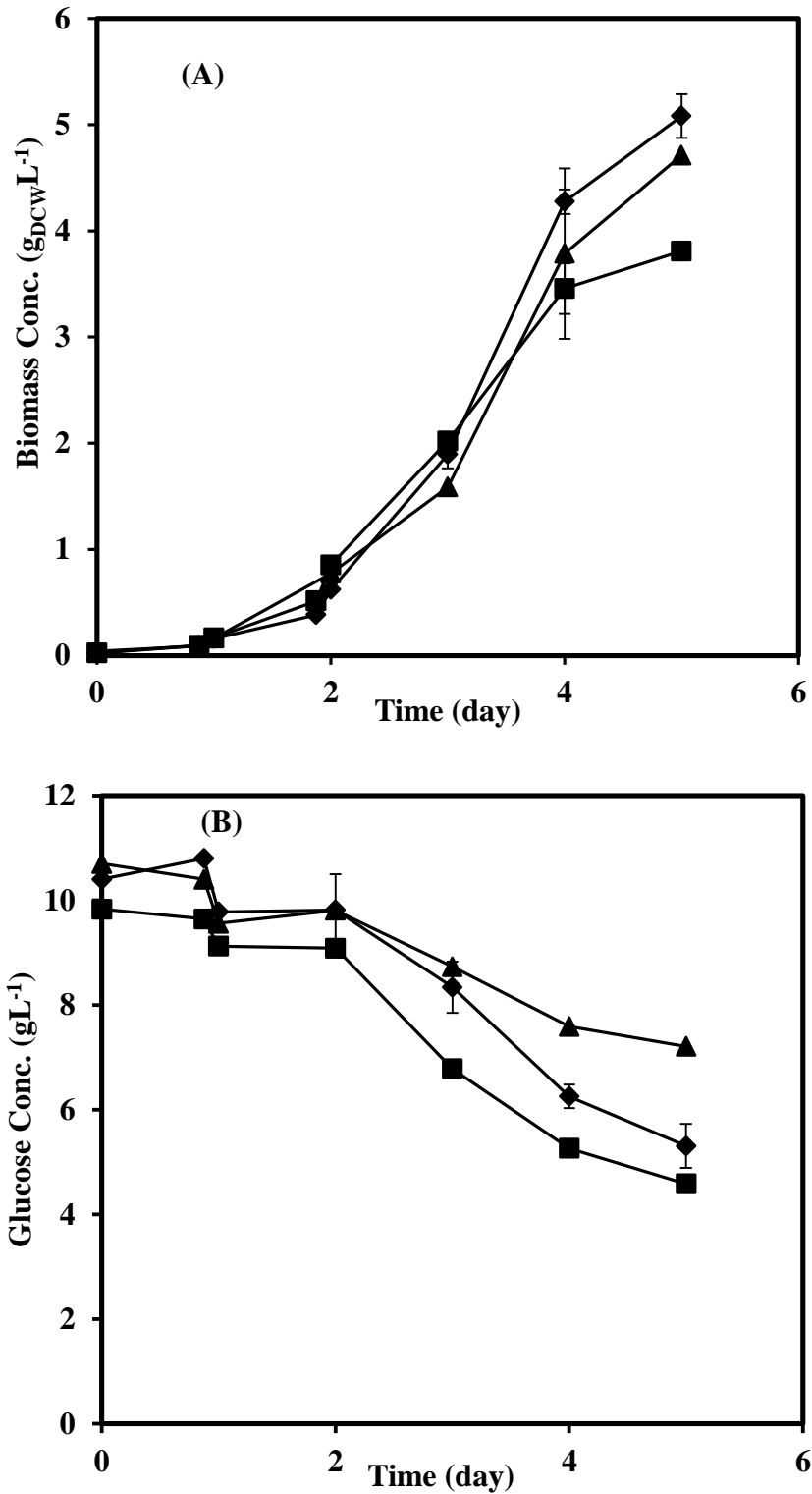
Figure 5.5: Comparison of culture kinetics during batch culture of *C. sorokiniana* at high k_La conditions: (A) biomass concentration (B) glucose concentration. Conditions in (▲) 24-well mPBr; (■) 250 mL shake flasks and (♦) 7.5 L STR are: V_f = 4 mL, 100 mL and 4 L respectively. Error bars represent one standard deviation about the mean (n=3). Experiments performed as described in Section 2.7 and Section 2.9.1.

147

Figure 5.6: Comparison of culture pH during batch culture of *C. sorokiniana* at high k_La conditions: Conditions in (▲) 24-well mPBr; (■) 250 mL shake flasks and (♦) 7.5 L STR are: V_f = 4 mL, 100 mL and 4 L respectively. Error bars represent one standard deviation about the mean (n=3). Experiments performed as described in Section 2.7 and Section 2.9.1.

.

Table 5-3: Comparison of heterotrophic growth kinetics for *C. sorokiniana* culture at high $k_L a$ conditions. Cultures performed at matched $k_L a$ as described in Section 2.7. (na: not applicable).

	24-well mPBr	Shake flasks	7.5 L STR
Engineering Conditions: High $k_L a$			
Shaking/stirring frequency	300	300	300
Air flow rate (vvm)	na	na	1
Shaken diameter (mm)	25	25	nd
Culture kinetic parameters			
μ_{max} **(d^{-1})**	0.87	0.69	0.81
X_{final} **(gL^{-1})**	4.71	3.81	5.10
Yx/s_{NH4} **(gg^{-1})**	0.75	0.60	0.81
$Y_{x/sglucose}$ **(gg^{-1})**	1.35	0.73	1.00

Where, μ_{max} = specific growth rate, X_{final} = final biomass concentration, Yx/s_{NH4} = biomass yield on ammonia, $Y_{x/sglucose}$ = biomass yield on glucose.
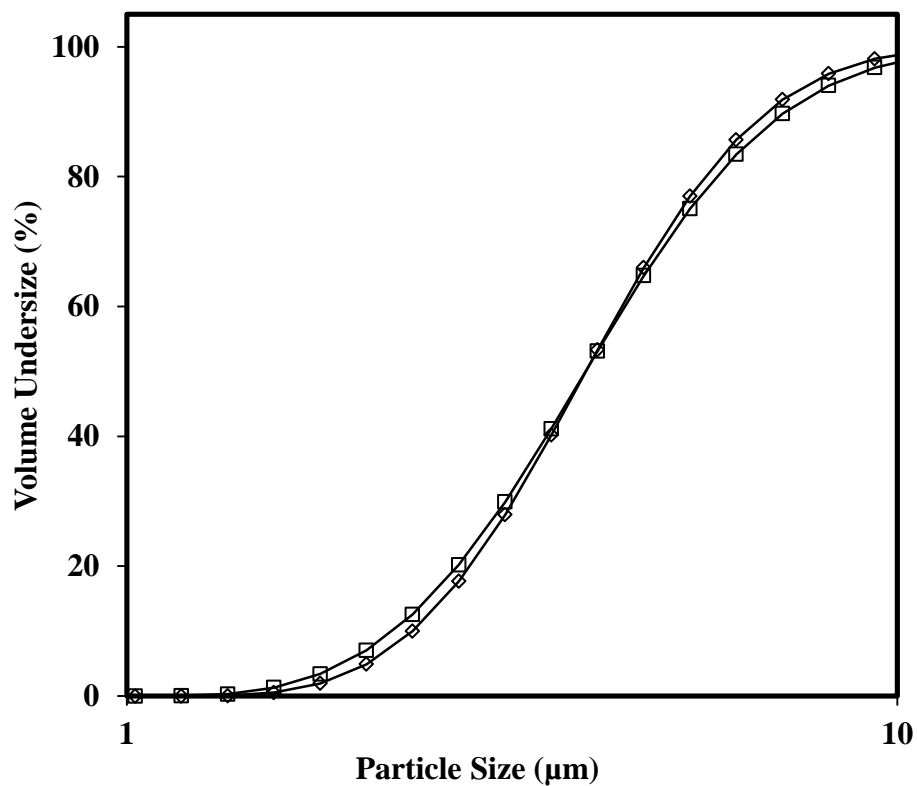
Figure 5.7: Cumulative size distribution during batch cultivation of *C. sorokiniana* at high $k_L a$ conditions in: (◊) 24 –well mPBr; (□) shake flasks and (Δ) 7.5 L STR. Each data point represents one standard deviation about the mean (n=3). Experiments performed as described in Section 2.9.7.

Overall, the results in this section show that operation at the high k_La conditions defined in Section 5.4 led to comparable growth performance between the mPBr and the STR representing an 1000-fold increase in scale. Further investigation of pigment and lipid production by *C. sorokiniana* was therefore conducted under high k_La operating conditions.

5.7   Chlorophyll and Total Lipid Production

5.7.1   Chlorophyll Production

Production of green pigment in microalgae is more often associated with phototrophic and mixotrophic cultivation of green microalgae (Mohsenpour et al., 2012). However, strains such as *C. sorokiniana* also produce green pigments under heterotrophic culture conditions. Pigment productivity depends largely on the chemical constituents of the media formulation used and the available nitrogen source (Perez-garcia et al., 2010). In this work chlorophyll concentration profiles were evaluated for *C. sorokiniana* cultured in all three bioreactor geometries and scales under high k_La conditions. As shown in Figure 5.8 (A&B) the results indicated similar kinetics for Chl a, b and Cppc (Figure 5.9) synthesis in each bioreactor. The corresponding final concentrations of the pigments were of 12.3, 4.2 and 4.5 mgL^{-1} respectively. Combined with the scalability of the mPBr growth data established in Section 5.6 these results further demonstrate the potential of the 24-well mPBr for early stage screening and optimisation of green pigment in different strains and under different culture conditions. Comparison of the final Chl a concentration obtain during heterotrophic culture with that obtained during phototropic culture in the mPBr under similar shaking conditions (Figure 3.8) indicates about a 50% reduction. This further establishes the importance of light and phototrophic culture conditions for increased production of green pigments.

5.7.2   Total Lipid Production

In this study it was sought to enhance lipid production by using a limited amount of ammonium salt in the media formulated (Table 2-1). During nitrogen limitation, the rate of protein synthesis is reduced leading to reduced carbon fixation via glycosylate cycle. This consequently leads to increase in the intracellular fatty acid acyl Co-A

and activation of diacylglycerol acyl transferase, which converts fatty acid acyl Co-A to triglyceride (Hsieh and Wu, 2009). Patil et al., (2011) also suggested higher lipid productivity in nitrogen deprived condition due to the decrease in the protein synthesis rate, resulting in a feedback inhibition in the citric acid cycle.

Total lipid production by *C. sorokiniana* cultured under high $k_L a$ conditions is shown in Figure 5.10. No significant difference in the percentage of lipid produced was found between the 24-well mPBr and the 7.5 L STR with an average value of approximately 45%. In contrast the lipid produced in shake flask cultures showed a reduced value of 38%. The reason for this reduced lipid production is unclear but may be due to the prevalent and uncontrolled environmental conditions in the shake flask during the culture e.g. pH or dissolved CO_2 levels.

The estimated lipid yields on glucose and ammonium consumption and the total lipid productivity showed a similar trend as indicated in Table 5-4. Results for the 24-well mPBr and the 7.5 L STR are very similar, given the 1000-fold difference in scale, while the values for the shake flask cultures are significantly lower.

Table 5-4: Summary of lipid productivity for heterotrophic batch cultivation of *C. sorokiniana* at high $k_L a$ conditions. Data calculated from Figure 5.7 and Figure 5.10. Glucose and ammonium measured as described in Section 2.9.3.

	24-well mPBr	Shake Flask	7.5 L STR
Lipid productivity ($mgg_{dcw}^{-1}day^{-1}$)	92.2	57.2	87.5
$Y_{XL/Sglucose}$	0.31	0.22	0.33
$Y_{XL/SNH4}$	0.21	0.16	0.25
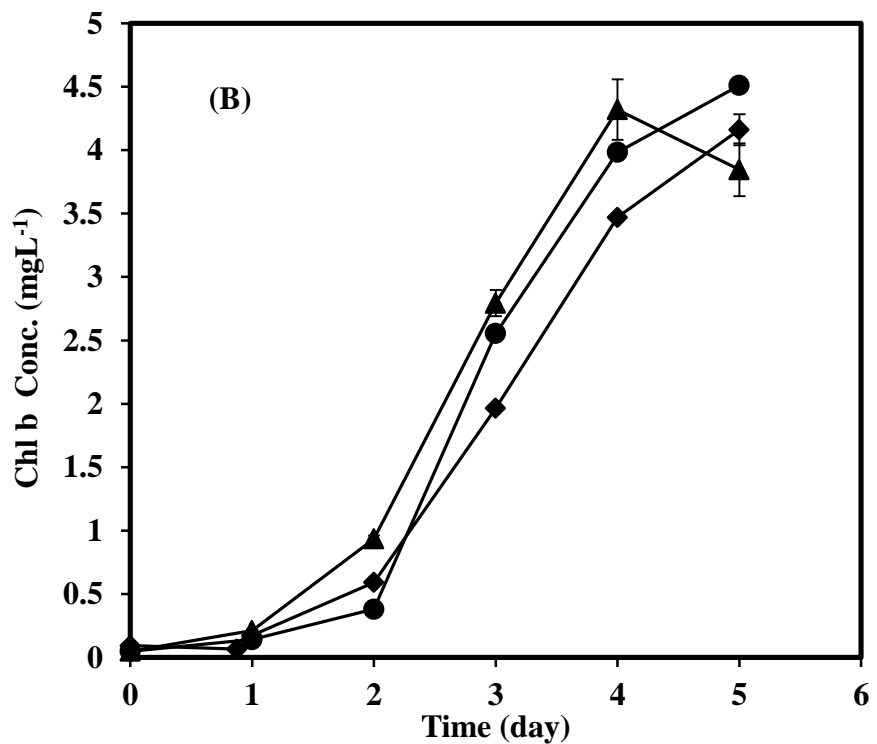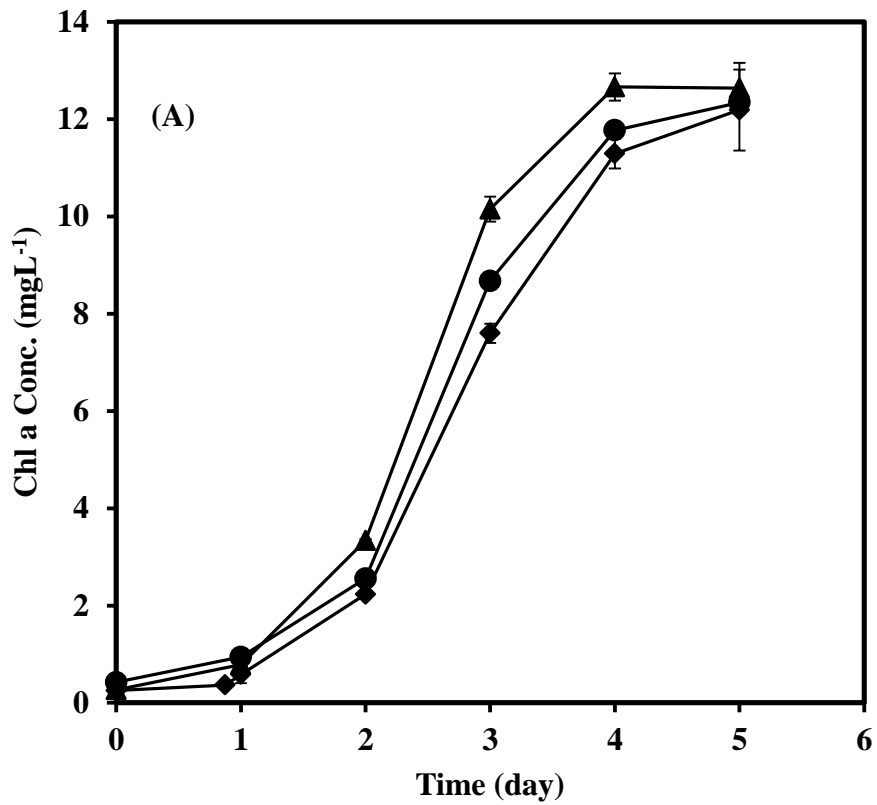
Figure 5.8: Comparison of chlorophylls produced during batch culture of *C. sorokiniana* at high $k_L a$ conditions as described in Figure 5.4 for (▲) shake flasks (♦) 7.5 L STR (●) 24 − well mPBr: (A) Chl a (B) Chl b. Error bars represent one standard deviation about the mean (n=3). Experiments performed as described in Section 2.9.2.
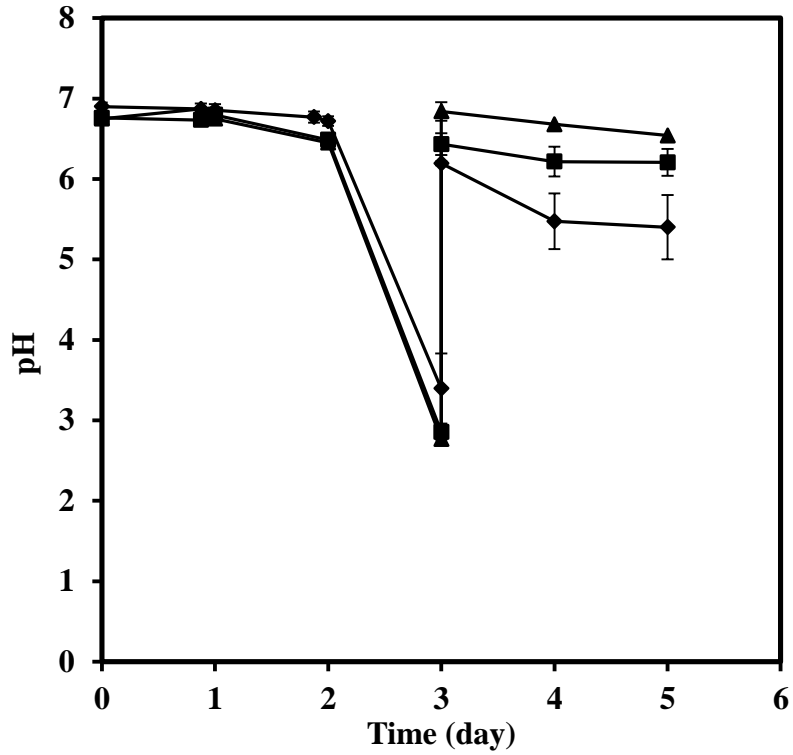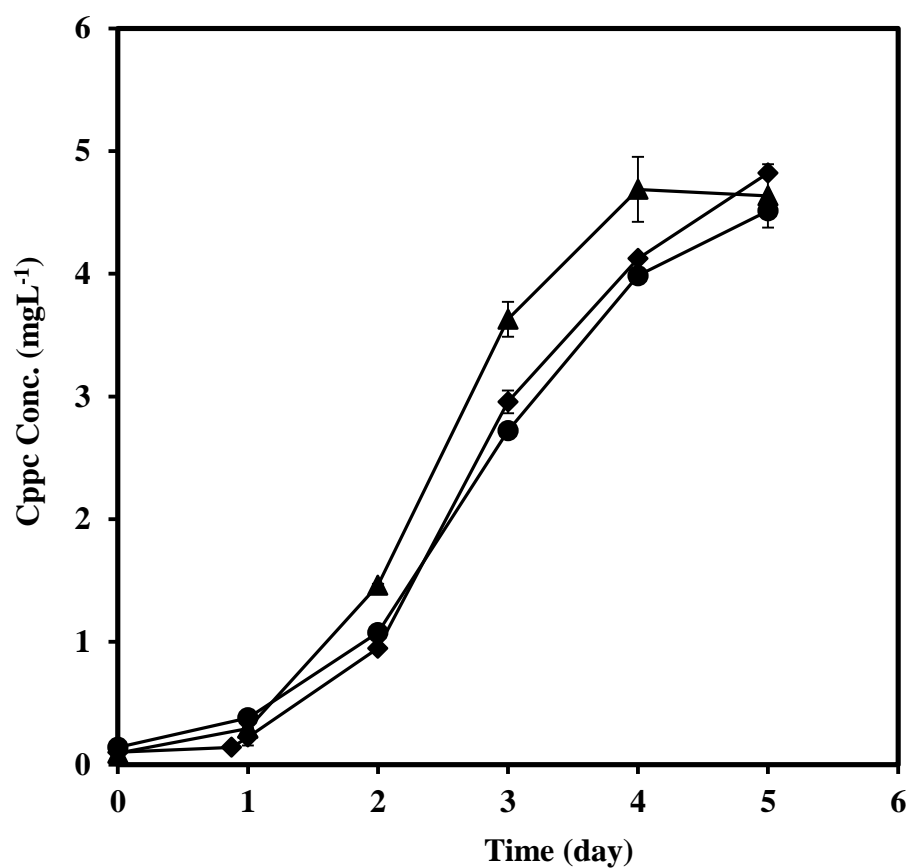
Figure 5.9: Comparison of carotenoids produced during batch culture of *C. sorokiniana* at high k_La conditions as described in Figure 5.4 for (▲) shake flasks (♦) 7.5 L STR (●) 24 – well mPBr. Error bars represent one standard deviation about the mean (n=3). Experiments performed as described in Section 2.9.2.
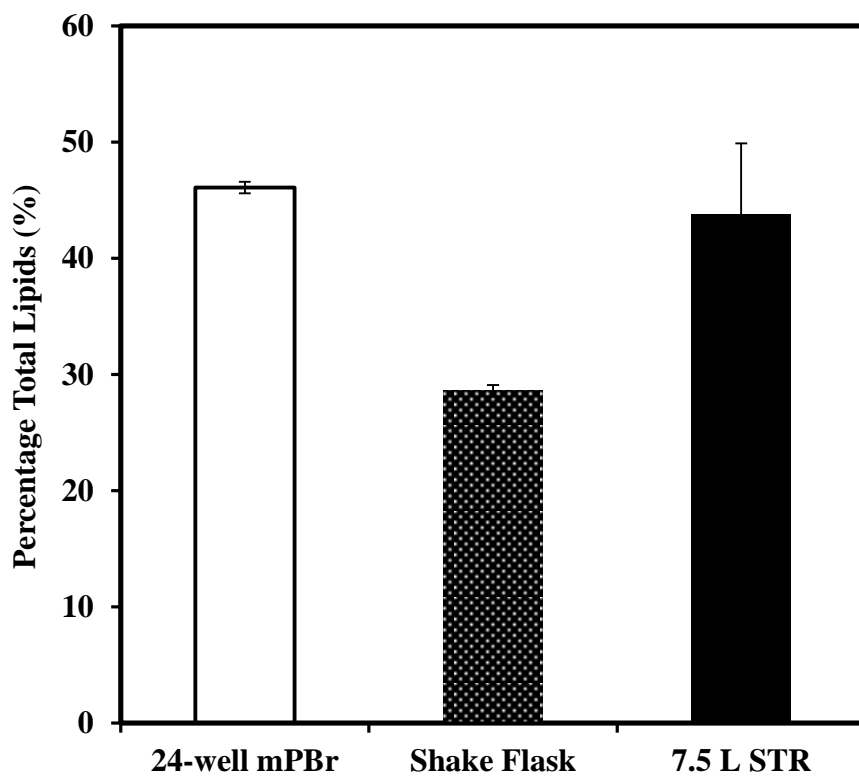
Figure 5.10: Total lipid production as a percentage of dry biomass during batch cultivation of *C. sorokiniana* at high k_La conditions in: 24 – well mPBr; shake flask and 7.5 L STR formats. Error bars represent one standard deviation about the mean (n=3). Experiments performed as described in Section 2.9.3.

5.8   Fatty Acid Methyl Esters (FAME) Evaluation

A quantitative evaluation of the percentage composition of individual FAMEs is shown in Figure 5.11 for *C. sorokiniana* produced in each of the three bioreactor formats. The composition data is grouped based on the degree of saturation. SFA, monounsaturated fatty acids (MUFA), PUFA and C16 – C18 chain length fatty acids are known for their useful biofuel properties (Lu et al., 2012). The prominence of SFA was seen in all three bioreactor formats with C10:0 accounting for approximately 50% of the total FAME produced. Others such as C13:0, C14:0, and C16:0 were present at ~ 2%, with some others in trace amount as shown in Table 5-5. These have been known for their use in preparation of several antibacterial agents, antioxidants, anti-inflammatory and anti-carcinogenic agents (Good rum and Geller, 2005). Others such as C14:0 are used in preparation of biofuels and lubricating oils while C17:0 is used in diesel engines (Gasparini et al., 2011). C21:0 and above were not detected in all the three bioreactor formats tested. This may be due to the absence of tris-acetate which triggers the glutamate pathway responsible for the formation of long chain hydrocarbons.

The average percentage of UFA produced across the three bioreactor formats was 42.2 of total FAME. In all the bioreactors, the key biofuel components, C18:1-3, show comparable concentrations. Other FAME were produced in in trace amount such as cis-10-pentadecanoic and heptadecanoic acid methyl ester. Most of the UFA are known for their application as combustion fuel, emulsifier, solubilisers, and lubricators. The total concentration of UFA was low in all three bioreactor formats. This may be due to differences in cultivation temperature amongst other factors such as the media formulation and type of carbon source as reported by Li et al., (2013). Overall the data shows comparable FAME compositions and concentration across the three systems tested.
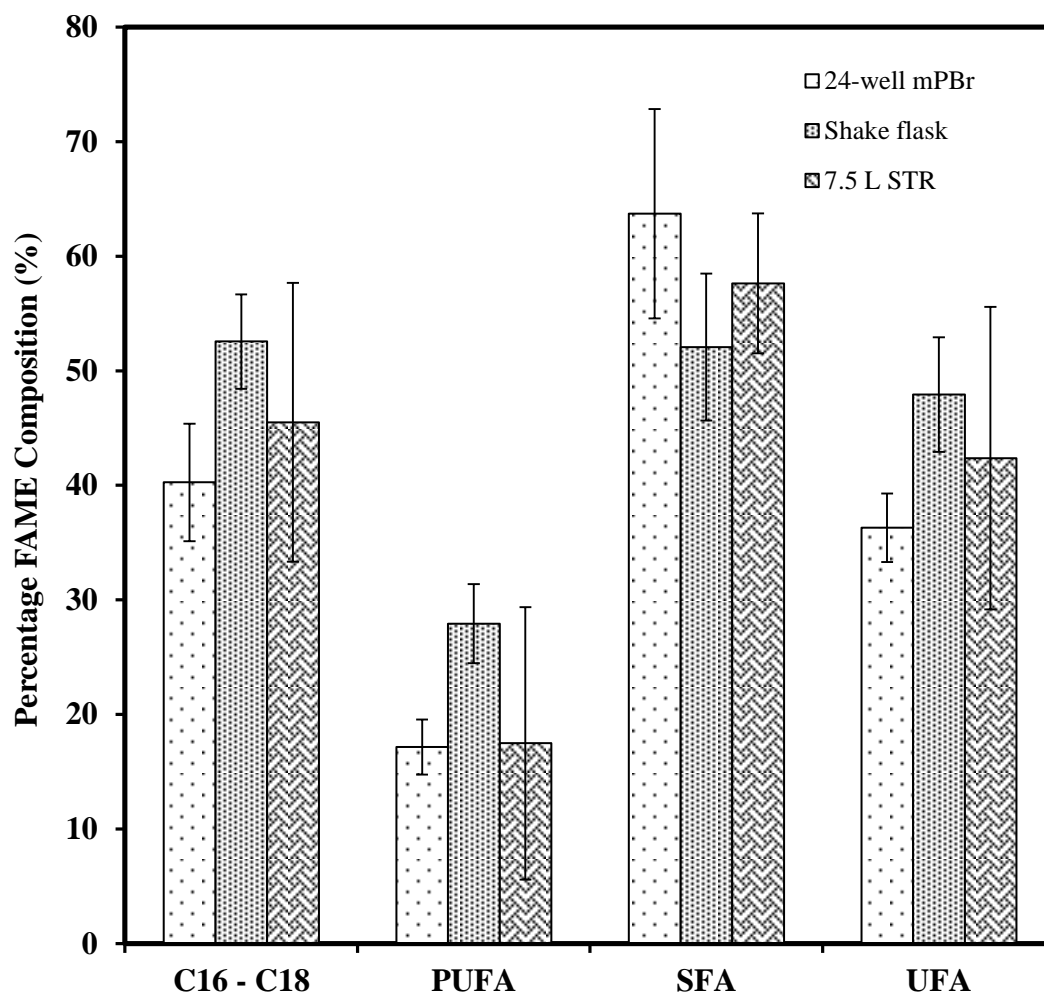
Figure 5.11: Comparison of FAME compositions during batch cultivation of *C. sorokiniana* at high k_La conditions in the three bioreactor formats. Error bars represent one standard deviation about the mean (n=3). Experiments performed as described in Section 2.9.5.

Table 5-5: Detailed comparison of FAME production during batch cultivation of *C. sorokiniana* at high k_La conditions in the three different bioreactor formats. Error levels represent one standard deviation about the mean (n=3). Experiments performed as described in Section 2.9.5. FAME composition quantified as described in Section 2.9.5.

FAME (% wt)	Structure	24-well mPBr	Shake flask	7.5L STR
Butyric Acid	C4	0.51 ± 0.09	0.21 ± 0.03	0.19 ± 0.16
Caproic Acid	C6	1.15 ± 0.11	0.10 ± 0.01	0.06 ± 0.00
Caprylic Acid	C8	0.60 ± 0.09	0.17 ± 0.03	0.24 ± 0.02
Capric Acid	C10	42.56 ± 4.59	36.96 ± 5.16	44.44 ± 3.14
Undecanoic Acid	C11	1.89 ± 0.26	0.03 ± 0.02	0.00 ± 0.00
Lauric Acid	C12	0.39 ± 0.06	0.18 ± 0.02	0.24 ± 0.02
Tridecanoic Acid	C13	2.68 ± 0.34	3.04 ± 0.19	2.33 ± 1.49
Myristic Acid	C14	2.90 ± 0.36	1.13 ± 0.11	2.43 ± 0.89
Myristoleic Acid	C14:1	1.13 ± 0.14	0.69 ± 0.06	0.41 ± 0.03
Pentadecanoic Acid	C15	1.64 ± 0.21	0.33 ± 0.03	0.53 ± 0.03
cis-10-Pentadecanoic Acid	C15:1	0.33 ± 0.05	0.35 ± 0.03	0.23 ± 0.01
Palmitic Acid	C16	5.56 ± 0.72	6.20 ± 0.53	5.57 ± 0.29
Hepatdecanoic Acid	C17	1.25 ± 0.24	0.49 ± 0.04	0.29 ± 0.02
cis-10-Hepatdecanoic Acid	C17:1	1.41 ± 0.17	2.20 ± 0.16	1.81 ± 0.10
Stearic Acid	C18	1.28 ± 2.00	1.67 ± 0.15	0.00 ± 0.00
Oleic/Elaidic Acid	C18:1n9c	15.14 ± 0.06	14.94 ± 1.16	20.59 ± 1.07
Linoleic Acid	C18:1n9t	1.13 ± 0.16	1.82 ± 0.14	1.86 ± 0.10
Linolelaidic Acid	C18:2n6c	15.03 ± 1.92	24.82 ± 1.92	14.97 ± 10.58
y-Linoleic Acid	C18:3n6	0.07 ± 0.01	3.06 ± 0.22	0.00 ± 0.00
α-Linoleic Acid	C18:3n3	2.04 ± 0.26	0.04 ± 0.2	2.51 ± 0.14
Arachidic Acid	C20:0	1.30 ± 0.07	1.58 ± 0.08	1.31 ± 0.06

5.9   Summary

The results presented in this Chapter have demonstrated the potential of the 24-well mPBr (without illumination) for the heterotrophic batch cultivation of different *Chlorella strains* notably *C. sorokiniana* and *C. protothecoides* (Figure 5.4). More importantly, it has been shown that cultivation under matched k_La conditions (35-40 h^{-1}) enables predictive scale-up of culture kinetics for *C. sorokiniana* between 24-well mPBr and 7.5 L STR scales representing a 1000-fold scale translation (Figure 5.5). The results indicate matched growth kinetics (Figure 5.5 & 5.6) and biomass yield (Table 5-3), substrate utilisation (Table 5-3), particle size distribution at harvest (Figure 5.7), total lipid production (Figure 5.10) and comparable lipid composition in terms of individual FAME produced (Figure 5.11 and Table 5-5).

Successful implementation of the mPBr for batch heterotrophic culture suggests this approach might be extended to fed-batch culture with well-defined feeding strategies. A higher biomass concentration would be expected with the extent depending on media formulation and feeding strategies adopted. At higher biomass concentration, decrease in pH below the range tolerable by the strain used would be expected due to increased bicarnonate concentration. However, as previously described in Section 2.1.3, further optimisation of the tris-base concentration used to keep the pH within an acceptable range at high culture density should be possible. The impact on product and lipid formation should also be further investigated. An increased understanding of the impact of tris-base of culture kinetics would further enable its application for both phototrophic and heterotrophic microalgae cultivation.

Overall, the 24-well mPBr appears superior to conventionally used shake flask systems offering a reduction in volume and an increase in experimental throughput. Importantly, the growth rates and productivities achieved provide a better match to those determined at the larger 7.5 L STR scale compared to the shake flasks. While the scope of this study was constrained to scale-up to the 7.5 L STR it would be interesting to explore the scalability of mPBr results to larger pilot scale (>100L) bioreactor systems.

6. CONCLUSIONS AND FUTURE WORK

6.1 Conclusions

At the start of this project a key challenge in microalgae bioprocess development was identified as the lack of a suitable platform for early stage evaluation of microalgae cultivation conditions (Section 1.2.4). For phototrophic cultivation in particular, small-scale photobioreactor technologies were not available. As previously highlighted in Section 1.2.4, creation of a miniature photobioreactor system, with the ability to mimic large-scale photobioreactor performance has the potential to reduce the costs, risks and time taken to bring microalgal products to market. The development of a generic microscale cultivation platform and establishment of effective engineering bases for scale translation was therefore considered novel and had not previously been reported in the literature. This thesis has described the development, characterisation and application of a generic mPBr cultivation platform suitable for both phototrophic and heterotrophic cultivation. Validated scale-out and scale-up strategies up to a 2 L SUPBr (phototrophic cultivation) and a 7.5 L STR (heterotrophic cultivation) have also been defined.

The initial objective was to develop a generic microscale platform for phototrophic cultivation of microalgae. The model test organism *C. sorokiniana* was used in all the experiments due to its high growth rates and biomass yields (Figure 3.8 and Figure 4.7) hence requirements for light and CO_2. The initial work focused on development of a 24-well mPBr (Figure 2.1) on a novel orbitally shaken and illuminated platform as illustrated in Figure 2.3. The platform enables parallel evaluation of up to six scaled-out 24-well mPBr plates which is equivalent to performing 144 separate experiments. The humidity controlled orbital shaking incubator that housed the illuminated shaking platform and the mPBr enabled effective control of evaporation over extended culture periods (Figure 3.5 (A)). As described in Chapter 3 the mPBr platform allowed a reduction in scale of 25-fold and

a concomitant increase in experimental throughput of 40-fold compared to conventional shake flask systems.

For culture of *C. sorokiniana*, a light intensity of 380 $\mu molm^{-2}s^{-1}$ with 5% CO_2 enriched air were found to provide optimum cultivation conditions (Figure 3.10). FAME compositions suitable for biodiesel production were also obtained under these optimal conditions (Figure 3.12). This work demonstrated the suitability of the mPBr system for screening different strains for production of biofuels and other polyunsaturated FAME of commercial importance. Furthermore, it was shown that reformulation of the commonly used TAP medium allowed adequate control of the culture pH (Figure 3.6).

To facilitate scale-up studies for the phototrophic cultivation of *C. sorokiniana* the shaking incubator platform was redesigned to enable operation with a SUPBr bag as shown in Figure 2.6. The SUPBr performance was investigated in terms of key engineering characteristics as described in Section 2.4. The overall oxygen mass transfer coefficient, k_La, in the mPBr and the SUPBr were evaluated as a function of shaking frequency, alongside the fluid hydrodynamics and mixing time (Section 4.2-4.4). Fluid hydrodynamics exhibited out-of-phase condition at shaking frequencies $\geq$ 300 and $\geq$ 180 rpm for mPBr and SUPBr respectively (Figure 3.3 and Figure 4.4). Further engineering characterisation in terms of mixing in the SUPBr showed t_m values to be in the range 15-30 s (Figure 4.6) with no significant difference in values above shaking frequencies of 70 rpm.

The growth performance for batch culture of *C. sorokiniana* using the SUPBr showed comparable results with other PBr designs reported in the literatures (Table 4-2). In addition, growth performances were similar at matched scale-up criteria as discussed in Section 4.6. This investigation concluded that successful scale-up was achieved on the basis of constant light intensity and path length as shown in Figure 4.9. The maximum biomass concentration was found to be around 6 gL^{-1} at the matched conditions. Further details on the fabrication, application, optimisation and scale translation of mPBr results to the SUPBr for early stage microalgal bioprocess development were discussed in detail in Chapter 3 - 4.

In order to prove the wider generic applicability of the mPBr, heterotrophic cultivation of *C. sorokiniana* was also undertaken (Chapter 5) and the potential for scale-up to conventional shake flasks and a 7.5 L STR demonstrated (Figure 5.5). Successful scale translation was based on matched k_La (while maintaining effective fluid mixing) as shown in Figure 5.2. In the heterotrophic scale translation studies good agreement was found between biomass concentration, pH, specific growth rate and chlorophyll concentration as reported in Figure 5.5 and Table 5-3 respectively. The 24-well mPBr has thus proven to be a valuable tool for heterotrophic cultivation on the basis of the scalability of culture performance to a conventional laboratory STR.

In summary, the work reported in this thesis has met the original aim of evaluating wider application of the miniature photobioreactor for heterotrophic cultivation of various microalgae strains and establishment of scale-up criteria from the mPBr to a conventional 7.5 L STR. The application of the mPBr was demonstrated for both phototrophic and heterotrophic culture of various *Chlorella* strains.

6.2 Future Work

The work in this thesis has demonstrated and validated the suitability of the scaled-out mPBr system for high-throughput cultivation and optimisation of microalgal growth conditions with reproducible and scalable results. Suggestions for future work are summarised below:

- Exploration of different feeding/cultivation strategies. Further studies similar to those described in Chapter 3 should be performed to explore the use of the mPBr with other microalgae strains and more challenging culture conditions such as the culture of flagellate microalgae which potentially cannot withstand rigorous agitation and high levels of hydrodynamic shear (Zhang et al., 2008). High density culture should also be tested by developing suitable substrate feeding regimes. Initial studies during the course of this thesis were undertaken on fed-batch phototrophic cultivation suggesting that such cultivation methods are possible at the mPBr scale.

- Modeling and simulation of gas-liquid distribution and liquid phase mixing times. In order to provide a more rigorous and comprehensive understanding and predictive capability of culture performance in the mPBr and SUPBr, liquid phase mixing times and also gas-liquid distribution within each system should be investigated in more detail. This will require the application of theoretical approaches, such as CFD modeling of fluid flow, as well as further high speed video studies to validate the model predictions.

- Multi-strain screening and the application of statistical Design of Experiments (DoE). The utility of using the mPBr alongside DoE methods should be demonstrated to increase experimental throughput and further optimise culture conditions. DoE approaches should examine critical variables such as media formulation, light regime, carbon dioxide concentration and mixing rate. Optimum relationships should be established between cell growth rate/yield and lipid production which it was not possible to fully explore during this project.

- Redesign of the geometry systems. Based on the observed hydrodynamics in the SUPBr, redesigning of the SUPBr having a flat rectangular base with the hemispherical top could better enhance optimised light utilisation and mixing.

- Predictive modeling of growth kinetics. Based on the experimental data generated in this thesis for growth kinetics under different culture conditions it would be useful to develop a mathematical model for prediction of *C. sorokiniana* growth kinetics based on radiance transfer equations and liquid hydrodynamics (Béchet et al., 2013; Zhang et al., 2008).

- Redesign for commercialisation. Finally, it would be necessary to redesign the shaking and control systems for reliable, long term operation. This would be a vital step before commercialisation of the technology could be considered. Such work would ideally be pursued through industrial collaboration.

References

Abdollahi J, Dubljevic S. 2012. Lipid production optimization and optimal control of heterotrophic microalgae fed-batch bioreactor. *Chem. Eng. Sci.* **84**:619–627.

Agrawal SC, Manisha. 2007. Growth, survival and reproduction in *Chlorella vulgaris* and *C. variegata* with respect to culture age and under different chemical factors. *Folia Microbiol. (Praha).* **52**:399–406.

Aiba S. 1982. Growth Kinetics of Photosynthetic Microorganisms. *Adv. Biochem. Eng.* **23**:85–156.

Allard B, Templier J. 2001. High molecular weight lipids from the trilaminar outer wall (TLS)-containing microalgae *Chlorella emersonii*, *Scenedesmus communis* and Tetraedron minimum. *Phytochemistry* **57**:459–467.

Allard B, Rager MN, Templier J. 2002. Occurrence of high molecular weight lipids (C80 +) in the trilaminar outer cell walls of some freshwater microalgae. A reappraisal of algaenan structure. *Org. Geochem.* **33**:789–801.

Barrett TA, Wu A, Zhang H, Levy MS, Lye GJ. 2010. Microwell engineering characterization for mammalian cell culture process development. *Biotechnol. Bioeng.* **105**:260–75.

Béchet Q, Shilton A, Fringer OB, Munoz R, Guieysse B. 2010. Mechanistic modeling of broth temperature in outdoor photobioreactors. *Environ. Sci. Technol.* **44**:2197–2203.

Béchet Q, Shilton A, Guieysse B. 2013. Modeling the effects of light and temperature on algae growth: state of the art and critical assessment for productivity prediction during outdoor cultivation. *Biotechnol. Adv.* **31**:1648–63.

Béchet Q, Shilton A, Park JBK, Craggs RJ, Guieysse B. 2011. Universal temperature model for shallow algal ponds provides improved accuracy. *Environ. Sci. Technol.* **45**:3702–3709.

Becker EW (1994). Microalgae: Biotechnology and Microbioloby, Cambridge University Press, Pg 263.

Bellou S, Aggelis G. 2012. Biochemical activities in Chlorella sp. and Nannochloropsis salina during lipid and sugar synthesis in a lab-scale open pond simulating reactor. *J. Biotechnol.* **164**:318–29.

Betts JPJ, Warr SRC, Finka GB, Uden M, Town M, Janda JM, Baganz F, Lye GJ. 2014. Impact of aeration strategies on fed-batch cell culture kinetics in a single-use 24-well miniature bioreactor. *Biochem. Eng. J.* **82**:105–116.

Betts JI, Baganz F. 2006. Miniature bioreactors: current practices and future opportunities. *Microb. Cell Fact.* **5**:21.

Betts JI, Doig SD, Baganz F. 2006. Characterization and application of a miniature 10 mL stirred-tank bioreactor, showing scale-down equivalence with a conventional 7 L reactor. *Biotechnol. Prog.* **22**:681–8.

Bligh EG, Dyer WJ. 1959. A rapid method of total lipid extraction and purification. *Can. J. Biochem. Physiol.* **37**.

Blumreisinger M, Meindl D, Loos E. 1983. Cell wall composition of chlorococcal algae. *Phytochemistry.*

Borowitzka M. 1999. Commercial production of microalgae: ponds, tanks, tubes and fermenters. *J. Biotechnol.* **70**:313–321.

Bosma R, Van Zessen E, Reith JH, Tramper J, Wijffels RH. 2007. Prediction of volumetric productivity of an outdoor photobioreactor. *Biotechnol. Bioeng.* **97**:1108–1120.

Brecht R. 2009. Disposable Bioreactors : Maturation into Pharmaceutical Glycoprotein Manufacturing. *Adv. Biochem. Eng. Biotechnol.* **115**:1 – 31.

Büchs J, Lotter S, Milbradt C. 2001. Out-of-phase operating conditions, a hitherto unknown phenomenon in shaking bioreactors. *Biochem. Eng. J.* **7**:135–141.

Büchs J, Maier U, Milbradt C, Zoels B. 2000a. Power consumption in shaking flasks on rotary shaking machines: II. Nondimensional description of specific power consumption and flow regimes in unbaffled flasks at elevated liquid viscosity. *Biotechnol. Bioeng.* **68**:594–601.

Büchs J, Maier U, Milbradt C, Zoels B. 2000b. Power consumption in shaking flasks on rotary shaking machines: I. Power consumption measurement in unbaffled flasks at low liquid viscosity. *Biotechnol. Bioeng.* **68**:589–93.

Büchs J, Maier U, Lotter S, Peter CP. 2007. Calculating liquid distribution in shake flasks on rotary shakers at waterlike viscosities. *Biochem. Eng. J.* **34**:200–208.

Bumbak F, Cook S, Zachleder V, Hauser S, Kovar K. 2011. Best practices in heterotrophic high-cell-density microalgal processes: achievements, potential and possible limitations. *Appl. Microbiol. Biotechnol.* **91**:31–46.

Carpita NC. 1985. Tensile strength of cell walls of living cells. *Plant Physiol.* **79**:485–488.

Carvalho AP, Meireles L a, Malcata FX. 2006. Microalgal reactors: a review of enclosed system designs and performances. *Biotechnol. Prog.* **22**:1490–506.

Cha TS, Chen JW, Goh EG, Aziz A, Loh SH. 2011. Differential regulation of fatty acid biosynthesis in two *Chlorella species* in response to nitrate treatments and the potential of binary blending microalgae oils for biodiesel application. *Bioresour. Technol.* **102**:10633–40.

Chader S, Mahmah B, Chetehouna K, Mignolet E. 2011. Biodiesel production using *Chlorella sorokiniana* a green microalga. *Rev. des Energies Renouvelables* **14**:21–26.

Chen C, Chang J. 2006. Enhancing phototropic hydrogen production by solid-carrier assisted fermentation and internal optical-fiber illumination. *Process Biochem.* **41**:2041–2049.

Chen C-Y, Yang M-H, Yeh K-L, Liu C-H, Chang J-S. 2008. Biohydrogen production using sequential two-stage dark and photo fermentation processes. *Int. J. Hydrogen Energy* **33**:4755–4762.

Chen C-Y, Yeh K-L, Aisyah R, Lee D-J, Chang J-S. 2010a. Cultivation, photobioreactor design and harvesting of microalgae for biodiesel production: A critical review. *Bioresour. Technol.* **102**:71–81.

Chen C-Y, Yeh K-L, Aisyah R, Lee D-J, Chang J-S. 2011. Cultivation, photobioreactor design and harvesting of microalgae for biodiesel production: a critical review. *Bioresour. Technol.* **102**:71–81.

Chen C-Y, Yeh K-L, Su H-M, Lo Y-C, Chen W-M, Chang J-S. 2010b. Strategies to enhance cell growth and achieve high-level oil production of a *Chlorella vulgaris* isolate. *Biotechnol. Prog.* **26**:679–86.

Chen G-Q, Chen F. 2006. Growing phototrophic cells without light. *Biotechnol. Lett.* **28**:607–16.

Cheng Y, Zhou W, Gao C, Lan K, Gao Y, Wu Q. 2009. Biodiesel production from Jerusalem artichoke (Helianthus Tuberosus L.) tuber by heterotrophic microalgae *Chlorella protothecoides*. *J. Chem. Technol. Biotechnol.* **84**:777–781.

Chisti Y. 2007. Biodiesel from microalgae. *Biotechnol. Adv.* **25**:294–306.

Chiu SY, Tsai MT, Kao CY, Ong SC, Lin CS. 2009. The air-lift photobioreactors with flow patterning for high-density cultures of microalgae and carbon dioxide removal. *Eng. Life Sci.* **9**:254–260.

Chiu S-Y, Kao C-Y, Chen C-H, Kuan T-C, Ong S-C, Lin C-S. 2008. Reduction of CO2 by a high-density culture of *Chlorella sp*. in a semicontinuous photobioreactor. *Bioresour. Technol.* **99**:3389–3396.

Cordero BF, Obraztsova I, Couso I, Leon R, Vargas MA, Rodriguez H. 2011. Enhancement of lutein production in *Chlorella sorokiniana* (Chorophyta) by

improvement of culture conditions and random mutagenesis. *Mar. Drugs* **9**:1607–24.

Cornet JF, Dussap CG. 2009. A simple and reliable formula for assessment of maximum volumetric productivities in photobioreactors. *Biotechnol. Prog.* **25**:424–435.

Cuaresma M, Janssen M, Vílchez C, Wijffels RH. 2009. Productivity of *Chlorella sorokiniana* in a short light-path (SLP) panel photobioreactor under high irradiance. *Biotechnol. Bioeng.* **104**:352–9.

Devi MP. 2013. Nutritional mode influence lipid accumulation in microalgae with the function of carbon sequestration and nutrient supplementation. *Bioresour. Technol.* **112**:116–123.

Dindore V, Brilman D, Versteeg G. 2005. Hollow fiber membrane contactor as a gas liquid model contactor. *Chem. Eng. Sci.* **60**:467–479.

Doig SD, Ortiz-Ochoa K, Ward JM, Baganz F. 2005. Characterization of oxygen transfer in miniature and lab-scale bubble column bioreactors and comparison of microbial growth performance based on constant k(L)a. *Biotechnol. Prog.* **21**:1175–82.

Doig SD, Pickering SCR, Lye GJ, Woodley JM. 2002. The use of microscale processing technologies for quantification of biocatalytic Baeyer-Villiger oxidation kinetics. *Biotechnol. Bioeng.* **80**:42–9.

Doran PM. 1995. Bioprocess Engineering Principles. *Technology*. Vol. 9.

Doucha J, Lívanský K. 2008. Influence of processing parameters on disintegration of *Chlorella* cells in various types of homogenizers. *Appl. Microbiol. Biotechnol.* **81**:431–40.

Duetz WA. 2007. Microtiter plates as mini-bioreactors: miniaturization of fermentation methods. *Trends Microbiol.* **15**:469–75.

Duetz WA, Witholt B. 2004. Oxygen transfer by orbital shaking of square vessels and deepwell microtiter plates of various dimensions. *Biochem. Eng. J.* **17**:181–185.

Eibl D. 2014. Disposable Bioreactors II. Ed. Dieter Eibl, Regine Eibl. *Adv. Biochem. Eng. Biotechnol.* **138**.

Eibl D, Eibl R, Köhler P. 2012. Single-use technology in biopharmaceutical production. Dechema Biotechnology.

Eibl R, Kaiser S, Lombriser R, Eibl D. 2010. Disposable bioreactors: the current state-of-the-art and recommended applications in biotechnology. *Appl. Microbiol. Biotechnol.* **86**:41–9.

Eibl R, Werner S, Eibl D. 2009. Bag bioreactor based on wave-induced motion: characteristics and applications. *Adv. Biochem. Eng. Biotechnol.* **115**:55–87.

Elmahdi I. 2003. pH control in microwell fermentations of *S. erythraea CA340*: influence on biomass growth kinetics and erythromycin biosynthesis. *Biochem. Eng. J.* **16**:299–310.

Fernandes P, Cabral JMS. 2006. Microlitre/millilitre shaken bioreactors in fermentative and biotransformation processes – a review. *Biocatal. Biotransformation* **24**:237–252.

Funke M, Diederichs S, Kensy F, Müller C, Büchs J. 2009. The baffled microtiter plate: Increased oxygen transfer and improved online monitoring in small scale fermentations. *Biotechnol. Bioeng.* **103**:1118–1128.

Gasparini F, de O. Lima JR, Ghani Y a., Hatanaka RR, Sequinel R, Flumignan DL, de Oliveira JE. 2011. EN 14103 Adjustments for biodiesel analysis from different raw materials, including animal tallow containing C17. *Bioenergy Technol.*101–108.

Gehl KA, Colman B. 1985. Effect of External pH on the Internal pH of *Chlorella saccharophila*. *Plant Physiol.* **77**:917–921.

Ghoshal D, Goyal A. 2001. Oxygen inhibition of dissolved inorganic carbon uptake in unicellular green algae. *Phycol. Res.* **49**:319–324.

Gill NK, Appleton M, Baganz F, Lye GJ. 2008a. Quantification of power consumption and oxygen transfer characteristics of a stirred miniature bioreactor for predictive fermentation scale-up. *Biotechnol. Bioeng.* **100**:1144–55.

Gill NK, Micheletti M, Lye GJ. 2011. Engineering characterisation of single-use , wave-type bioreactors and scale- up considerations for early phase cell culture process development. http://microsite.sartorius.com/fileadmin/Image_Archive/ microsite/biostat_cultibag/pdf/11-06-21/Esact%20Europe_may%202011.pdf

Gill NK, Appleton M, Baganz F, Lye GJ. 2008b. Design and characterisation of a miniature stirred bioreactor system for parallel microbial fermentations. *Biochem. Eng. J.* **39**:164–176.

Gouveia L, Oliveira AC. 2009. Microalgae as a raw material for biofuels production. *J. Ind. Microbiol. Biotechnol.* **36**:269–274.

Grobbelaar JU. 2009. Factors governing algal growth in photobioreactors: The "open" versus "closed" debate. *J. Appl. Phycol.* **21**:489–492.

Guedes a C, Amaro HM, Malcata FX. 2011. Microalgae as sources of high added-value compounds--a brief review of recent work. *Biotechnol. Prog.* **27**:597–613.

Harun R, Singh M, Forde GM, Danquah MK. 2010. Bioprocess engineering of microalgae to produce a variety of consumer products. *Renew. Sustain. Energy Rev.* **14**:1037–1047.

Halim R, Harun R, Webley PA, Danquah MK. (2013). Bioprocess engineering aspects of biodiesel and biothanol production from microalgae. Adv. Biofuels and Bioprod. 601-628.

Hermann R, Lehmann M, Büchs J. 2003. Characterization of gas-liquid mass transfer phenomena in microtiter plates. *Biotechnol. Bioeng.* **81**:178–86.

Hillig F, Annemüller S, Chmielewska M, Pilarek M, Junne S, Neubauer P. 2013. Bioprocess Development in Single-Use Systems for Heterotrophic Marine Microalgae. *Chemie Ing. Tech.* **85**:153–161.

Hillig F, Pilarek M, Junne S, Neubauer P. 2014a. Cultivation of marine microorganisms in single-use systems. *Adv. Biochem. Eng. Biotechnol.* **138**:179–206.

Hillig F, Porscha N, Junne S, Neubauer P. 2014b. Growth and docosahexaenoic acid production performance of the heterotrophic marine microalgae *Crypthecodinium cohnii* in the wave-mixed single-use reactor CELL-tainer. *Eng. Life Sci.* **14**:254–263.

Hsieh C-H, Wu W-T. 2009. Cultivation of microalgae for oil production with a cultivation strategy of urea limitation. *Bioresour. Technol.* **100**:3921–6.

Hsueh HT, Chu H, Yu ST. 2007. A batch study on the bio-fixation of carbon dioxide in the absorbed solution from a chemical wet scrubber by hot spring and marine algae. *Chemosphere* **66**:878–86.

Hu Q, Sommerfeld M, Jarvis E, Ghirardi M, Posewitz M, Seibert M, Darzins A. 2008. Microalgal triacylglycerols as feedstocks for biofuel production: perspectives and advances. *Plant J.* **54**:621–39.

Huang G, Chen F, Wei D, Zhang X, Chen G. 2010. Biodiesel production by microalgal biotechnology. *Appl. Energy*.

Hussain W, Moens N, Veraitch FS, Hernandez D, Mason C, Lye GJ. 2013. Reproducible culture and differentiation of mouse embryonic stem cells using an automated microwell platform. *Biochem. Eng. J.* **77**:246–257.

IEA. 2011. Technology Roadmap Biofuels for Transport. *Int. Energy Agency Fr.*52.

Illman A, Scragg A, Shales S. 2000. Increase in *Chlorella strains* calorific values when grown in low nitrogen medium. *Enzyme Microb. Technol.* **27**:631–635.

Ip PF, Chen F. 2005. Production of astaxanthin by the green microalga *Chlorella zofingiensis* in the dark. *Process Biochem.* **40**:733–738.

Isett K, George H, Herber W, Amanullah A. 2007. Twenty-four-well plate miniature bioreactor high-throughput system : Assessment for microbial cultivations. *Biotechnol. Bioeng.* **98**:1017–1028.

Islam RS, Tisi D, Levy MS, Lye GJ. 2008. Scale-up of *Escherichia coli* growth and recombinant protein expression conditions from microwell to laboratory and pilot scale based on matched k(L)a. *Biotechnol. Bioeng.* **99**:1128–39.

James GO, Hocart CH, Hillier W, Chen H, Kordbacheh F, Price GD, Djordjevic M a. 2011. Fatty acid profiling of *Chlamydomonas reinhardtii* under nitrogen deprivation. *Bioresour. Technol.* **102**:3343–51.

Janssen M, Tramper J, Mur LR, Wijffels RH. 2003. Enclosed outdoor photobioreactors: light regime, photosynthetic efficiency, scale-up, and future prospects. *Biotechnol. Bioeng.* **81**:193–210.

Jeffrey SW, Humphrey GF. 1975. New spectrophotometric equations for determining chlorophyll a , b , c1 and c2 in higher plants , algae and. *Biochem. Physiol. Pflanz* **167**:191–194.

Jeong ML, Gillis JM, Hwang J. 2003. Carbon dioxide mitigation by microalgal photosynthesis **24**:1763–1766.

Jimenez C, Belen R. C, Diego L, F. Xavier N. 2003. The Feasibility of industrial production of *Spirulina* (Arthrospira) in Southern Spain. *Aquaculture* **217**:179–190.

Kalmbach A, Bordás R, Oncül A a, Thévenin D, Genzel Y, Reichl U. 2011. Experimental characterization of flow conditions in 2- and 20-L bioreactors with wave-induced motion. *Biotechnol. Prog.* **27**:402–9.

Katarzyna C, Facundo-Joaquin M-R. 2004. Kinetic and stoichiometric relationships of the energy and carbon metabolism in the culture of microalgae. *biotechnology(Faisalabad)*.

Kauling J, Brod H, Jenne M, Waldhelm A, Langer U, Bödeker B. 2013. Novel, rotary oscillated, scalable single-use bioreactor technology for the cultivation of animal cells. *Chemie Ing. Tech.* **85**:127–135.

Khalil ZI, Asker MMS, El-Sayed S, Kobbia I a. 2009. Effect of pH on growth and biochemical responses of Dunaliella bardawil and *Chlorella ellipsoidea*. *World J. Microbiol. Biotechnol.* **26**:1225–1231.

Kirk T V, Szita N. 2013. Oxygen transfer characteristics of miniaturized bioreactor systems. *Biotechnol. Bioeng.* **110**:1005–19.

Klöckner W, Büchs J. 2012. Advances in shaking technologies. *Trends Biotechnol.* **30**:307–14.

Krienitz L, Takeda H, Hepperle D. 1999. Ultrastructure, cell wall composition, and phylogenetic position of *Pseudodictyosphaerium jurisii* (Chlorococcales, Chlorophyta) including a comparison with other picoplanktonic green algae. *Phycologia*.

Kumar K, Das D. 2012. Growth characteristics of *Chlorella sorokiniana* in airlift and bubble column photobioreactors. *Bioresour. Technol.* **116**:307–13.

Kumar S, Wittmann C, Heinzle E. 2004. Minibioreactor. *Biotechnol. Lett.* **26**:1–10.

Lehana M. 1990. Kinetic analysis of the growth of *Chlorella vulgaris*. *Biotechnol. Bioeng.* **36**:198–206.

Lehmann N, Rischer H, Eibl D, Eibl R. 2013. Wave-mixed and orbitally shaken single-use photobioreactors for diatom algae propagation. *Chemie Ing. Tech.* **85**:197–201.

Li M, Hu CW, Zhu Q, Kong ZM, Liu ZL. 2007a. Outdoor mass culture of the marine microalga *Pavlova viridis* (Prymnesiophyceae) for production of eicosapentaenoic acid (EPA). *Cryptogam. Algol.* **28**:397–410.

Li Q, Du W, Liu D. 2008. Perspectives of microbial oils for biodiesel production. *Appl. Microbiol. Biotechnol.* **80**:749–756.

Li T, Zheng Y, Yu L, Chen S. 2013. High productivity cultivation of a heat-resistant microalga *Chlorella sorokiniana* for biofuel production. *Bioresour. Technol.* **131**:60–7.

Li X, Xu H, Wu Q. 2007b. Large-scale biodiesel production from microalga *Chlorella protothecoides* through heterotrophic cultivation in bioreactors. *Biotechnology* **98**:764–771.

Liang Y, Sarkany N, Cui Y. 2009. Biomass and lipid productivities of *Chlorella vulgaris* under autotrophic, heterotrophic and mixotrophic growth conditions. *Biotechnol. Lett.* **31**:1043–1049.

Liao Q, Li L, Chen R, Zhu X. 2014. A novel photobioreactor generating the light/dark cycle to improve microalgae cultivation. *Bioresour. Technol.* **161**:186–191.

Linek V, Kordač M, Fujasová M, Moucha T. 2004. Gas-liquid mass transfer coefficient in stirred tanks interpreted through models of idealized eddy structure of turbulence in the bubble vicinity. *Chem. Eng. Process. Process Intensif.* **43**:1511–1517.

Liu J, Huang J, Fan KW, Jiang Y, Zhong Y, Sun Z, Chen F. 2010. Production potential of *Chlorella zofingienesis* as a feedstock for biodiesel. *Bioresour. Technol.* **101**:8658–63.

Löffelholz C, Husemann U, Greller G, Meusel W, Kauling J, Ay P, Kraume M, Eibl R, Eibl D. 2013. bioengineering parameters for single-use bioreactors: overview and evaluation of suitable methods. *Chemie Ing. Tech.* **85**:40–56.

Löffelholz C, Kaiser SC, Kraume M, Eibl R, Eibl D. 2014. Dynamic single-use bioreactors used in modern liter- and m(3)- scale biotechnological processes: engineering characteristics and scaling up. *Adv. Biochem. Eng. Biotechnol.* **138**:1–44.

Lopes AG. 2013. Single-use in the biopharmaceutical industry: A review of current technology impact, challenges and limitations. *Food Bioprod. Process.*1–17.

Lu S, Wang J, Niu Y, Yang J, Zhou J, Yuan Y. 2012. Metabolic profiling reveals growth related FAME productivity and quality of *Chlorella sorokiniana* with different inoculum sizes. *Biotechnol. Bioeng.* **109**:1651–62.

Lye G, Infors HT. 2010. Application note Analysis of evaporation in Box for Microtitre Plates.

Lye GJ, Ayazi-Shamlou P, Baganz F, Dalby P a, Woodley JM. 2003. Accelerated design of bioconversion processes using automated microscale processing techniques. *Trends Biotechnol.* **21**:29–37.

Mairet F, Bernard O, Lacour T, Sciandra A. 2011. Modelling microalgae growth in nitrogen limited photobiorector for estimating biomass , carbohydrate and neutral lipid. *Int. Fed. Autom. Control*:10591–10596.

Marques MPC, Cabral JMS, Fernandes P. 2010. Bioprocess scale-up: quest for the parameters to be used as criterion to move from microreactors to lab-scale. *J. Chem. Technol. Biotechnol.* **85**:1184–1198.

Mata TM, Martins AA, Caetano NS. 2010. Microalgae for biodiesel production and other applications: A review. *Renew. Sustain. Energy Rev.* **14**:217–232.

Mattos ER, Singh M, Cabrera ML, Das KC. 2012. Effects of inoculum physiological stage on the growth characteristics of *Chlorella sorokiniana* cultivated under different CO_2 concentrations. *Appl. Biochem. Biotechnol.* **168**:519–30.

Merchuk JC, Sheva B, College J. 2011. Photobioreactors − Models of Photosynthesis and Related Effects. *Compr. Biotechnol.* **1**:227–248.

Merseburger T, Pahl I, Müller D, Tanner M. 2014. A risk analysis for production processes with disposable bioreactors. *Adv. Biochem. Eng. Biotechnol.* **138**:273–88.

Metting F. 1996. Biodiversity and application of microalgae. *Ind. Microbiol. ans Biotechnol.* **17**:477–489.

Meusel W, Kauling J, Löffelholz C. 2013. Single-use technologies for biopharmaceutical production: report from the working group bioprocess technology - upstream processing. *Chemie Ing. Tech.* **85**:23–25.

Miao X, Wu Q. 2006. Biodiesel production from heterotrophic microalgal oil. *Bioresour. Technol.* **97**:841–6.

Micheletti M, Barrett T, Doig S, Baganz F, Levy M, Woodley J, Lye G. 2006. Fluid mixing in shaken bioreactors: Implications for scale-up predictions from microlitre-scale microbial and mammalian cell cultures. *Chem. Eng. Sci.* **61**:2939–2949.

Micheletti M, Lye GJ. 2006. Microscale bioprocess optimisation. *Curr. Opin. Biotechnol.* **17**:611–8.

Mirón AS, Gómez AC, Camacho FG, Grima EM, Chisti Y. 1999. Comparative evaluation of compact photobioreactors for large-scale monoculture of microalgae. *Prog. Ind. Microbiol.* **35**:249–270.

Mohsenpour SF, Richards B, Willoughby N. 2012. Spectral conversion of light for enhanced microalgae growth rates and photosynthetic pigment production. *Bioresour. Technol.* **125**:75–81.

Morita M, Watanabe Y, Saiki H. 2002. Photosynthetic productivity of conical helical tubular photobioreactor incorporating *Chlorella sorokiniana* under field conditions. *Biotechnol. Bioeng.* **77**:155–162.

Mukhopadhyay TK, Allison N, Charlton S, Ward J, Lye GJ. 2011. Use of microwells to investigate the effect of quorum sensing on growth and antigen production in *Bacillus anthracis Sterne* 34F2. *J. Appl. Microbiol.* **111**:1224–34.

Muthuraj M, Kumar V, Palabhanvi B, Das D. 2014. Evaluation of indigenous microalgal isolate *Chlorella sp.* FC2 IITG as a cell factory for biodiesel production and scale up in outdoor conditions. *J. Ind. Microbiol. Biotechnol.* **41**:499–511.

Ngangkham M, Ratha SK, Prasanna R, Saxena AK, Dhar DW, Sarika C, Prasad RBN. 2012. Biochemical modulation of growth, lipid quality and productivity in mixotrophic cultures of *Chlorella sorokiniana*. *Springerplus* **1**:33.

O'Grady J, Morgan J a. 2010. Heterotrophic growth and lipid production of *Chlorella protothecoides* on glycerol. *Bioprocess Biosyst. Eng.*121–125.

Oncül AA, Kalmbach A, Genzel Y, Reichl U, Thévenin D. 2009. Characterization of flow conditions in 2 L and 20 L wave bioreactors using computational fluid dynamics. *Biotechnol. Prog.* **26**:101–10.

Orus MI, Marco E, Martinez F. 1991. Suitability of *Chlorella vulgaris* UAM 101 for heterotrophic biomass production. In: . *Bioresour. Technol.*, Vol. 38, pp. 179–184.

Packer A, Li Y, Andersen T, Hu Q, Kuang Y, Sommerfeld M. 2011. Growth and neutral lipid synthesis in green microalgae: A mathematical model. *Bioresour. Technol.* **102**:111–117.

Perez-Garcia O, Escalante FME, de-Bashan LE, Bashan Y. 2011. Heterotrophic cultures of microalgae: metabolism and potential products. *Water Res.* **45**:11–36.

Perez-garcia O, Escalante FME, Luz E, Bashan Y. 2010. Heterotrophic cultures of microalgae : Metabolism and potential products. *Water Res.* **45**:11–36.

Perner-Nochta I, Posten C. 2007. Simulations of light intensity variation in photobioreactors. *J. Biotechnol.* **131**:276–285.

Pradhan K, Pant T, Gadgil M. 2012. In situ pH maintenance for mammalian cell cultures in shake flasks and tissue culture flasks. *Biotechnol. Prog.* **28**:1605–10.

Prathima Devi M, Swamy Y V, Venkata Mohan S. 2013. Nutritional mode influences lipid accumulation in microalgae with the function of carbon sequestration and nutrient supplementation. *Bioresour. Technol.* **142**:278–86.

Pruvost J, Pottier L, Legrand J. 2006. Numerical investigation of hydrodynamic and mixing conditions in a torus photobioreactor. *Chem. Eng. Sci.* **61**:4476–4489.

Pulz O, Gross W. 2004. Valuable products from biotechnology of microalgae. *Appl. Microbiol. Biotechnol.* **65**:635–48.

Pyle DJ, Garcia R a, Wen Z. 2008. Producing docosahexaenoic acid (DHA)-rich algae from biodiesel-derived crude glycerol: effects of impurities on DHA production and algal biomass composition. *J. Agric. Food Chem.* **56**:3933–9.

Qiao H, Wang G. 2009. Effect of carbon source on growth and lipid accumulation in *Chlorella sorokiniana* GXNN01. *Chinese J. Oceanol. Limnol.* **27**:762–768.

Raoof B, Kaushik B, Prasanna R. 2006. Formulation of a low-cost medium for mass production of *Spirulina*. *Biomass and Bioenergy* **30**:537–542.

Ratledge C. 2002. Regulation of lipid accumulation in oleaginous micro-organisms. *Biochem. Soc. Trans.* **30**:1047–50.

Raval K, Kato Y, Buchs J. 2007. Comparison of torque method and temperature method for determination of power consumption in disposable shaken bioreactors. *Biochem. Eng. J.* **34**:224–227.

Robertson P, Jane F. 2010. Studies on *Chlorella vulgaris* II . Further Evidence that *Chlorella* Cells form a Growth- Inhibiting Substance. *America (NY).* **27**:431–436.

Rodolfi L, Zittelli GC, Bassi N, Padovani G, Biondi N, Bonini G, Tredici MR. 2009. Microalgae for oil: Strain selection, induction of lipid synthesis and outdoor mass cultivation in a low-cost photobioreactor. *Biotechnol. Bioeng.* **102**:100–112.

Rupprecht J. 2009. From systems biology to fuel--*Chlamydomonas reinhardtii* as a model for a systems biology approach to improve biohydrogen production. *J. Biotechnol.* **142**:10–20.

Sakthivel R, Elumalai S, Mohommad M. 2011. Microalgae lipid research , past , present : A critical review for biodiesel production , in the future. *Plant Biol.* **2**:29–49.

Scott S a, Davey MP, Dennis JS, Horst I, Howe CJ, Lea-Smith DJ, Smith AG. 2010. Biodiesel from algae: challenges and prospects. *Curr. Opin. Biotechnol.* **21**:277–286.

Scragg AH, Illman AM, Carden A, Shales SW. 2002. Growth of microalgae with increased calorific values in a tubular bioreactor. *Biomass and Bioenergy* **23**:67–73.

Seletzky JM, Noak U, Fricke J, Welk E, Eberhard W. 2007. Scale-up from shake flasks to fermenters in batch and continuous mode with *Corynebacterium glutamicum* on Lactic acid based on oxygen transfer and pH. *Biotechnol. Bioeng.* **98**:800–811.

Sharma KK, Schuhmann H, Schenk PM. 2012. High lipid induction in microalgae for biodiesel production. *Energies* **5**:1532–1553.

Sheyn D, Mizrahi O, Benjamin S, Gazit Z, Pelled G, Gazit D. 2010. Genetically modified cells in regenerative medicine and tissue engineering ☆. *Adv. Drug Deliv. Rev.* **62**:683–698.

Shukla A a, Gottschalk U. 2013. Single-use disposable technologies for biopharmaceutical manufacturing. *Trends Biotechnol.* **31**:147–54.

Silk NJ, Denby S, Lewis G, Kuiper M, Hatton D, Field R, Baganz F, Lye GJ. 2010. Fed-batch operation of an industrial cell culture process in shaken microwells. *Biotechnol. Lett.* **32**:73–8.

Singh A, Nigam PS, Murphy JD. 2011. Mechanism and challenges in commercialisation of algal biofuels. *Bioresour. Technol.* **102**:26–34.

Singh V. 1999. Disposable bioreactor for cell culture using wave-induced agitation. *Cytotechnology* **30**:149–58.

Soletto D, Binaghi L, Ferrari L, Lodi A, Carvalho JCM, Zilli M, Converti A. 2008. Effects of carbon dioxide feeding rate and light intensity on the fed-batch pulse-feeding cultivation of *Spirulina platensis* in helical photobioreactor. *Biochem. Eng. J.* **39**:369–375.

Spolaore P, Joannis-Cassan C, Duran E, Isambert A. 2006. Commercial applications of microalgae. *J. Biosci. Bioeng.* **101**:87–96.

Steiger N, Eibl R. 2013. Interlaboratory Test for detection of cytotoxic leachables arising from single-use bags. *Chemie Ing. Tech.* **85**:26–28.

Stephens E, Ross IL, King Z, Mussgnug JH, Kruse O, Posten C, Borowitzka M a, Hankamer B. 2010. An economic and technical evaluation of microalgal biofuels. *Nat. Biotechnol.* **28**:126–8.

Strickland JD., Parsons TR. 1972. A Practical Handbook of Seawater Analysis. Ed. J.C. Stevenson, J. Watson, J.M. Reinhart, D.G. Cook. *Fish. Res. Board Canada, Ottawa. Bull.* **167**:311.

Sugiyama J, Vuong R, Chanzy H. 1991. Electron diffraction study on the two crystalline phases occurring in native cellulose from an algal cell wall. *Macromolecules* **24**:4168–4175.

Suresh S, Srivastava V, Mishra I. 2009. Techniques for oxygen transfer measurement in bioreactors: a review. *J. Chem. Technol. Biotechnol.* **84**:1091–1103.

Szarafinski D. 2013. Flexible, Scalable and configurable single-use systems for biopharmaceutical research and manufacture. *Chemie Ing. Tech.* **85**:34–39.

Tam NFY, Wong YS. 1996. Effect of ammonia concentrations on growth of *Chlorella vulgaris* and nitrogen removal from media. *Bioresour. Technol.* **57**:45–50.

Tan R, Eberhard W, Jochen B. 2011. Measurement and characterization of mixing time in shake flasks. *Chem. Eng. Sci.* **66**:440–447.

Tang D, Han W, Li P, Miao X, Zhong J. 2011. CO2 biofixation and fatty acid composition of *Scenedesmus obliquus* and *Chlorella pyrenoidosa* in response to different CO2 levels. *Bioresour. Technol.* **102**:3071–6.

Tanner W. 2000. The Chlorella hexose/H(+)-symporters. *Int. Rev. Cytol.* **200**:101–141.

Tissot S, Farhat M, Hacker DL, Anderlei T, Kühner M, Comninellis C, Wurm F. 2010. Determination of a scale-up factor from mixing time studies in orbitally shaken bioreactors. *Biochem. Eng. J.* **52**:181–186.

Ugwu CU, Ogbonna JC, Tanaka H. 2005. Light/dark cyclic movement of algal culture (*Synechocystis aquatilis*) in outdoor inclined tubular photobioreactor

equipped with static mixers for efficient production of biomass. *Biotechnol. Lett.* **27**:75–8.

Vallejos JR, Kostov Y, Ram A, French JA, Marten MR. 2006. Optical analysis of liquid mixing in a minibioreactor. *Biotechnol. Bioeng.* **93**:1–6.

Weber A, Husemann U, Chaussin S, Adams T, Wilde D De, Gerighausen S, Greller G, Fenge C. 2013. Development and qualification of a scalable, disposable bioreactor for GMP-Compliant cell culture. *Bioprocess Int.* **11**.

Wijffels RH, Barbosa MJ. 2010. An outlook on microalgal biofuels. *Science* **329**:796–9.

Xin L, Hu H, Ke G, Sun Y. 2010. Effects of different nitrogen and phosphorus concentrations on the growth, nutrient uptake, and lipid accumulation of a freshwater microalga *Scenedesmus sp. Bioresour. Technol.* **101**:5494–500.

Xiong W, Li X, Xiang J, Wu Q. 2008. High-density fermentation of microalga *Chlorella protothecoides* in bioreactor for microbio-diesel production. *Appl. Microbiol. Biotechnol.* **78**:29–36.

Xu H, Miao X, Wu Q. 2006a. High quality biodiesel production from a microalga *Chlorella protothecoides* by heterotrophic growth in fermenters. *J. Biotechnol.* **126**:499–507.

Xu H, Miao X, Wu Q. 2006b. High quality biodiesel production from a microalga *Chlorella protothecoides* by heterotrophic growth in fermenters. *J. Biotechnol.* **126**:499–507.

Xu L, Wim Brilman DWF, Withag J a M, Brem G, Kersten S. 2011. Assessment of a dry and a wet route for the production of biofuels from microalgae: energy balance analysis. *Bioresour. Technol.* **102**:5113–22.

Yoo C, Jun S-Y, Lee J-Y, Ahn C-Y, Oh H-M. 2010. Selection of microalgae for lipid production under high levels carbon dioxide. *Bioresour. Technol.* **101 Suppl** S71–S74.

Yun YS, Park JM. 2003. Kinetic modeling of the light-dependent photosynthetic activity of the green microalga *Chlorella vulgaris*. *Biotechnol. Bioeng.* **83**:303–311.

Zanzotto A, Szita N, Boccazzi P, Lessard P, Sinskey AJ, Jensen KF. 2004. Membrane-aerated microbioreactor for high-throughput bioprocessing. *Biotechnol. Bioeng.* **87**:243–54.

Zhang H, Lamping S, Pickering S, Lye G, Shamlou P. 2008. Engineering characterisation of a single well from 24-well and 96-well microtitre plates. *Biochem. Eng. J.* **40**:138–149.

Zhang Q, Yong Y, Mao Z-S, Yang C, Zhao C. 2009. Experimental determination and numerical simulation of mixing time in a gas–liquid stirred tank. *Chem. Eng. Sci.* **64**:2926–2933.

Zhang T. 2013. Dynamics of fluid and light intensity in mechanically stirred photobioreactor. *J. Biotechnol.* **168**:107–116.

Zheng Y, Li T, Yu X, Bates PD, Dong T, Chen S. 2013. High-density fed-batch culture of a thermotolerant microalga *Chlorella sorokiniana* for biofuel production. *Appl. Energy* **108**:281–287.

Zhou H, Purdie J, Wang T, Ouyang A. 2009. pH measurement and a rational and practical pH control strategy for high throughput cell culture system. *Biotechnol. Prog.* **26**:872–80.

Zhu Y, Bandopadhayay PC, Wu J. 2001. Measurement of gas-liquid mass transfer in an agitated vessel. A Comparison between Different Impellers. *J. Chem. Eng. Japan* **34**:579–584.

Zimmermann HF, John GT, Trauthwein H, Dingerdissen U, Huthmacher K. 2003. Rapid evaluation of oxygen and water permeation through microplate sealing tapes. *Biotechnol. Prog.* **19**:1061–3.

Appendix I   Examples of standard calibration curves

Calibration of offline OD_{750nm}, OD_{540nm}, and online peak area measurements with biomass dry cell weight, total lipids and FAME concentrations respectively.
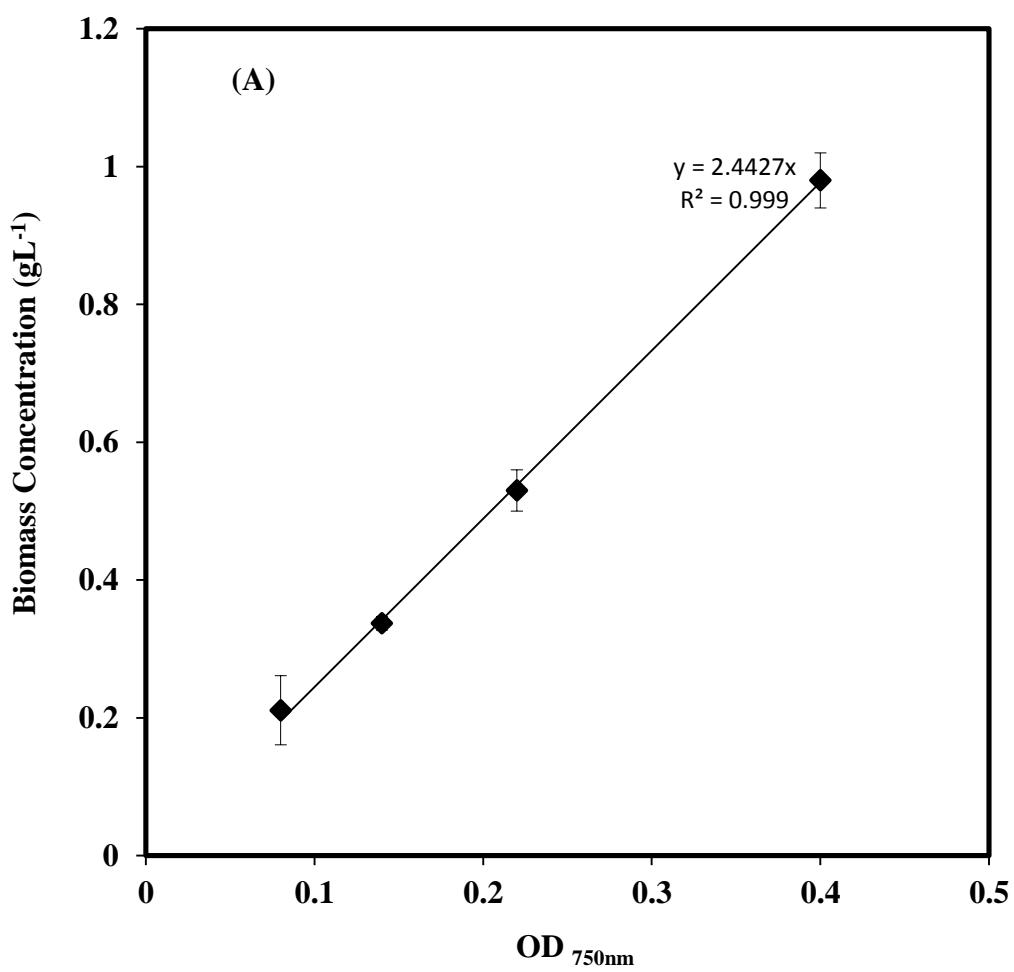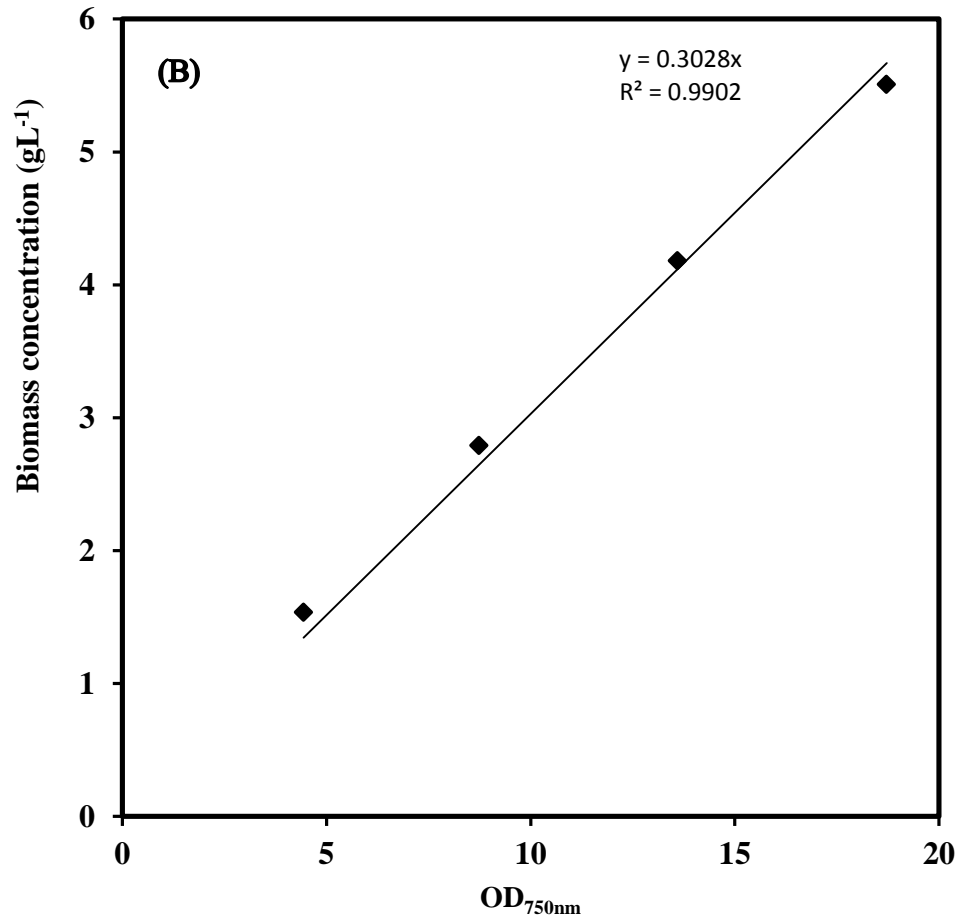
Figure I.1: Calibration curve showing the relationship between biomass concentration (dry cell weight) and OD for *C. sorokiniana*; (A) measured using microwell plate reader for phototrophic cultivation and (B) phototrophically using heterotrophically. Data points represent mean value of triplicate sample preparations. Experiment performed as described in Section 2.9.1.
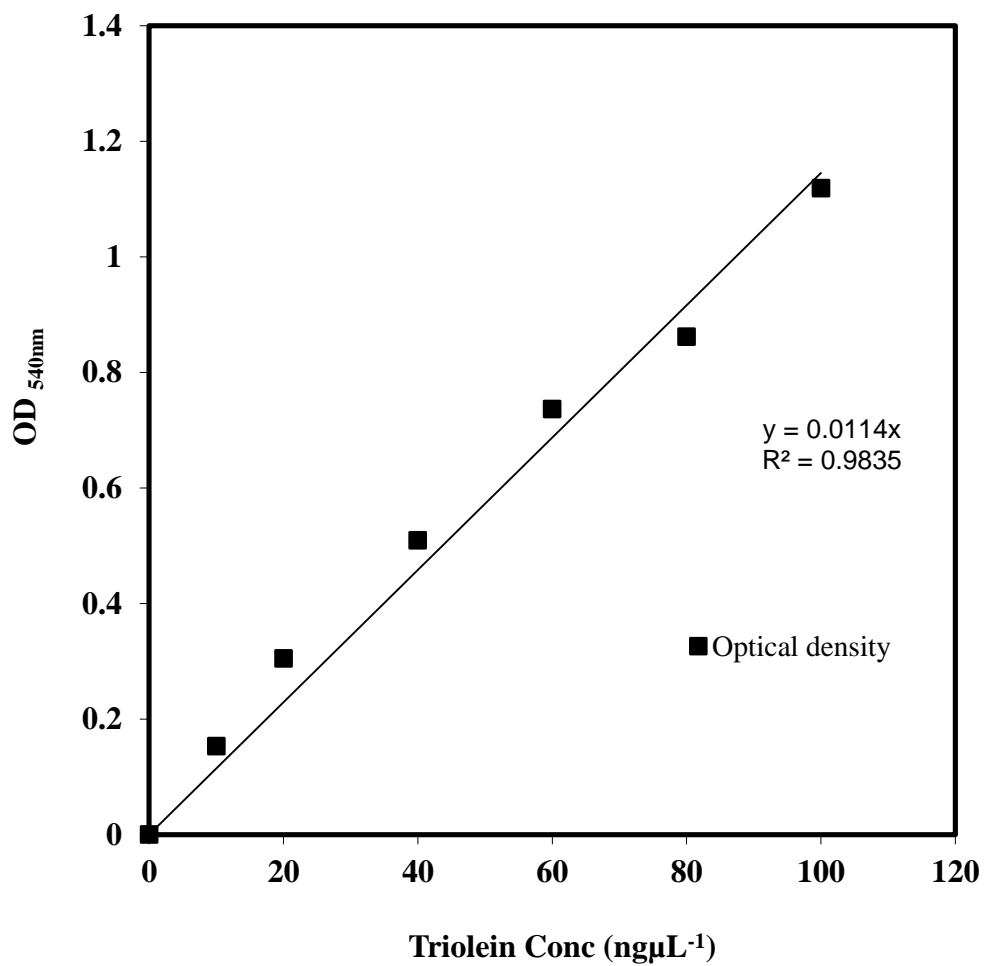
Figure I.2: Triolein calibration curve. Data points represent mean value of triplicate sample in individual wells. Experiment performed as described in Section 2.9.4.

(A)

y = 0.0007x
R² = 0.9895

◆ Capric Acid Methyl Ester (C10:0)

(B)

y = 0.0014x
R² = 0.9754

◆ Myristic Acid Methyl Ester (C14:0)

(F)

$y = 0.0027x$
$R^2 = 0.9862$

Linoleic Acid Methyl Ester (C18:2n6c)

(H

$y = 0.0039x$
$R^2 = 0.9904$

Arachidic Acid Methyl Ester (C20:0)
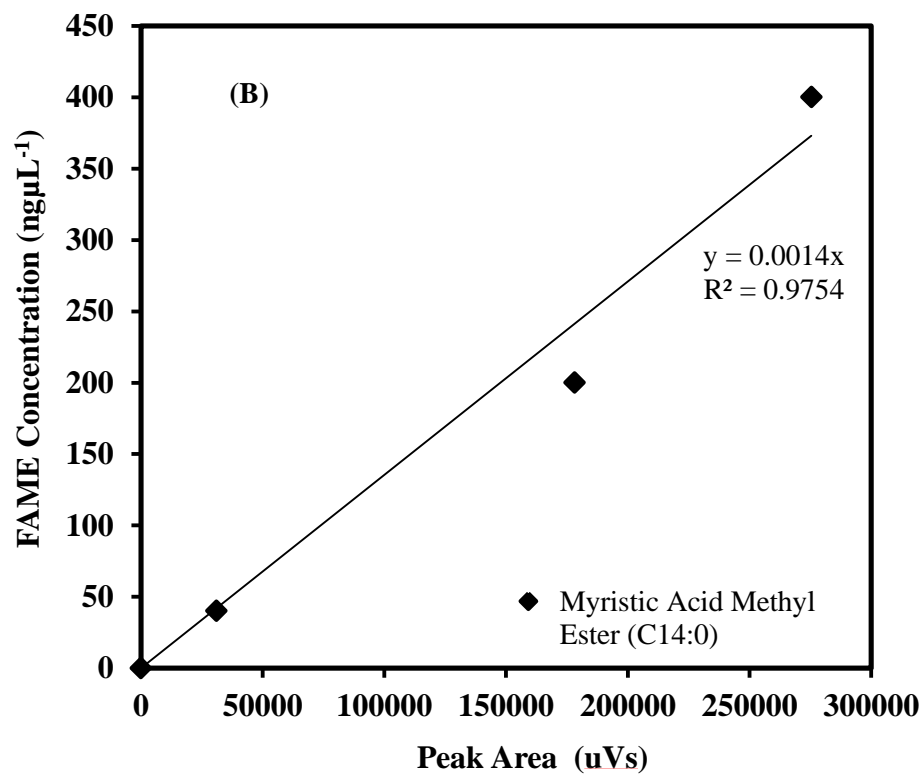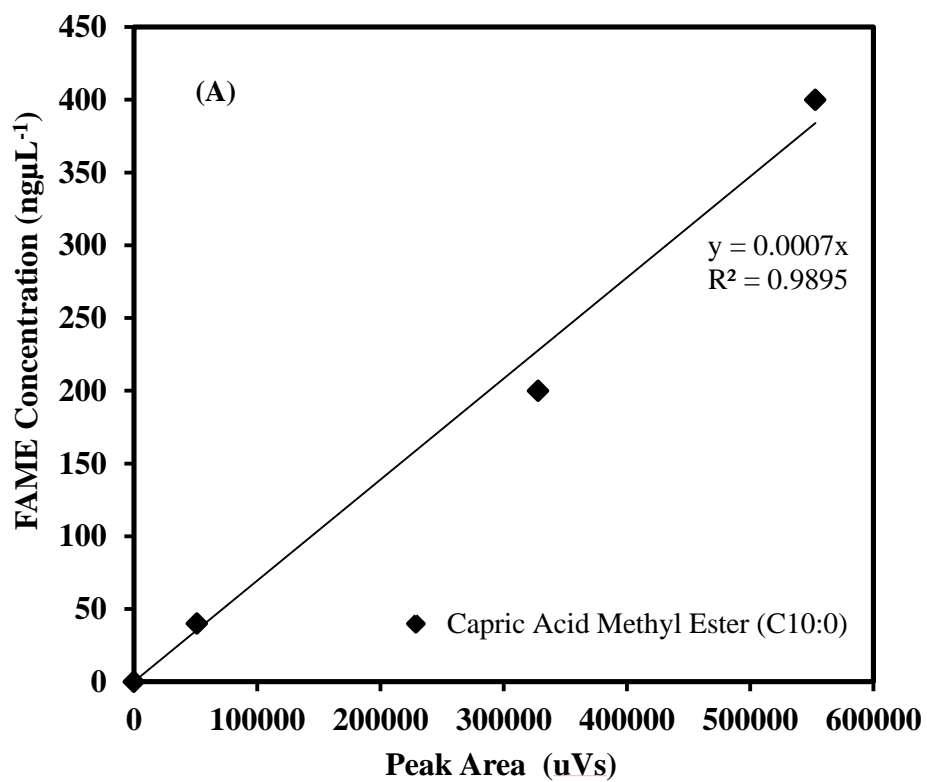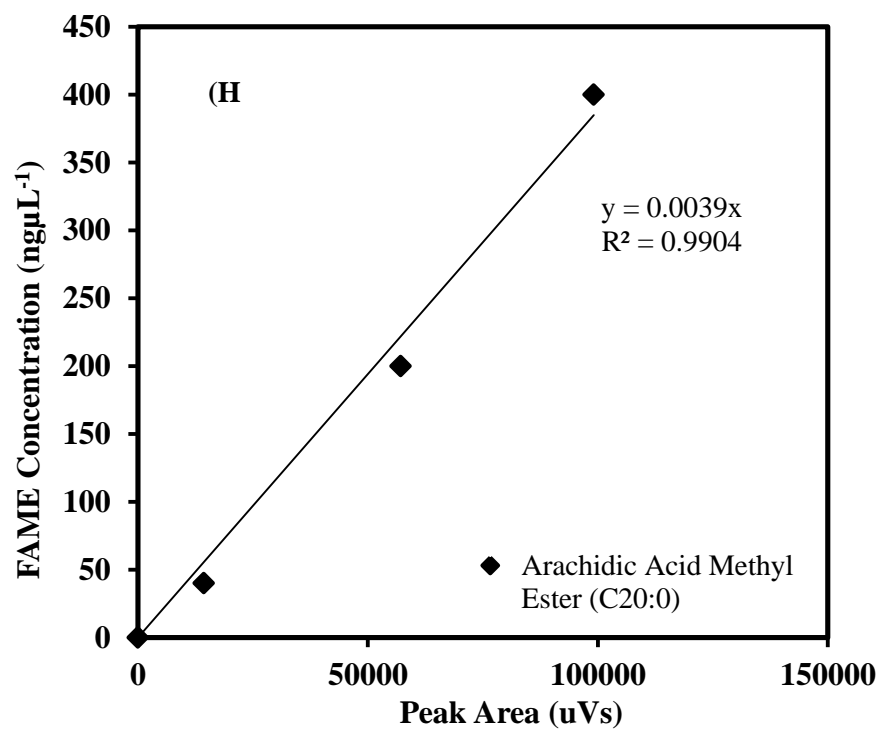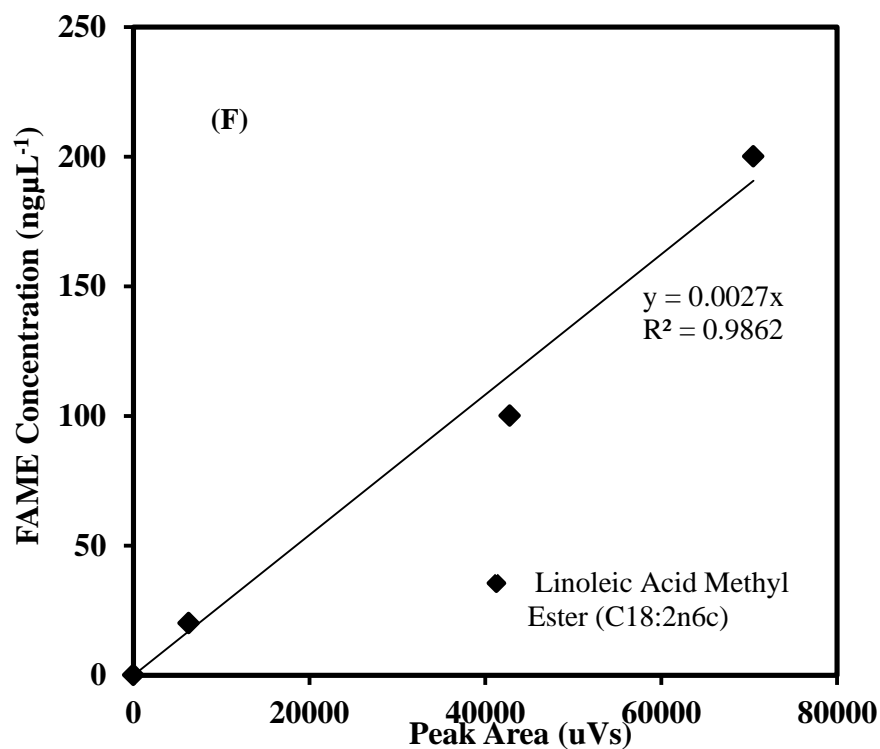
Figure I.3: Calibration curves for selected fatty acid methyl esters (A) capric acid, (B) myristic acid (C) linolenic acid (D) arachidic acid. Each point represents mean value of triplicate standard preparation in dichloromethane. Experiment performed as described in Section 2.9.5.

Appendix II   Engineering characterisation of SUB and example GC chromatographs for FAME.

1ms,	0.2s,	0.4s,
0.6s,	0.8s,	1.0s,
1.4s,	1.8s,	2s,
3s,	4s,	4.5s,
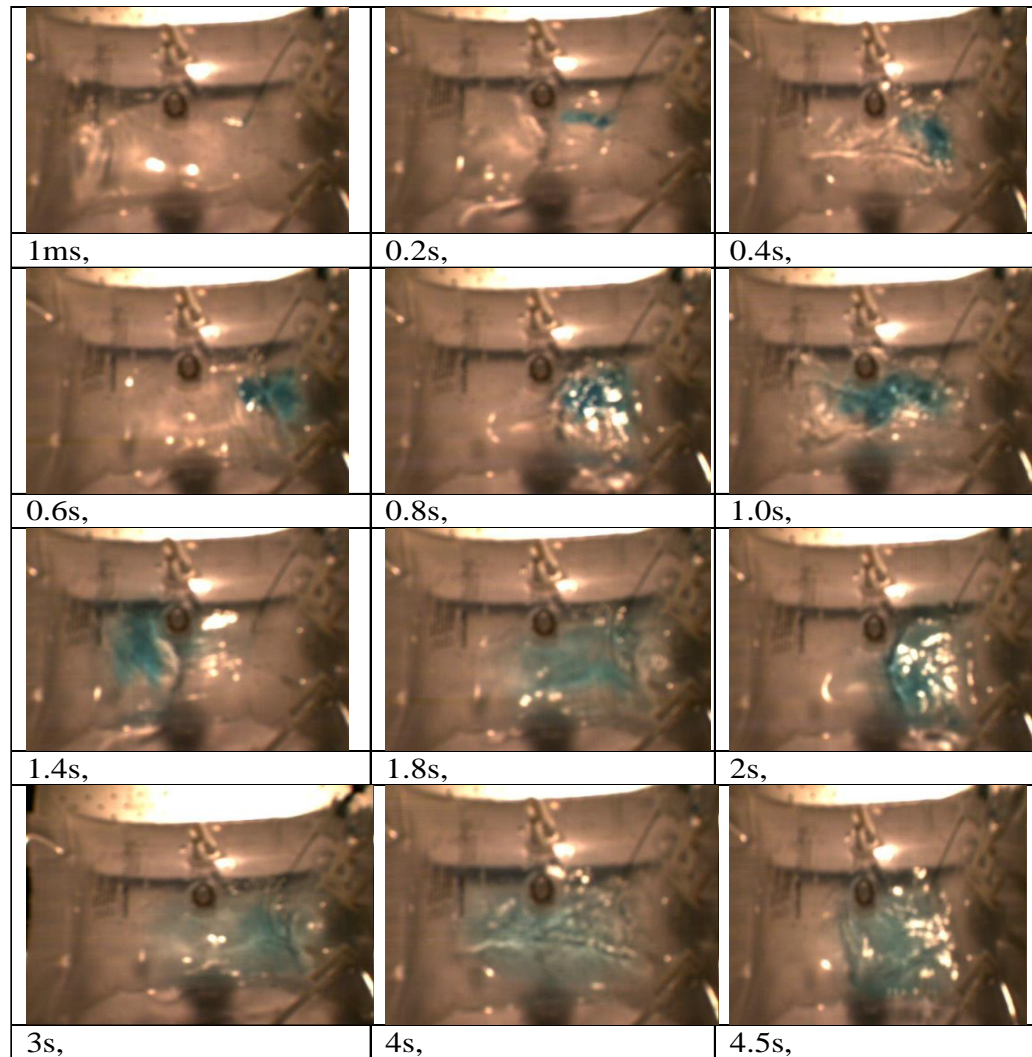
Figure II.4: Visualisation and time estimation of dye dispersion in an orbitally shaken Biostat Cultibag^{TM} showing different position of dye at micro-milliseconds internal of sample images obtained from continuous video footage. Experimental conditions: $V_f = 0.25$, $d_o = 25$ mm, $N_f = 180$ rpm, $V_s = 250$ fps. Experiment performed as described in Section 2.4.4.
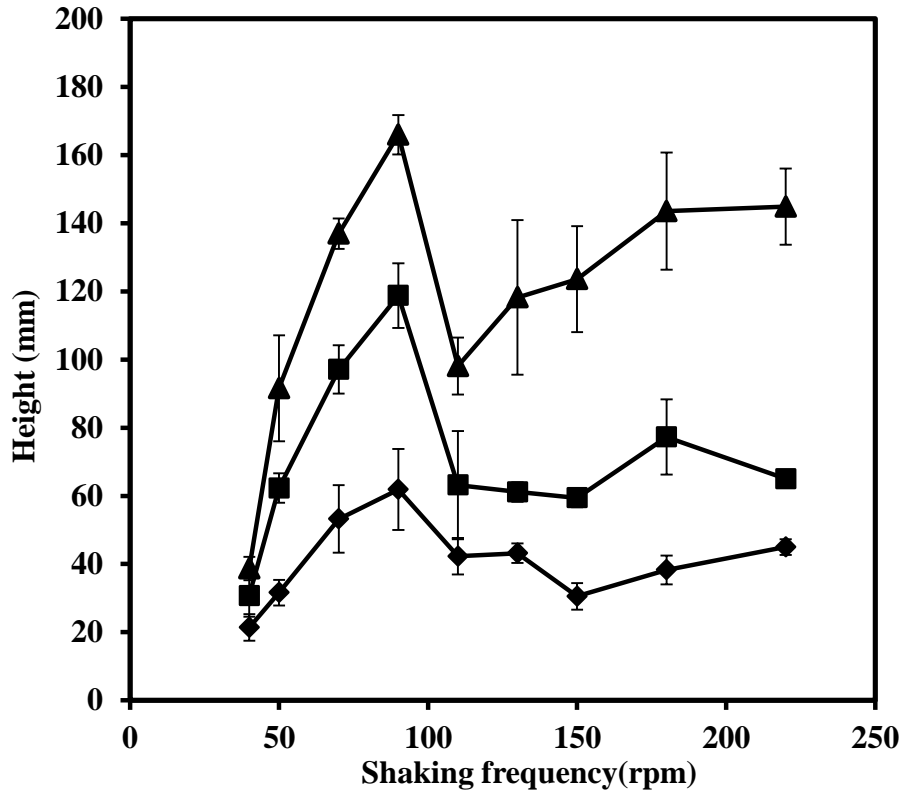
Example calculation; where Ho is the fill volume height at 0 rpm.

$H_{actual} = 172 - (H_1 - Init) - x$

where initial point is most often 0

$H_{actual} = 172 - H_1 - x$

where;

$H = 172 - H_1$

$H_{actual} = H - Ho$

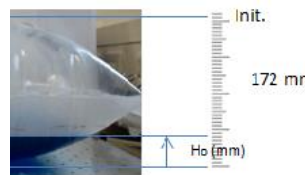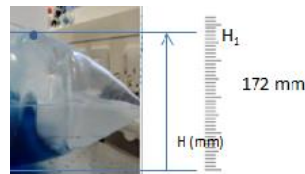Normalising Hactual; divide by x

$$H_{actual} = \frac{H - Ho}{Ho}$$

Figure II.5: Effect of shaking frequency on fluid hydrodynamics in the single-use photobioreactor as determined by the maximum height attained by the shaken liquid at d_o = 25 mm as described in Section 2.4.5; and normalised as shown in Figure 4.3. The image was calibrated using image J software for height determination.
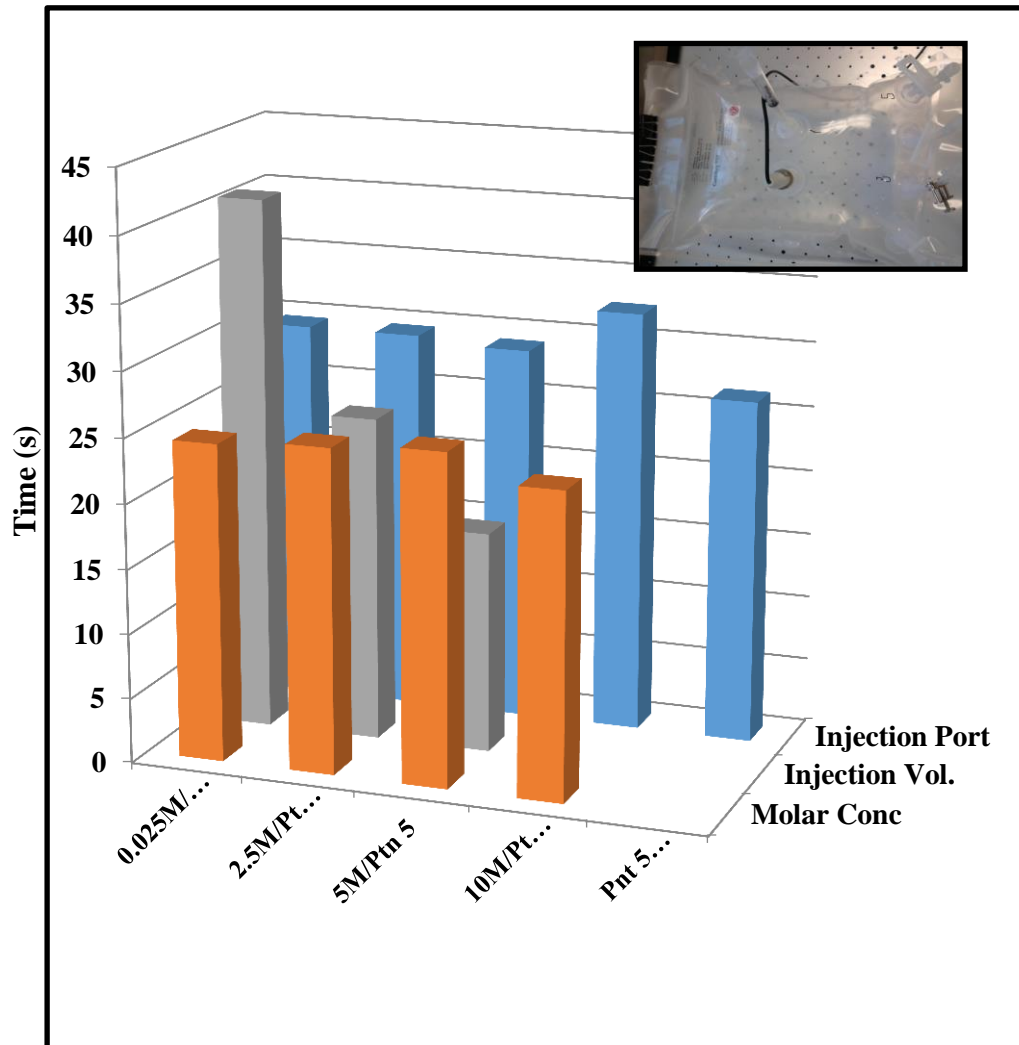
Figure II.6: Estimation of mixing time in the CultiBag^{TM} based on pH-tracer method to determine the effect of molar concentration of acid and base, injection volume and injection port on the total time it takes to form a homogeneous fluid. Experimental conditions are: $V_f = 0.25$, do = 25 mm, N = 180 rpm. Experiment performed as described in Section 2.4.3.
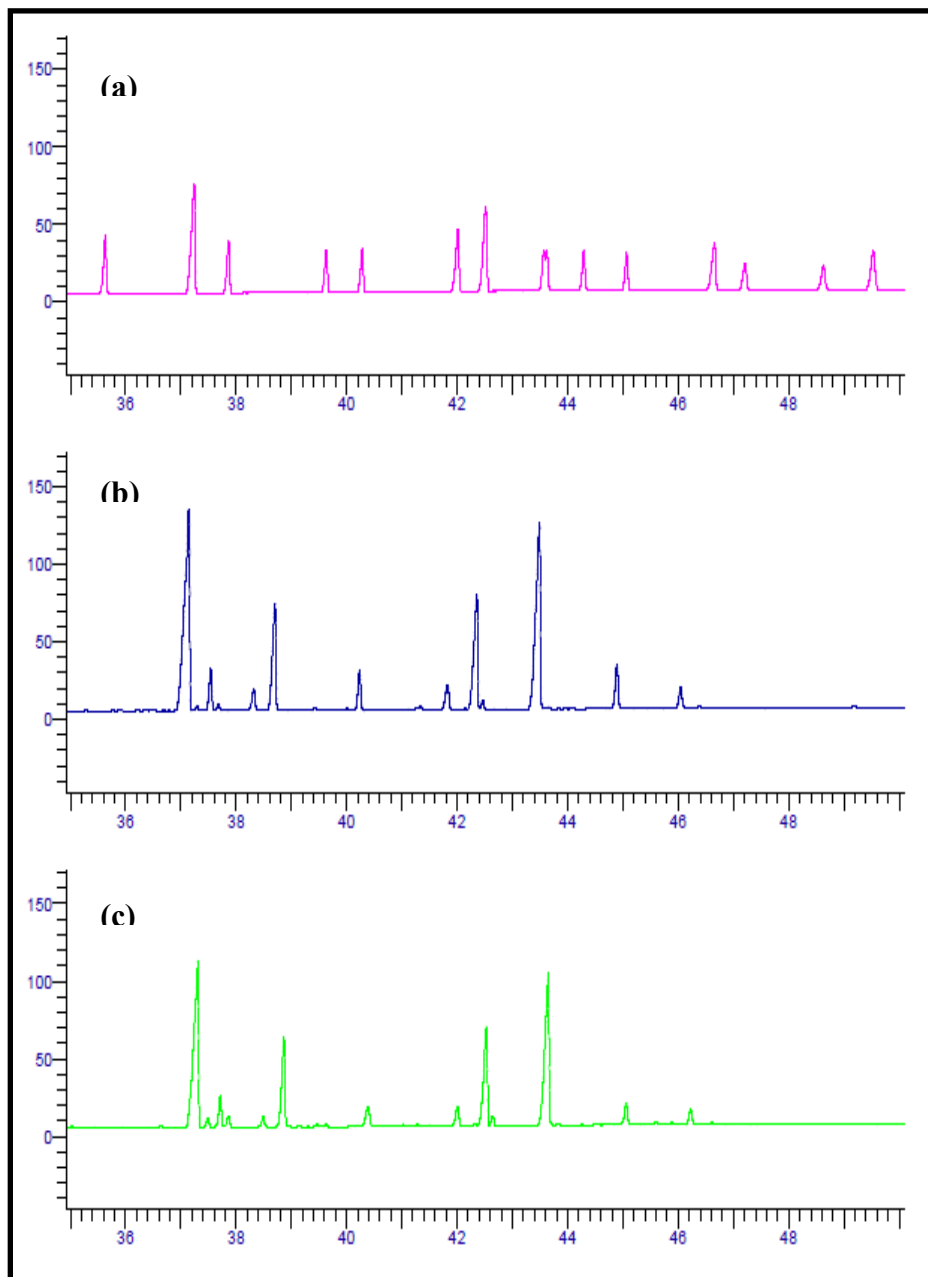
Figure II.7: Example gas chromatograph showing cross sections of esterified lipid sample for FAME identification. a – c represent three samples from the same stock. The results showed consistency and reproducibility of sample results. Experiment performed as described in Section 2.9.5.
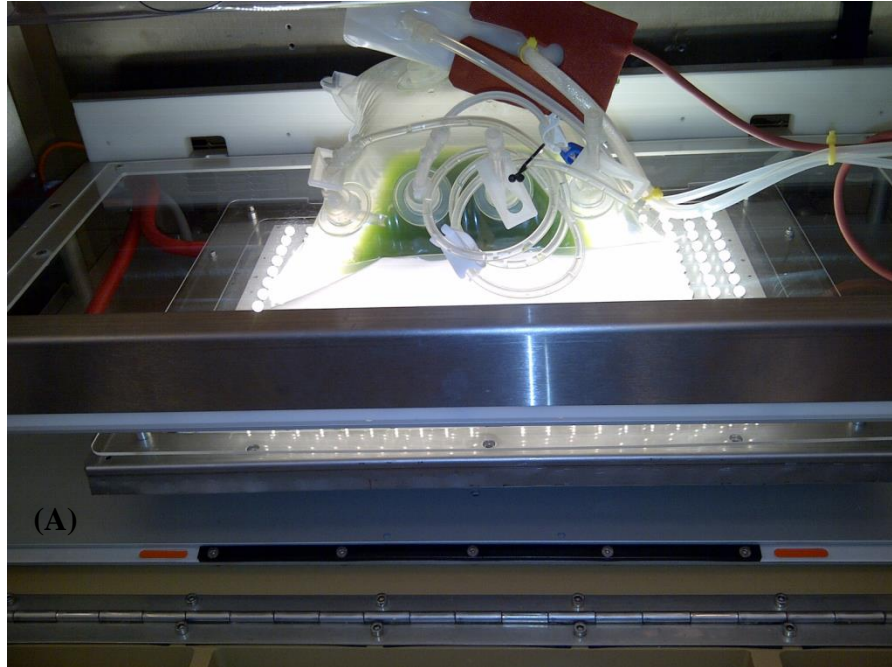
Figure II.8: Example images showing (A) set-up and utilisation of the SUPBr containing four days culture of *C. sorokiniana*. (B) a cross section of the suspended high power LED and the novel platform designed for the SUPBr. Light intensity in both cases were 180 μmols.m^{-2}.s^{-1}. Experiment performed as described in Section 2.3.2 & 2.5.3.
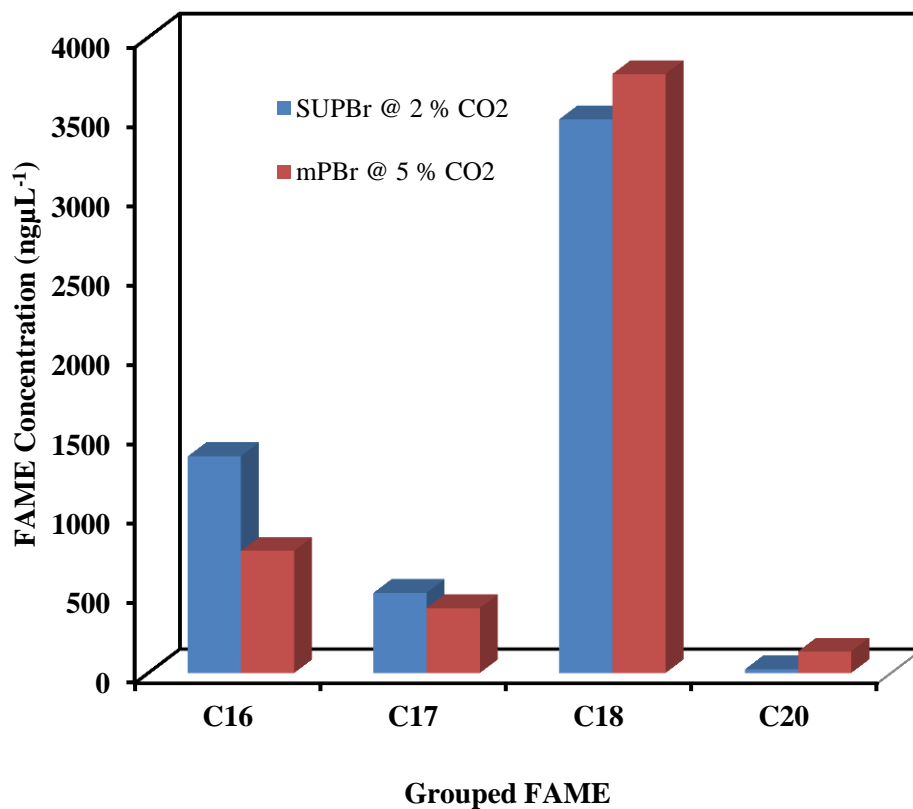
Figure II.9: Comparison of grouped FAME concentrations between the SUPBr and mPBr showing comparable performance at matched scale-up criteria for cultivation. Experiment performed as described in Section 2.9.5.